SOLPLAN

FOUNDATION ANALYSIS SOFTWARE

PILE GROUP ANALYSIS · THREE-DIMENSIONAL, NONLINEAR

Solgroup

Technical Reference

Pile-group mechanics, soil-response curves, cap models, numerical solution and verification.

Release **1.0.16** · Document **SPL-SG-003** · Revision **A**

DOCUMENT TITLE	DOCUMENT NO.	REVISION	ISSUE DATE
Solgroup — Technical Reference	**SPL-SG-003**	**A**	**2026-11-23**
STATUS	SOFTWARE RELEASE	PAGES	LANGUAGE
Issued for release	**1.0.16**	**66**	**English**

© 2026 Solplan. All rights reserved.

Solplan · Indonesia

Document control

Document	SPL-SG-003 — Solgroup Technical Reference
Applies to	Solgroup 1.0.16 and later releases until superseded
Revision / date	A / 2026-11-23
Status	Issued for release
Publisher	Solplan

Revision history

Rev.	Date	Description
A	2026-11-23	First issue for Solgroup 1.0.16.

Solgroup documentation set

No.	Title	Content
SPL-SG-001	Solgroup — End-User Licence Agreement	Terms under which Solgroup is licensed to its users.
SPL-SG-002	Solgroup — User Manual	Building, running and reporting three-dimensional pile group analyses with Solgroup.
SPL-SG-003	Solgroup — Technical Reference	Pile-group mechanics, soil-response curves, cap models, numerical solution and verification.
SPL-SG-004	Solgroup — Release Notes	Scope, requirements and known limitations of release 1.0.16.
SPL-SG-005	Solgroup — Third-Party Software Notices	Open-source components distributed with Solgroup and their licences.

This document is uncontrolled when printed or copied. The current revision is the one distributed with the installed release of Solgroup. The information in this document is subject to change without notice and does not represent a commitment on the part of the publisher.

© 2026 Solplan. All rights reserved. Solplan and Solgroup are names used by the publisher for its company and products. Other product and company names mentioned in this document may be trademarks of their respective owners and are used for identification only.

Contents

1 Scope and conventions 5
1.1 Purpose of this document 5
1.2 Overview of the model 5
1.3 Methods of analysis of pile groups 6
1.4 Behaviour of closely spaced piles 6
1.5 Three-dimensional analysis 7
1.6 Coordinates and sign conventions 7
1.7 Units 7

2 Mechanics of the pile group 8
2.1 Guiding concept 8
2.2 Assumptions 8
2.3 Rigid cap 8
2.4 Flexible cap 10
2.5 Loads 11
2.6 Load cases and combinations 11
2.7 Axial force along the piles 11

3 The pile group in the analysis of the structure 12
3.1 Foundation and superstructure 12
3.2 Coupling of translation and rotation 12
3.3 An isolated pile under combined loads 12
3.4 Dynamic and seismic analyses 13

4 Analysis of a single pile 14
4.1 Lateral response 14
4.2 Axial response 16
4.3 Torsional response 17

5 Soil response: p-y curves 18
5.1 General 18
5.2 Soft clay 21
5.3 Stiff clay with free water 22
5.4 Stiff clay without free water 23
5.5 Sand (Reese) 24
5.6 API sand 25
5.7 Liquefied sand 26
5.8 Cemented soils with cohesion and friction 27
5.9 Rock 28
5.10 Other models 31
5.11 Selection of a p-y criterion 33
5.12 Battered piles 33
5.13 Layered soil 34
5.14 Default parameters 34

6 Soil response for axial loading 36
6.1 Load-transfer curves 36
6.2 Driven piles 36
6.3 Drilled shafts 37
6.4 Curves of the pile head 38
6.5 Estimated ultimate values 38

7 Group effects 40
7.1 Closely spaced piles 40
7.2 Factors by rows 40
7.3 Factors for each pile from the positions of all piles 40
7.4 Factors for each pile by direction 41

© 2026 Solplan. All rights reserved.

7.5 Reduction along the depth 42
7.6 Effect of the spacing 42
7.7 Axial group effects 42

8 Axial resistance of pile groups 43
8.1 Efficiency of a group 43
8.2 Piles in cohesionless soils 43
8.3 Piles in cohesive soils 43
8.4 Settlement of the group 43

9 Section mechanics 44
9.1 Method 44
9.2 Concrete 44
9.3 Confined concrete 44
9.4 Reinforcing and structural steel 45
9.5 Prestressed sections 45
9.6 Bending stiffness in the pile analysis 46
9.7 Section options 47

10 Structural checks of the piles 48
10.1 Elastic section with a specified moment capacity 48
10.2 Total stress of elastic sections 48
10.3 Demand/capacity ratios 49

11 Embedded pile cap 51
11.1 Soil resistance on the cap 51
11.2 Method of analysis 51
11.3 Effect on the lateral response 51

12 Foundation stiffness and pushover 53
12.1 Stiffness of the foundation 53
12.2 Pushover analysis 54

13 Parametric studies 55
13.1 Length of the piles 55
13.2 Batter of the piles 55
13.3 Free length and axial load 56
13.4 Number of piles 57
13.5 Rotational restraint of the pile heads 57
13.6 Thickness of a flexible cap 58
13.7 Mesh of a flexible cap 58
13.8 Depth of a soil movement 59
13.9 Choice of the p-y criterion 60

14 Verification 61
14.1 Long pile on a linear subgrade 61
14.2 Symmetric group under a rigid cap 61
14.3 Equilibrium of the worked example 61
14.4 Independence of the position of the group 62
14.5 Axial forces in a ring of piles 62
14.6 Equilibrium of battered piles 62
14.7 A rectangular section in its two planes 63
14.8 Moment–curvature of a steel pipe 63
14.9 Torsion of a rigid cap 63
14.10 p-y curves against the published equations 64

Appendix A References 65

© 2026 Solplan. All rights reserved.

1 Scope and conventions

1.1 Purpose of this document

This document describes the engineering model on which Solgroup 1.0.16 rests: the representation of the piles, the soil and the pile cap, the soil-response curves, the solution of the equilibrium of the group, and the verification of the program. It is intended for engineers who need to judge whether the model suits a design problem and how its results should be interpreted. The use of the program is described in the User Manual (SPL-SG-002).

The soil-response curves are empirical. Their validity rests on the field tests reported in the publications cited with each curve. Solgroup implements these published relations; it does not extend them beyond the conditions for which they were derived.

1.2 Overview of the model

A pile group is a set of piles joined at their heads by a pile cap. The model has three parts:

1. **Piles.** Each pile is a beam-column of given length, cross-section and orientation. Along its length it is supported by nonlinear soil springs: lateral springs defined by p-y curves in two perpendicular planes, axial springs along the shaft (t-z curves) and at the tip (Q-w curve), and torsional springs. The bending stiffness can depend on the bending moment (nonlinear sections).
2. **Cap.** The cap is either rigid, with six degrees of freedom, or flexible, represented by plate elements. The piles are connected to the cap at their heads, with a connection that ranges from fixed to pinned.
3. **Loads.** Forces and moments act on the cap, on joints and along the piles; the soil can move horizontally around the piles.

For each load case the program finds the displacements of the cap for which the forces exerted by the piles balance the applied loads, and the response of every pile under the movement of its head. Because the soil springs are nonlinear, the solution is iterative.

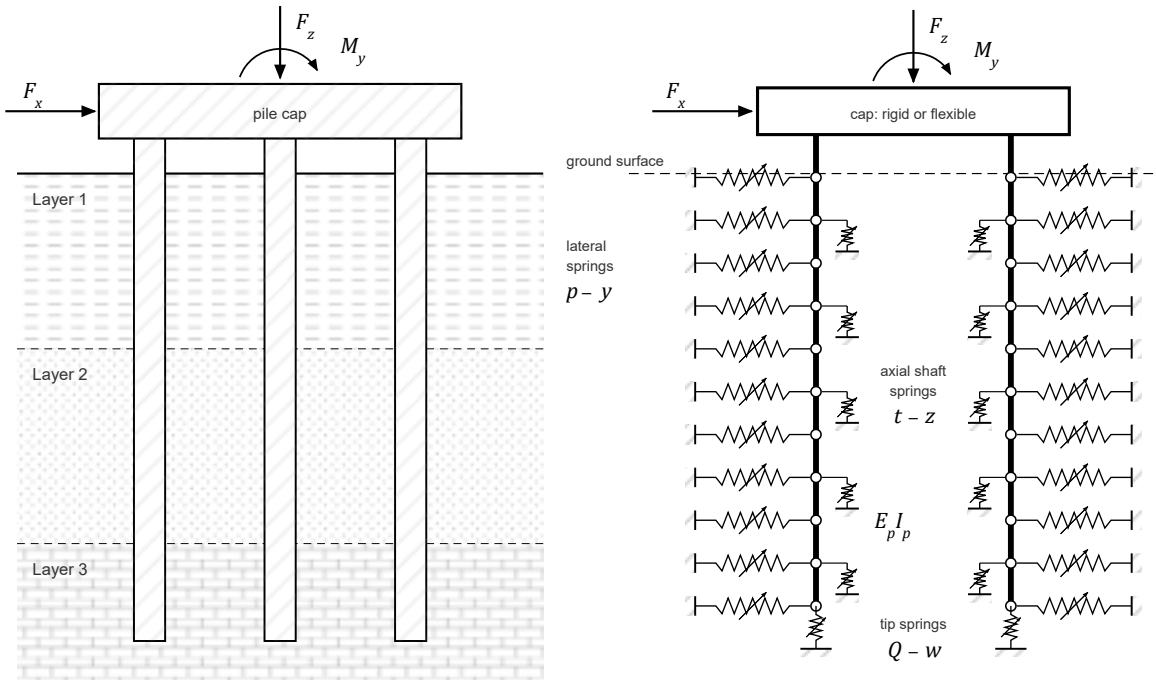

(a) Pile group and soil **(b) Piles on nonlinear springs, joined by the cap**

Figure 1.1 — Model of a pile group: piles on nonlinear soil springs, joined by a cap

© 2026 Solplan. All rights reserved.

1.3 Methods of analysis of pile groups

Several families of methods are used to analyse a group of piles under combined loads. They differ in how the soil is represented and, as a consequence, in how the nonlinearity of the soil and the interaction between the piles are treated.

Elastic continuum methods. The soil is an elastic half-space, and the displacement of each pile is obtained by integrating the solution for a point load in the continuum over the surface of the pile (Poulos and Davis, 1980). The interaction between two piles follows naturally from the continuum and is often expressed by interaction factors: the additional displacement of one pile caused by an equal load on another pile, as a fraction of the displacement of the loaded pile alone. These methods describe the interaction of closely spaced piles at small loads well, but the soil responds linearly; a nonlinear soil can only be approximated by reducing the modulus, and the yield of the soil near the ground surface, which governs the lateral response at working loads, is not represented.

Load-transfer methods. The soil around each pile is replaced by nonlinear springs whose properties are derived from full-scale tests on instrumented piles: p-y curves for the lateral resistance, t-z curves for the shaft resistance and a Q-w curve for the tip. The response of each pile follows from the solution of a beam-column on these springs, and the piles are joined through the cap by the conditions of equilibrium and compatibility (Reese, O'Neill and Smith, 1970; Bryant and Matlock, 1977; O'Neill, Ghazzaly and Ha, 1977). The springs reproduce the nonlinear behaviour of real soils as measured, including the effects of repeated loading and of free water; the interaction through the soil is introduced by factors derived from tests on groups. Solgroup belongs to this family.

Numerical continuum methods. Finite-element or finite-difference models of the soil and the piles can represent the soil with an elastoplastic constitutive model and the interaction between the piles directly. They require the parameters of a constitutive model, which are seldom available from a routine site investigation, they are sensitive to the representation of the interface between pile and soil, and their computing cost makes it difficult to study many load cases and variations of the parameters. They are mostly used for special problems and for research.

For the design of pile foundations the load-transfer method has two advantages: its springs are calibrated against the measured response of real piles, and it is fast enough for every load case and for the variation of uncertain parameters to be analysed. Its limitation is that the interaction between closely spaced piles through the soil is not computed but introduced by empirical factors.

1.4 Behaviour of closely spaced piles

When piles are far apart, each pile responds as a single pile, and the group can be analysed as a set of independent piles joined by the cap. Field and model tests show that the response changes when the spacing is less than about seven diameters in the direction of loading and about four diameters across it (Brown, Morrison and Reese, 1988; Rollins, Peterson and Weaver, 1998):

- Under lateral load, a pile that follows another pile in the direction of movement acts in soil that has already been pushed by the leading pile, and its resistance is lower. This shadowing effect is strongest for the second row and increases only slightly for the rows behind it. Piles side by side share the soil between them, which also reduces their resistance, but less. The leading row carries a larger share of the load than the trailing rows, and its piles have the largest bending moments.
- Under axial load, the zones of soil stressed by the shafts and the tips of neighbouring piles overlap. In loose sand, driving the piles densifies the soil and the group can carry more than the sum of the single piles; in clay the capacity of a closely spaced group can be governed by the failure of the block of soil that contains the piles, and the settlement of the group is larger than that of a single pile at the same load per pile (Chapter 8).

Solgroup represents these effects by multipliers on the soil resistance of each pile: p-multipliers on the p-y curves, computed from the positions of the piles or entered by rows (Chapter 7), and reduction factors on the axial load–displacement curves entered by the user.

© 2026 Solplan. All rights reserved.

1.5 Three-dimensional analysis

Solgroup analyses every model in three dimensions: the cap has six degrees of freedom, each pile bends in two planes, and the axial and torsional responses of the piles are included. A two-dimensional idealisation, in which the cap moves in one vertical plane, is exact only for a group that is symmetric about that plane and loaded in it; for any other group, and for loads in two directions or with a torque, it can mis-estimate the forces of the piles at the corners and the torsion of the cap. The three-dimensional analysis needs no such assumption and costs little more, because the number of unknowns of the cap is six for any number of piles.

1.6 Coordinates and sign conventions

The global axes are X and Y in the horizontal plane and Z vertical, positive upward; the system is right-handed. Coordinates may be large (for example site or map coordinates); the solution does not depend on the position of the group in the global system.

Each pile has local axes: axis 1 along the pile from the head to the tip, and axes 2 and 3 in the plane of the cross-section. For a vertical pile without a rotation of its section, local axes 2 and 3 are parallel to global X and Y. The deflection of a pile in the direction of local axis 2 is resisted by the bending stiffness EI_{33} and is reported as “plane 2”; the deflection along local axis 3 as “plane 3”.

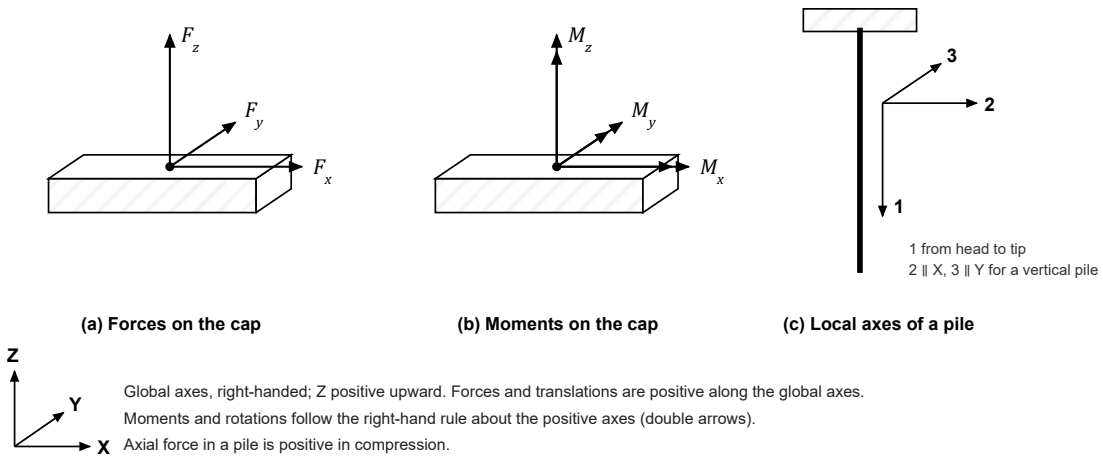

Figure 1.2 — Global axes, loads on the cap and local axes of a pile

Table 1.1 — Sign conventions of the results

Quantity	Positive sense
Cap translation	along the positive global axis
Cap rotation	right-hand rule about the positive global axis
Axial force in a pile	compression
Shear and moment in a pile	in the local axes of the pile; the moment sign convention of the reports is chosen in the preferences
Soil reaction *p*	opposing the deflection of the pile relative to the soil

1.7 Units

The analysis is carried out in SI units internally. Input and results are converted to the unit system of the model (kN, m; kgf, m; tonf, m; N, mm; kip, in; kip, ft). Where a published relation is dimensional, its constants are applied in the units of the publication and the result is converted.

© 2026 Solplan. All rights reserved.

2 Mechanics of the pile group

2.1 Guiding concept

A pile foundation transfers the loads of a structure to the ground through piles that are joined at their heads by a pile cap. The load on the cap is shared between the piles in proportion to their stiffness, and the stiffness of a pile depends on the load it carries: a pile in soft ground or near its capacity is softer than a lightly loaded pile in stiff ground. The distribution of the load is therefore found together with the response of the piles, by requiring that the cap is in equilibrium under the applied loads and the forces of the piles, and that every pile head moves with the cap.

Solgroup describes each pile by its own nonlinear response to the movement of its head – lateral in two planes, axial and torsional – computed from the soil around it (Chapter 4), and finds the movement of the cap for which the forces of all piles balance the loads. This approach, introduced for pile groups by Reese, O'Neill and Smith (1970) and developed by Bryant and Matlock (1977), O'Neill, Ghazzaly and Ha (1977) and Reese and Van Impe (2011), keeps the full nonlinearity of the soil and of the pile sections while the number of unknowns of the group remains small.

2.2 Assumptions

- **Interaction through the cap.** The piles interact through the cap that joins them. The interaction of closely spaced piles through the soil is represented by reduction factors on the soil resistance of each pile (Chapter 7); it is not computed from a continuum model of the soil.
- **Lateral and axial response.** The lateral response of a pile in each of its two bending planes, its axial response and its torsional response are computed separately and coupled through the movement of the pile head. The axial force of a pile enters its lateral response as the axial thrust of a beam-column (Section 4.1).
- **Cap.** A rigid cap does not deform; its movement is described by three translations and three rotations. A flexible cap deforms as a plate (Section 2.4).
- **Small displacements.** Equilibrium is written for the undeformed geometry of the cap; the effect of the axial thrust on the bending of a pile is included.
- **Static loading.** Loads are applied statically. The effect of repeated loading is included through the cyclic forms of the soil-response curves, not by a dynamic analysis.

2.3 Rigid cap

2.3.1 Kinematics

The movement of a rigid cap is described at its reference point by the vector

$$\mathbf{U} = \left(U_x,\ U_y,\ U_z,\ \theta_x,\ \theta_y,\ \theta_z \right)^{\mathrm{T}} \tag{2.1}$$

of three translations and three rotations in the global axes. The head of pile i, at the position $\mathbf{r}_i$ relative to the reference point, translates and rotates with the cap:

$$\mathbf{u}_i = \mathbf{A}_i\,\mathbf{U}, \qquad \mathbf{A}_i = \begin{bmatrix} \mathbf{I} & -[\mathbf{r}_i]_\times \\ 0 & \mathbf{I} \end{bmatrix}, \qquad [\mathbf{r}]_\times = \begin{bmatrix} 0 & -r_z & r_y \\ r_z & 0 & -r_x \\ -r_y & r_x & 0 \end{bmatrix} \tag{2.2}$$

The movement of the head is resolved into the local axes of the pile with the rotation matrix $\mathbf{T}_i$ of the pile, whose rows are the unit vectors of local axes 1, 2 and 3 in global coordinates:

$$\bar{\mathbf{u}}_i = \begin{bmatrix} \mathbf{T}_i & 0 \\ 0 & \mathbf{T}_i \end{bmatrix} \mathbf{u}_i = \Lambda_i\,\mathbf{u}_i \tag{2.3}$$

© 2026 Solplan. All rights reserved.

Axis 1 points along the pile from the head to the tip; for a battered pile it follows the batter, and a rotation of the section turns axes 2 and 3 about axis 1. The local components are the axial movement of the head, its lateral deflections in planes 2 and 3, the torsional rotation and the slopes in the two bending planes.

2.3.2 Pile-head forces

For a given head movement each pile responds with the head forces

$$\bar{\mathbf{f}}_i = \left(N_i,\ V_{2,i},\ V_{3,i},\ T_i,\ M_{2,i},\ M_{3,i} \right)^{\mathsf{T}} \tag{2.4}$$

where the axial force N follows from the axial load–displacement curve of the pile, the torque T from its torque–rotation curve, and the shear forces and moments from the analysis of the pile as a beam-column on nonlinear soil springs in each bending plane, with the head deflection and slope (or the head moment, depending on the connection) imposed (Chapter 4). The head connection sets which movements the cap imposes on the pile:

Table 2.1 — Pile-head connections

Connection	Conditions at the head, in each bending plane
Fixed	The deflection and the slope of the head are those of the cap; the head carries a moment.
Pinned	The deflection is that of the cap; the head moment is zero. A pile pinned in both planes carries no torque.
Elastically restrained	The deflection is that of the cap; the head moment is $M = k_\theta(\theta_{\text{cap}} - S)$, where S is the slope of the pile head and k_θ the rotational stiffness of the connection.

The connection can differ between the two bending planes of a pile. The forces are transformed back to the global axes and to the reference point of the cap:

$$\mathbf{f}_i = \Lambda_i^{\mathsf{T}}\, \bar{\mathbf{f}}_i, \qquad \mathbf{F}_{\text{piles}}(\mathbf{U}) = \sum_i \mathbf{A}_i^{\mathsf{T}}\, \mathbf{f}_i \tag{2.5}$$

2.3.3 Equilibrium and its solution

The cap is in equilibrium when the resultant of the pile-head forces balances the applied load $\mathbf{F}$, reduced to the reference point:

$$\mathbf{R}(\mathbf{U}) = \mathbf{F} - \sum_i \mathbf{A}_i^{\mathsf{T}}\, \Lambda_i^{\mathsf{T}}\, \bar{\mathbf{f}}_i \left(\Lambda_i \mathbf{A}_i \mathbf{U} \right) = 0 \tag{2.6}$$

Because the pile responses are nonlinear, (2.6) is solved iteratively. From the current estimate $\mathbf{U}^{(k)}$ the residual load $\mathbf{R}$ is computed, the tangent stiffness of the group is formed from the tangent stiffness $\mathbf{k}_i = \partial \bar{\mathbf{f}}_i / \partial \bar{\mathbf{u}}_i$ of every pile head,

$$\mathbf{K} = \sum_i \mathbf{A}_i^{\mathsf{T}}\, \Lambda_i^{\mathsf{T}}\, \mathbf{k}_i\, \Lambda_i\, \mathbf{A}_i \tag{2.7}$$

and the cap movement is corrected:

$$\mathbf{K}\, \Delta\mathbf{U} = \mathbf{R}\left(\mathbf{U}^{(k)} \right), \qquad \mathbf{U}^{(k+1)} = \mathbf{U}^{(k)} + \Delta\mathbf{U} \tag{2.8}$$

This is the method of successive displacement correction (a Newton–Raphson iteration). The stiffness of a pile head is found numerically, by small changes of each component of the head movement. The analyses of the individual piles in one iteration are independent and are carried out in parallel when several processors are available.

2.3.4 Convergence

The iteration stops when the correction of the cap movement is small compared with the movement itself, separately for translations and rotations:

$$\frac{\left\| \Delta\mathbf{U}_t \right\|}{\left\| \mathbf{U}_t \right\|} < \varepsilon_{cap}, \qquad \frac{\left\| \Delta\mathbf{U}_r \right\|}{\left\| \mathbf{U}_r \right\|} < \varepsilon_{cap} \tag{2.9}$$

© 2026 Solplan. All rights reserved.

where $\mathbf{U}_t$ and $\mathbf{U}_r$ are the translational and rotational parts of $\mathbf{U}$ and ε_{cap} is the relative cap tolerance of the load case. Optionally the iteration also stops when the absolute corrections fall below given values of displacement and rotation. Each single-pile analysis inside an iteration has its own limit on the number of iterations and its own tolerance on the deflection of the pile. When the limit on the number of iterations of the group is reached without convergence, the case is reported as not converged together with its last iterate, which is not a solution.

2.3.5 Load steps

A strongly nonlinear problem may not converge when the full load is applied at once. The load is then applied in steps. The load factor λ starts at zero; a step of size $\Delta\lambda$, initially the *initial step* of the load case, is attempted from the last converged state. A step that converges is accepted ($\lambda \leftarrow \lambda + \Delta\lambda$); a step that fails is halved and attempted again. When the step would become smaller than the *minimum step*, the analysis stops. If the full load ($\lambda = 1$) is not reached, the results of the last converged load factor are reported together with the fraction of the load they represent. All loads of the case – cap loads, loads along the piles, soil movements and prescribed displacements – are scaled by the same factor. With the default initial and minimum steps of 1, the load is applied at once.

2.3.6 Prescribed movements

Any degree of freedom of the cap can be controlled by a prescribed displacement or rotation instead of a force. The prescribed components are removed from the unknowns of (2.8), and the reaction needed to impose them is part of the result.

2.4 Flexible cap

When the stiffness of the cap is not large compared with that of the piles, the cap deforms and the piles under its stiffer parts receive more load. A flexible cap is represented by a mesh of quadrilateral plate elements in the mid-plane of the cap, at the elevation of the cap, with the thickness of the cap section and the elastic properties of its material. Every node of the mesh has six degrees of freedom: three translations and three rotations.

2.4.1 Plate elements

Each element combines two actions:

- **Bending.** The plate follows the theory of Reissner and Mindlin, in which the deflection w and the rotations of the normal are independent, so that transverse shear deformation is included and thick caps are described correctly. With the curvatures $\boldsymbol{\kappa}$ and the shear strains $\boldsymbol{\gamma}$, the moments and shear forces per unit width are

$$\mathbf{m} = \begin{pmatrix} m_{xx} \\ m_{yy} \\ m_{xy} \end{pmatrix} = \frac{E\,t^3}{12(1-\nu^2)} \begin{bmatrix} 1 & \nu & 0 \\ \nu & 1 & 0 \\ 0 & 0 & \frac{1-\nu}{2} \end{bmatrix} \boldsymbol{\kappa}, \qquad \mathbf{q} = \begin{pmatrix} q_x \\ q_y \end{pmatrix} = \kappa_s\, G\, t\, \boldsymbol{\gamma} \tag{2.10}$$

with the thickness t, Young's modulus E, Poisson's ratio ν, the shear modulus G and the shear correction factor κ_s = 5/6. The element interpolations follow Ibrahimbegovic (1993), which avoids shear locking of thin plates.

- **Membrane.** The in-plane forces n_{xx}, n_{yy} and n_{xy} follow plane-stress elasticity. The membrane element of Ibrahimbegovic, Taylor and Wilson (1990) includes a rotation about the normal (drilling rotation) at every node, so that the in-plane rotation of the cap is resisted and the pile heads can transmit torsion and moments in all directions to the cap.

2.4.2 Connection of the piles and solution

Each pile head is connected to a node of the mesh and moves with it according to its head connection. The plate mesh is linear; the piles are nonlinear. The degrees of freedom of the nodes without piles are eliminated by static condensation, and the equilibrium of the remaining nodes with the forces of their piles is solved by the iteration of (2.8), now with the condensed plate stiffness added to the stiffness of the pile heads. The movements of the other nodes and the forces in the plates follow from the converged movement of the pile nodes. Loads act at points of the cap and as distributed pressures on selected plates.

© 2026 Solplan. All rights reserved.

2.4.3 Mesh

The mesh is generated on a grid of lines in plan that pass through every pile head, every corner of the cap outline and every point load on the cap, so that these points are nodes of the mesh. Each interval between two grid lines is divided into equal parts no longer than the element size chosen by the user, and the cells whose centre lies inside the outline form the mesh; the edge of a cap that is not rectangular is therefore stepped at the scale of the element size. A finer mesh describes the bending of the cap more accurately; the mesh is fine enough when a further refinement does not change the pile-head forces noticeably. The model check warns when the stored mesh no longer matches the outline of the cap, the positions of the piles or the cap section.

2.5 Loads

Table 2.2 — Loads and how they enter the analysis

Load	Treatment
Point forces and moments on the cap	Reduced to the reference point of a rigid cap, including the moment of a force applied away from it; applied at its own node of a flexible cap.
Point forces and moments at a joint	Act on the cap at the position of the joint (for example a pile head or a reference point), and are reduced to the reference point like other cap loads.
Distributed load on cap plates	A pressure on the selected plates of a flexible cap.
Distributed lateral load along a pile	The load $w(x)$ of (4.1) over a part of the pile, in global or local directions; an axial component is added to the axial force along the pile.
Point force along a pile	A concentrated force at a point of the pile, applied at a node of the difference mesh.
Free-field soil movement	A horizontal movement of the ground that loads the piles through the soil (Section 4.1.7).

NOTE The weight of the piles is not applied: it is close to the weight of the soil the piles replace. The weight of the cap is applied as a vertical load at the cap through the Self weight multiplier of a load pattern: the weight per unit volume of the cap material × the cap thickness × its plan area, times the multiplier summed over the patterns of the load case. Check Model reports a multiplier that adds nothing because the cap material has no unit weight.

2.6 Load cases and combinations

A load case multiplies its load patterns by scale factors and is analysed as one nonlinear problem. It also sets the soil behaviour (static or cyclic, with the number of cycles), the control of each degree of freedom of the cap, the limits and tolerances of the iteration and the load steps. Every load case starts from the unloaded state.

Because the response is nonlinear, the results of load cases cannot in general be superposed. A *Linear Add* combination is therefore analysed again with the sum of its factored loads; its result is the response to those loads, not the sum of the results of its members. An *Envelope* combination reports, for every quantity, the largest and the smallest value among its members, together with the member that gives each extreme. The extremes of different quantities may come from different members, so that a row of an envelope is not a state that occurs in any one case.

2.7 Axial force along the piles

The axial thrust P_x in the beam-column equation of a pile is, by default, the axial force at the head of the pile, constant along its length. When the variation of the axial force along the piles is included, the thrust at each node is the head force reduced by the shaft resistance mobilised above that node, as given by the axial analysis of the pile. The difference matters for long piles carrying large axial loads, where the second-order moment $P_x \cdot y$ is significant.

© 2026 Solplan. All rights reserved.

3 The pile group in the analysis of the structure

3.1 Foundation and superstructure

A bridge pier, a building or a jetty rests on its pile groups, and the forces in the structure depend on the stiffness of the foundations as much as the forces in the piles depend on the loads from the structure. For a statically indeterminate structure, a foundation that is stiffer or softer than assumed changes the distribution of the moments in the structure; for a pier or a jetty deck, the flexibility of the piles can govern the lateral sway and the natural period. The analysis of the structure and the analysis of the foundation should therefore be consistent: the springs that represent the foundation in the structural model must correspond to the loads that the structure applies to the foundation.

Because the response of the piles is nonlinear, no single set of springs is valid for every load. A practical procedure is iterative:

1. Estimate the loads at the base of the structure, for example from an analysis with fixed supports.
2. Analyse the pile group under these loads and compute its stiffness at the corresponding level of loading (Chapter 12).
3. Represent the foundation in the structural model by the 6×6 stiffness matrix, or by its diagonal terms where the structural program accepts only uncoupled springs, and analyse the structure again.
4. Repeat with the new base loads until the loads and the stiffness change by less than a chosen tolerance. One or two cycles are usually enough, because the stiffness of a group changes slowly with the load at working levels.
5. Analyse the pile group under the final base loads to obtain the forces, moments and displacements of the piles for their design.

For each load case or combination of the structure the procedure gives a stiffness matched to its own level of loading. Where many load cases must be analysed, the stiffness can be computed at the levels of the governing cases and the case with the largest loads used to check that the stiffness assumed for the others is not unconservative.

3.2 Coupling of translation and rotation

The stiffness matrix of a pile group is generally full. A horizontal force at the reference point of the cap produces, besides the horizontal translation, a rotation of the cap about the horizontal axis, because the soil resists the movement of the piles mostly near the ground surface and the resultant of the soil resistance lies below the cap. How much the coupling matters depends on the foundation. It is measured by $\rho = |K_{15}| \,/\, \sqrt{(K_{11}K_{55})}$; under a horizontal force alone the diagonal terms underestimate the horizontal movement by the factor $1 - \rho^2$. For a single pile of the examples (0.6 m diameter, head fixed to the cap, under 100 kN horizontal, 300 kN vertical and 60 kN·m) $\rho = 0.38$ and the true movement is 17% larger than the diagonal terms give. For the 3 × 3 group of the examples, whose rotational stiffness comes mostly from the axial stiffness of the piles, $\rho = 0.09$ and the difference is 0.8%. Replacing the matrix by its diagonal is therefore acceptable for a group of several rows of vertical piles, but not for a single pile or a single row loaded across it. If the structural program requires uncoupled springs, the reference point can be moved down by K_{15}/K_{11} (1.40 m for the single pile, 0.77 m for the group), where the coupling vanishes, or the effect of the coupling estimated by comparing the movements of the two representations under the governing loads.

3.3 An isolated pile under combined loads

A single pile under a combination of axial load, shear, moment and torque is a group of one pile. The axial thrust interacts with the bending through the beam-column action of the pile (Chapter 4), and the head forces follow from the connection of the pile to the structure. Analysing a single pile as a group gives the same response as an analysis of the pile alone, and lets the pile be connected to a cap whose movement is controlled by the structure, for example by specified displacements of the cap.

© 2026 Solplan. All rights reserved.

3.4 Dynamic and seismic analyses

The stiffness computed by Solgroup is a static secant stiffness. For a dynamic analysis of the structure it represents the foundation at the level of deformation of the earthquake or of the dynamic load considered, without the damping of the soil and without the frequency dependence of the stiffness of the foundation. Where the inertial interaction between the structure and the foundation is important, the stiffness should be computed at the level of the expected displacements, and its effect on the period of the structure checked. The pushover analysis of a group (Chapter 12) shows the capacity and the deformation of the foundation beyond the elastic range and is used in displacement-based seismic design of the foundation.

© 2026 Solplan. All rights reserved.

4 Analysis of a single pile

Within the group analysis every pile is analysed as a single pile whose head movement is imposed by the cap (Section 2.3). This chapter describes the three single-pile analyses: lateral, axial and torsional.

4.1 Lateral response

4.1.1 Governing equation

In each of its two bending planes a pile is a beam-column supported by nonlinear soil springs (Hetényi, 1946; Reese and Van Impe, 2011). The equilibrium of an element of length dx gives

$$\frac{d^2}{dx^2}\left(EI\,\frac{d^2y}{dx^2}\right) + P_x\,\frac{d^2y}{dx^2} - p(y,x) - w(x) = 0 \tag{4.1}$$

where x is the distance along the pile from the head, y the lateral deflection, EI the bending stiffness, P_x the axial thrust (compression positive), p the soil reaction per unit length, which opposes the deflection, and w a distributed load along the pile. The soil reaction is given by the p-y curve of the soil at depth x (Chapter 5). The slope, moment and shear force follow from the deflection:

$$S = \frac{dy}{dx}, \qquad M = EI\,\frac{d^2y}{dx^2}, \qquad V = \frac{dM}{dx} + P_x\,\frac{dy}{dx} \tag{4.2}$$

The two bending planes of a pile are its local planes 1-2 and 1-3. The deflection in the direction of local axis 2 is resisted by the bending stiffness EI_{33} of the section, and the deflection in the direction of local axis 3 by EI_{22}. The two planes are analysed separately, each with the head movement of that plane; for a section that is not circular the two stiffnesses differ.

4.1.2 Finite-difference discretisation

The pile is divided into N increments of equal length $h = L/N$ with nodes $m = 0$ (head) to N (tip); the number of increments is a property of each pile. Two imaginary nodes are added beyond each end to express the boundary conditions (Figure 4.1).

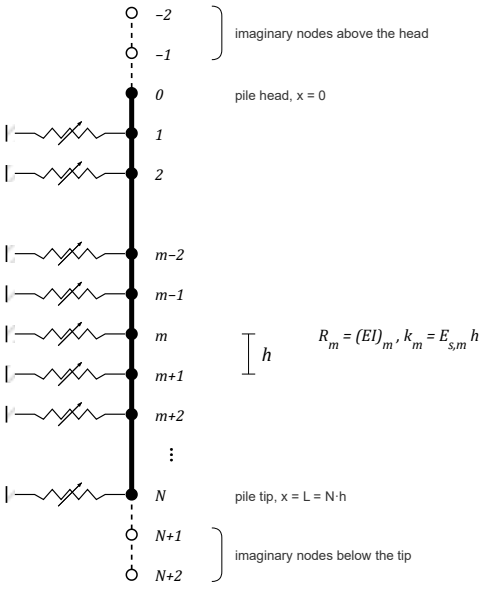

Figure 4.1 — Nodes of the finite-difference model of a pile

With $R_m = (EI)_m$ and the secant modulus of the soil $E_{s,m} = p_m/y_m$, central differences applied to (4.1) at node m give

© 2026 Solplan. All rights reserved.

$$R_{m-1}\,y_{m-2} + \left(-2R_{m-1} - 2R_m + P_x h^2\right) y_{m-1} + \left(R_{m-1} + 4R_m + R_{m+1} - 2P_x h^2 + E_{s,m} h^4\right) y_m + \left(-2R_m - 2R_{m+1} + P_x h^2\right) y_{m+1} + R_{m+1}\,y_{m+2} = W_m\,h^4 \tag{4.3}$$

where W_m is the distributed load at node m. At the ends the stiffness of the imaginary nodes equals that of the adjacent real node. The resulting system is banded and is solved directly.

4.1.3 Boundary conditions

At the head, the cap imposes the deflection y_t and, depending on the connection (Table 2.1), the slope, a zero moment or an elastic rotational restraint:

$$y_0 = y_t, \qquad \begin{cases} S_0 = \theta_t & \text{fixed} \\ M_0 = 0 & \text{pinned} \\ M_0 = k_\theta\,(\theta_t - S_0) & \text{elastically restrained} \end{cases} \tag{4.4}$$

where θ_t is the rotation of the cap in the plane considered. With central differences,

$$M_0 = \frac{R_0}{h^2}\left(y_{-1} - 2y_0 + y_1\right), \qquad S_0 = \frac{y_1 - y_{-1}}{2h} \tag{4.5}$$

At the tip the moment and the shear force are zero:

$$M_N = 0, \qquad V_N = 0 \tag{4.6}$$

The head shear and moment of the pile are recovered from the solution and are the forces the pile exerts on the cap.

4.1.4 Iteration

The nonlinearity of the soil, and of the bending stiffness of nonlinear sections, is treated by secant iteration:

1. Initial secant moduli are taken from the initial branch of each p-y curve.
2. The linear system is solved for the deflections.
3. At every node the secant modulus is updated from the p-y curve at the new deflection; for nonlinear sections the bending stiffness is updated from the moment–curvature relation at the new moment (Chapter 9).
4. Steps 2 and 3 are repeated until the largest change of nodal deflection between two iterations is smaller than the tolerance on the pile deflection, or until the iteration limit for a single pile is reached.

A curve whose secant modulus is unbounded at zero deflection is given a finite modulus in the range of very small deflections, so that nodes with negligible deflection are well conditioned. This does not affect the curve in the range of practical deflections.

4.1.5 Axial thrust

The axial thrust P_x is the axial force of the pile, which reduces its lateral stiffness when it is compressive (second-order effect $P_x \cdot y$). By default the axial force at the head is used over the whole length; optionally the thrust varies along the pile with the axial force from the axial analysis (Section 2.7). A pile in tension is stiffened by its axial force in the same way.

4.1.6 Loads along the pile

A distributed load $w(x)$ acts between two elevations of the pile, with linear variation between its values at the top and at the bottom. It is given in a local direction of the pile or in a global direction. A global load on a battered pile is resolved into the two bending planes and a part parallel to the pile axis; that part is integrated and applied as an axial force at the head when its inclusion is chosen, and is otherwise neglected. A point force along the pile, given by its elevation and its three global components, is applied at a node of the difference mesh placed at that elevation.

© 2026 Solplan. All rights reserved.

4.1.7 Free-field soil movement

A free-field soil movement $y_s(x)$ is a horizontal movement of the ground that would occur without the piles, for example next to an embankment, a slope or an excavation. It is given as a profile of horizontal movements in the two global horizontal directions (or in the local directions 2 and 3 of the pile) against depth below the ground surface, linearly interpolated between its points, and is assigned to piles and to a load pattern. The soil reaction then depends on the movement of the pile relative to the soil:

$$p = p\left(y - y_s(x),\ x\right) \tag{4.7}$$

and (4.1) is solved with this reaction. Where the soil moves more than the pile, the soil drives the pile; where it moves less, the soil resists. The movement may act on the piles alone, without any load on the cap, and then gives the forces that the moving ground induces in the foundation.

4.1.8 Lateral reduction factors along the depth

When the lateral reduction along depth is switched on in the analysis options, the soil resistance of a pile can be reduced by factors that vary along the pile. A reduction set lists, at depths measured vertically below the global elevation zero (along the pile from its head for piles with user-defined p-y curves), a p-factor P and a y-factor Y; at a node the soil reaction is multiplied by P/Y, with both factors interpolated linearly between the points of the set and equal to 1 outside its range. The factors act together with the group factors of Chapter 7.

4.2 Axial response

4.2.1 Load-transfer method

The axial response of a pile is that of a column supported by springs along its shaft and at its tip. The shaft resistance per unit length is a function $t(z, x)$ of the local movement z of the pile relative to the soil, and the tip resistance a function $Q(w)$ of the movement of the tip (Chapter 6). The equilibrium of an element of the pile gives

$$\frac{d}{dx}\left(EA\,\frac{du}{dx}\right) = t(u, x) \tag{4.8}$$

with the axial displacement u (positive towards the tip) and the axial stiffness EA. Solgroup solves (4.8) by the load-transfer method of Coyle and Reese (1966), as described by Reese, Isenhower and Wang (2006):

1. A movement w_N of the tip is chosen, and the tip force $Q_N = Q(w_N)$ follows from the tip curve.
2. Moving up the pile one increment at a time, the movement at the middle of the increment is estimated, the shaft resistance $t \cdot h$ at that movement is added to the axial force, and the shortening of the increment under the average force, $\Delta u = F_{avg} \cdot h/EA$, is added to the movement. Each increment is iterated until the movement at its middle no longer changes.
3. At the head this gives one point (head movement, head force) of the load–displacement curve.

Repeating the procedure for a series of tip movements gives the axial load–displacement (L-D) curve of the pile head. In uplift the shaft resistance acts with the same magnitude in the opposite direction, and the tip carries no resistance.

4.2.2 Use in the group analysis

The L-D curve is the axial spring of the pile head: the axial force for a given axial movement of the head is interpolated linearly on the curve. A curve can also be entered by the user for a pile, in place of the curve generated from the soil. When the axial movement of a head passes the last point of its curve, the pile has reached its axial capacity. By default it then carries no axial load at all and the run reports an apparent failure in bearing; when the curves are extended beyond their last point, the axial force is held at the value of the last point.

A reduction factor on the axial resistance of a pile multiplies its L-D curve (Section 7.7).

© 2026 Solplan. All rights reserved.

4.3 Torsional response

A pile resists a rotation about its own axis by the shaft friction acting on its perimeter. The torque per unit length of the shaft is the unit shaft resistance multiplied by the perimeter and the radius of the pile, at the tangential movement $r\theta$ of the shaft surface. The torque–rotation (T-R) curve of the pile head is found by the same marching procedure as the axial curve, with the torsional stiffness GJ of the section in place of EA, the rotation of the section in place of the axial movement, and no torsional resistance at the tip (Stoll, 1972; Reese and Van Impe, 2011). A T-R curve can also be entered by the user.

The torque of a pile head follows from its T-R curve at the torsional rotation of the head. A pile whose head is pinned in both bending planes carries no torque. In a group under horizontal load the torsional resistance of the individual piles is usually small compared with the resistance that the lateral forces of the piles give against a rotation of the cap about the vertical axis.

© 2026 Solplan. All rights reserved.

5 Soil response: p-y curves

5.1 General

A p-y curve gives the soil reaction p (force per unit length of pile) as a function of the lateral deflection y at one depth. Solgroup generates a curve at every node from the soil material of the layer that contains the node, the pile width b at that node, the depth and the vertical effective stress. Representative curves of the main models are shown in Figure 5.1.

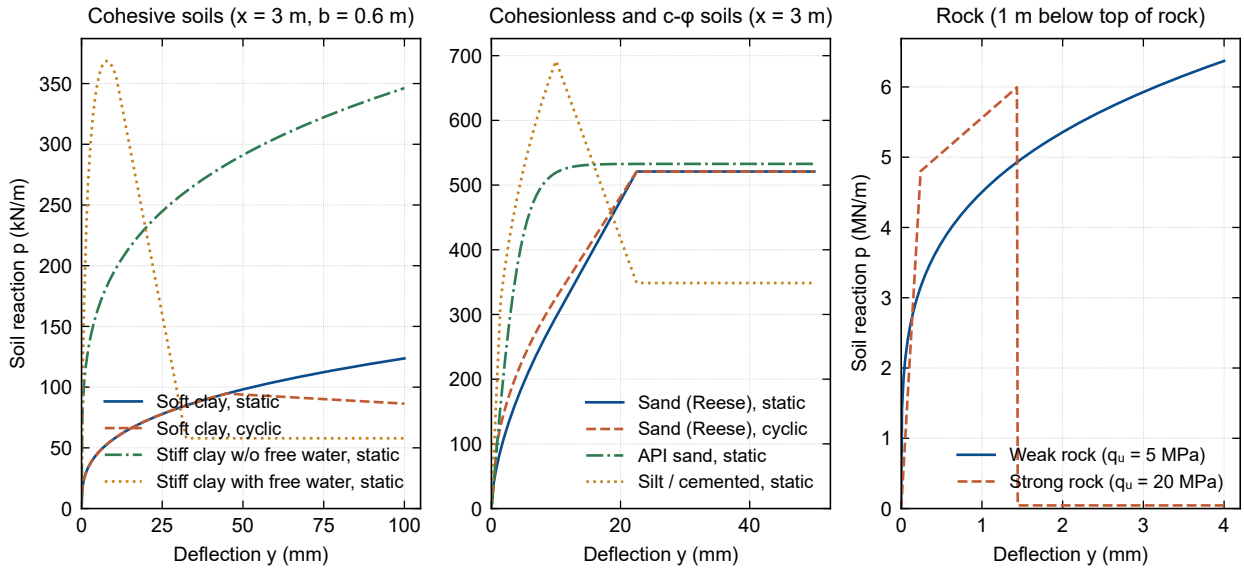

Figure 5.1 — p-y curves of the main models, computed by Solgroup for b = 0.6 m

5.1.1 Effective stress

The vertical effective stress is integrated from the ground surface:

$$\sigma'_v(x) = \int_0^x \gamma'(\zeta)\, d\zeta, \qquad \gamma' = \gamma \text{ above the water table}, \quad \gamma' = \gamma_{sat} - \gamma_w \text{ below} \tag{5.1}$$

with γ_w = 9.81 kN/m^3. In the expressions for the ultimate resistance of the shallow soil wedge, γ' denotes the average effective unit weight σ'_v/x. Depths in this chapter are measured below the ground surface.

5.1.2 Static and cyclic curves

Each model provides a static curve and, where the model defines one, a cyclic curve. The choice is made for each load case (its soil behaviour), with the default set in the analysis options.

Figure 5.2 compares the static and cyclic curves of the clay and sand models at a depth of 2 m below the top of a layer that starts at the ground surface (pile width 0.6 m, γ = 18 kN/m^3, no water table, 100 cycles where the model uses the number). The effect of cyclic loading differs between the models:

- In soft clay the cyclic curve is limited to $0.72p_u$ (66 against 86 kN/m at 2 m within the deflections shown). Above the transition depth x_r the resistance then falls with further deflection (56 kN/m at 100 mm); below it, as at 6 m, it stays at $0.72p_u$.
- Stiff clay with free water loses most of its resistance at large deflections even under static load, and cyclic loading reduces both the peak (198 against 366 kN/m) and the residual resistance; this is the effect of the scour of the clay by water pumped in and out of the gap behind the pile.
- Stiff clay without free water is reduced less (237 against 288 kN/m), because the clay is not washed away.
- In sand the cyclic curve of the Reese criterion is somewhat lower (267 against 290 kN/m). In the API criterion the factor A of the static curve, $3 - 0.8x/b$, cannot fall below the cyclic value 0.9, so below a depth of $2.625b$ the

© 2026 Solplan. All rights reserved.

static and cyclic curves coincide, as at 2 m here.

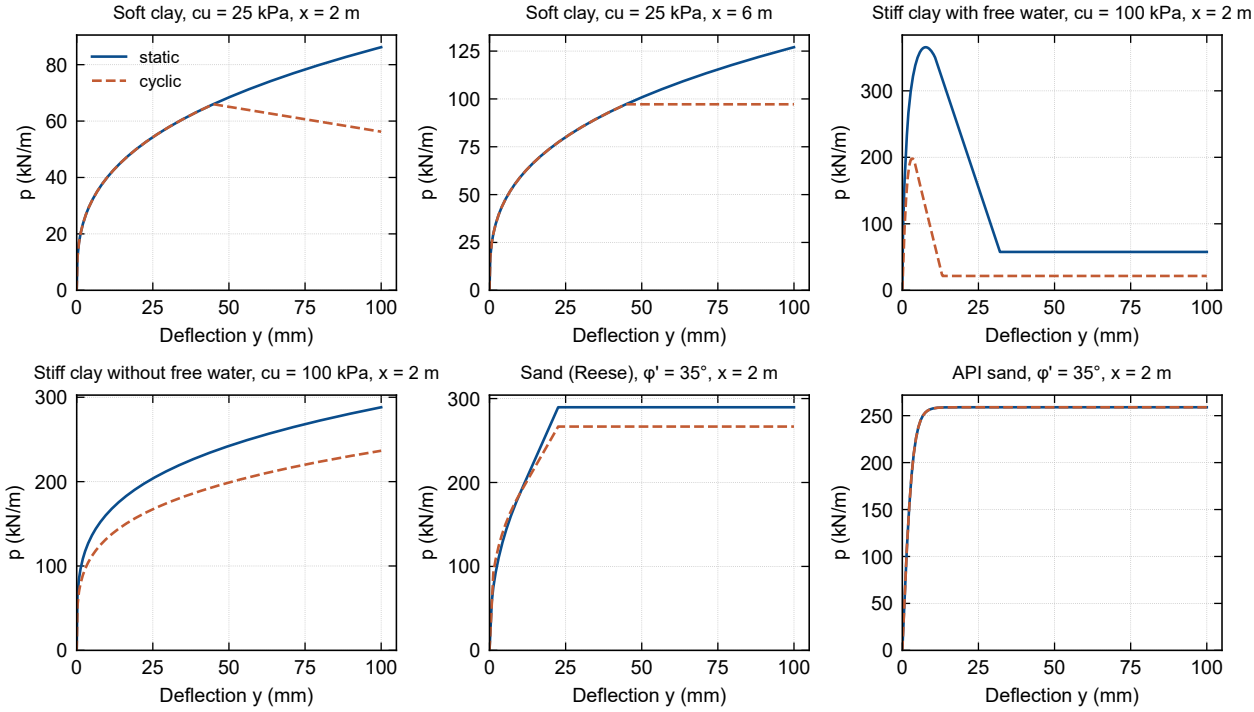

Figure 5.2 — Static (solid) and cyclic (dashed) p-y curves of the clay and sand models

5.1.3 Nature of loading

The response of soil to lateral load depends on how the load is applied (Reese and Van Impe, 2011):

- **Static loading** is applied once, slowly, as for dead loads and for loads of short duration that are applied only a few times. The static curves of the models apply.
- **Repeated (cyclic) loading**, from waves, wind, traffic or berthing ships, degrades the soil near the ground surface. In clay below free water the soil may be scoured away from the pile by the pumping action of water in the gap that opens behind the pile. The cyclic curves of the models represent the response after many cycles of load; they are not the result of a cyclic analysis. For the models whose cyclic curves depend on the number of cycles, that number is given with the load case.
- **Sustained loading**, as from earth pressure, can cause creep and consolidation of soft clay, which increase the deflections with time. The curves do not include this effect; it can be estimated by reducing the stiffness of the curves near the surface, for example with p-multipliers.
- **Dynamic loading**, as from earthquakes or machinery, involves inertia and damping, which a static analysis does not include. A static analysis with appropriate curves (for example for liquefied sand) and with the soil movements and loads of the event can be used as a simplified approach.

5.1.4 Ultimate resistance and depth

Near the ground surface the soil in front of a pile fails as a wedge that moves up and out; deeper, it flows around the pile in horizontal planes. The ultimate resistance of the criteria is the smaller of the two mechanisms, so that it grows quickly with depth near the surface and more slowly, or not at all, below the transition (Figure 5.3). For soft clay with c_u = 25 kPa and a pile of 0.6 m, the resistance increases from 68 kN/m at 1 m to the flow-around value $9c_u b$ = 135 kN/m, which is reached at the transition depth 3.86 m. In sand the resistance grows with the effective overburden stress at every depth, 151 kN/m at 1 m, 1,339 kN/m at 5 m and 5,030 kN/m at 10 m for φ' = 35°. Because the response of a laterally loaded pile is governed by the upper few diameters, where the resistance is small and grows quickly, the parameters of the soil near the surface matter most.

© 2026 Solplan. All rights reserved.

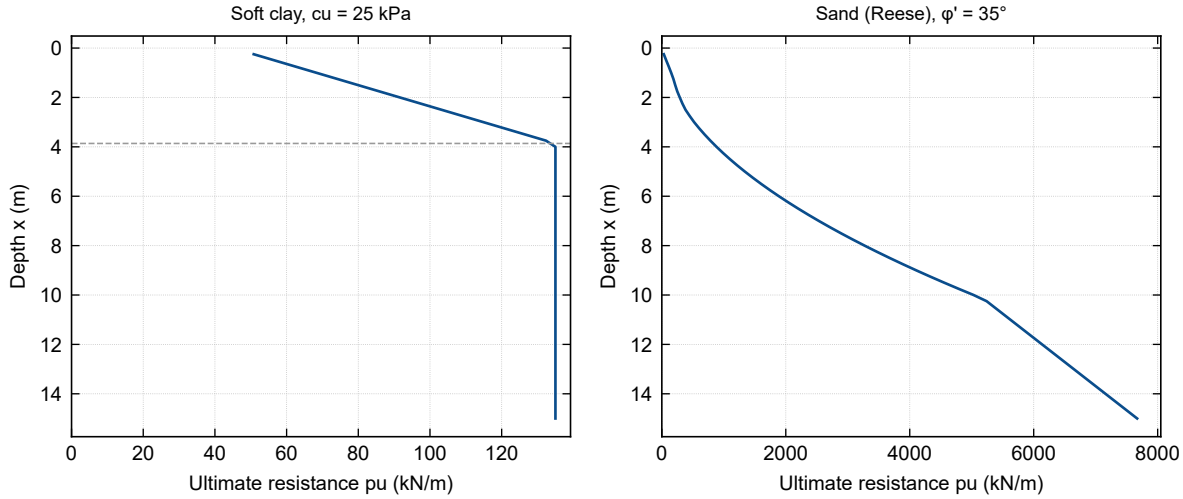

Figure 5.3 — Ultimate soil resistance against depth for soft clay and sand, pile width 0.6 m

5.1.5 Soil parameters and recommended tests

The quality of a p-y analysis depends on the soil parameters more than on any other input. The following table lists the main parameters of each family of models and the tests from which they are usually obtained.

Table 5.1 — Main parameters of the soil models and their sources

Models	Parameters	Usual sources
Soft and stiff clays	undrained shear strength c_u, ε_{50}, unit weight, k	unconsolidated-undrained triaxial tests on good-quality samples (c_u and ε_{50}, the strain at half the peak deviator stress); field vane and cone penetration tests for the profile of c_u; lateral load tests for k
Sands	friction angle φ', unit weight, k	correlations with the standard penetration test and the cone penetration test; triaxial tests on reconstituted samples; relative density
Liquefied sand	corrected blow count $(N_1)_{60\text{-}cs}$ or residual strength	standard penetration test with corrections for overburden, energy and fines content; liquefaction assessment
Silt / c-φ soils	c, φ', ε_{50}, k	consolidated-drained or consolidated-undrained triaxial tests
Weak and strong rock	q_u, E_{ir}, RQD, k_{rm}	unconfined compression tests on rock cores, core logging (RQD), pressuremeter or dilatometer tests for the modulus
Massive rock	q_u (σ_{ci}), m_i, GSI, E_i or E_m, v	unconfined compression tests, rock-mass classification (GSI) from core and exposures, published values of m_i for the rock type
Piedmont residual soil	one of N_{60}, q_c, E_D, E_M	standard penetration, cone penetration, flat dilatometer or Ménard pressuremeter test
Loess	cone tip resistance q_c	cone penetration test

Where a lateral load test on a pile at the site is available, the parameters should be adjusted until the computed response of the test pile matches the measured response, and the adjusted parameters used for the design piles.

5.1.6 Variants and options

Several models exist in variants that differ only in one parameter or in an initial straight branch; they are described with their parent model. The p-y curves of a node are modified afterwards by the layering correction (Section 5.13), by the group factors (Chapter 7) and by the lateral reduction factors along the depth (Chapter 4). For a battered pile

© 2026 Solplan. All rights reserved.

the depth used for the curves is, by default, measured vertically below the ground surface; when the option *Adjust Depth for Batter Piles* is off, it is measured along the pile.

5.2 Soft clay

Basis: Matlock (1970). The empirical factor J is 0.5 for the model *Soft Clay (Matlock)*; it is entered for the model *Soft Clay (API), User J* (API, 2000), whose default is 0.25, and for *Mod. Soft Clay with Initial k*, whose default is 0.5. Values from 0.25 to 0.5 are usual. The ultimate resistance is the smaller of the wedge and flow-around values:

$$p_u = \min\left[\left(3 + \frac{\gamma' x}{c_u} + \frac{J\,x}{b}\right) c_u\, b,\;\; 9\, c_u\, b\right] \tag{5.2}$$

$$y_{50} = 2.5\,\varepsilon_{50}\, b \tag{5.3}$$

Static loading:

$$p = 0.5\, p_u \left(\frac{y}{y_{50}}\right)^{1/3} \quad (y \le 8\, y_{50}), \qquad p = p_u \quad (y > 8\, y_{50}) \tag{5.4}$$

Cyclic loading: the curve follows the static curve up to $0.72 p_u$ at $y = 3y_{50}$ (precisely $0.5 \cdot 3^{1/3} = 0.7211$). Below the transition depth

$$x_r = \frac{6\, c_u\, b}{\gamma' b + J\, c_u} \;\ge\; 2.5\, b \tag{5.5}$$

the resistance remains $0.72 p_u$ beyond $3y_{50}$. Above it, the resistance decreases linearly from $0.72 p_u$ at $3y_{50}$ to $0.72 p_u \cdot x/x_r$ at $15y_{50}$ and remains constant thereafter.

Modified soft clay with initial k. The curve of the model *Mod. Soft Clay with Initial k* is the Matlock curve limited by an initial straight line whose slope increases linearly with depth, $p = k\, x\, y$; it avoids the infinite initial stiffness of the cubic parabola. k and ε_{50} may be entered as zero to have them estimated from c_u (Section 5.14).

The criterion was derived from lateral load tests on instrumented steel pipe piles in soft clay below the water table in Texas, under static and cyclic loading (Matlock, 1970). The soil reaction along the piles was obtained from the measured bending moments, and the curves were fitted with the undrained shear strength and the strain ε_{50} of laboratory tests. The criterion is intended for normally consolidated and lightly overconsolidated clays; the variants with a user-defined J or an initial straight branch of slope $k\,x$ keep the same ultimate resistance.

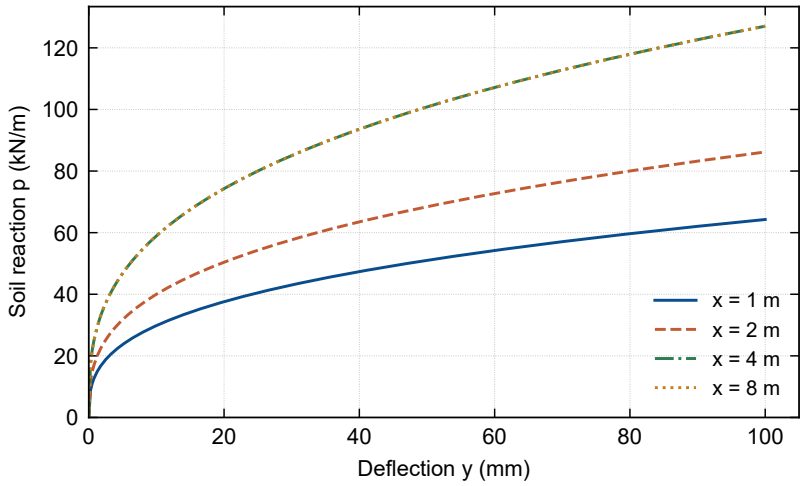

Figure 5.4 — p-y curves of soft clay (c_u = 25 kPa, static), computed for a pile of 0.6 m width at four depths below the top of the layer

© 2026 Solplan. All rights reserved.

5.3 Stiff clay with free water

Basis: Reese, Cox and Koop (1975). The ultimate resistance is

$$p_c = \min\left[2\,c_a\,b + \gamma' b\,x + 2.83\,c_a\,x,\;\; 11\,c\,b\right] \tag{5.6}$$

where c is the undrained shear strength at the depth considered and c_a the average value over the depth of the wedge, which equals c in a layer of uniform strength. With $y_{50} = \varepsilon_{50} b$ and the empirical coefficients $A_s(x/b)$ (static) and $A_c(x/b)$ (cyclic), which Solgroup evaluates from tabulated representations of the published charts, the static backbone curve is

$$p = 0.5\,p_c\left(\frac{y}{y_{50}}\right)^{0.5} \qquad (y \le A_s y_{50}) \tag{5.7}$$

$$p = 0.5\,p_c\left(\frac{y}{y_{50}}\right)^{0.5} - 0.055\,p_c\left(\frac{y - A_s y_{50}}{A_s y_{50}}\right)^{1.25} \qquad (A_s y_{50} < y \le 6A_s y_{50}) \tag{5.8}$$

$$p = 0.5\,p_c\sqrt{6A_s} - 0.411\,p_c - \frac{0.0625}{y_{50}}\,p_c\left(y - 6A_s y_{50}\right) \qquad (6A_s y_{50} < y \le 18A_s y_{50}) \tag{5.9}$$

$$p = p_c\left(0.5\sqrt{6A_s} - 0.75\,A_s - 0.411\right) \qquad (y > 18A_s y_{50}) \tag{5.10}$$

For cyclic loading, with $y_p = 4.1 A_s y_{50}$,

$$p = A_c\,p_c\left[1 - \left|\frac{y - 0.45\,y_p}{0.45\,y_p}\right|^{2.5}\right] \qquad (y \le 0.6\,y_p) \tag{5.11}$$

$$p = 0.936\,A_c\,p_c - \frac{0.085}{y_{50}}\,p_c\left(y - 0.6\,y_p\right) \qquad (0.6\,y_p < y \le 1.8\,y_p) \tag{5.12}$$

$$p = p_c\left(0.936\,A_c - 0.102 \cdot 4.1\,A_s\right) \qquad (y > 1.8\,y_p) \tag{5.13}$$

In both cases the curve is limited by the initial straight line $p = k\,x\,y$, where k is the initial modulus gradient: p = min(kxy, backbone).

The criterion was derived from tests on instrumented steel pipe piles of 610 mm diameter in overconsolidated stiff clay with water standing above the ground surface (Reese, Cox and Koop, 1975). Under cyclic loading the clay near the surface lost much of its resistance: a gap opened behind the pile and water pumped in and out of it eroded the clay. The cyclic curves represent this degradation, and the criterion is recommended where free water can reach the ground surface, for example offshore and at river crossings.

© 2026 Solplan. All rights reserved.

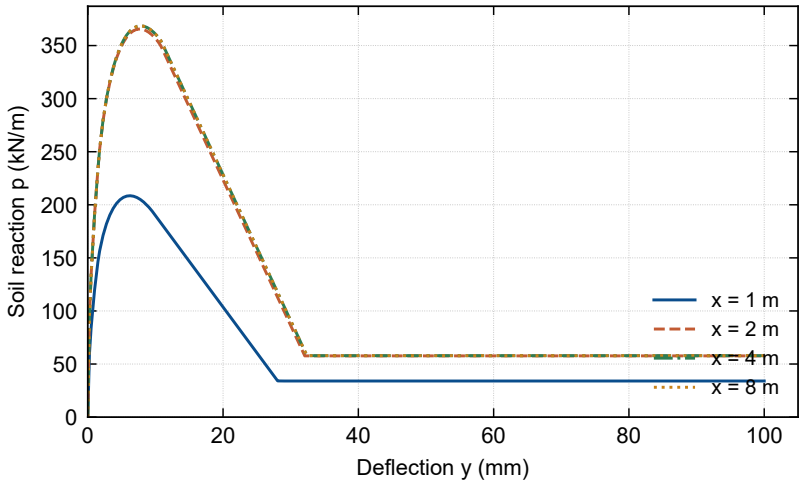

Figure 5.5 — p-y curves of stiff clay with free water (c_u = 100 kPa, static), computed for a pile of 0.6 m width at four depths below the top of the layer

5.4 Stiff clay without free water

Basis: Welch and Reese (1972). With

$$p_u = \min\left[\left(3 + \frac{\gamma' x}{c} + 0.5\,\frac{x}{b}\right) c\,b,\;\; 9\,c\,b\right], \qquad y_{50} = 2.5\,\varepsilon_{50}\,b \tag{5.14}$$

the static curve is

$$p = 0.5\,p_u \left(\frac{y}{y_{50}}\right)^{1/4} \quad (y \le 16\,y_{50}), \qquad p = p_u \quad (y > 16\,y_{50}) \tag{5.15}$$

For cyclic loading with N cycles the deflection at a given resistance increases, and the curve becomes

$$p = p_u \left(\frac{y}{y_{50}\,(16 + 9.6\log_{10} N)}\right)^{1/4} \le p_u \tag{5.16}$$

which reduces to (5.15) for N = 1.

Stiff clay with user k. The model *Stiff Clay with User k* uses the same curve, limited by the initial line $p = kxy$ with the modulus gradient k entered by the user. k should come from a lateral load test at the site.

The criterion was derived from tests on an instrumented drilled shaft in stiff clay above the water table (Welch and Reese, 1972). Without free water the clay does not erode under repeated loading, and the curves keep the shape of the soft-clay criterion with a flatter exponent. The variant with a user-defined k adds an initial straight branch whose slope should come from a lateral load test.

© 2026 Solplan. All rights reserved.

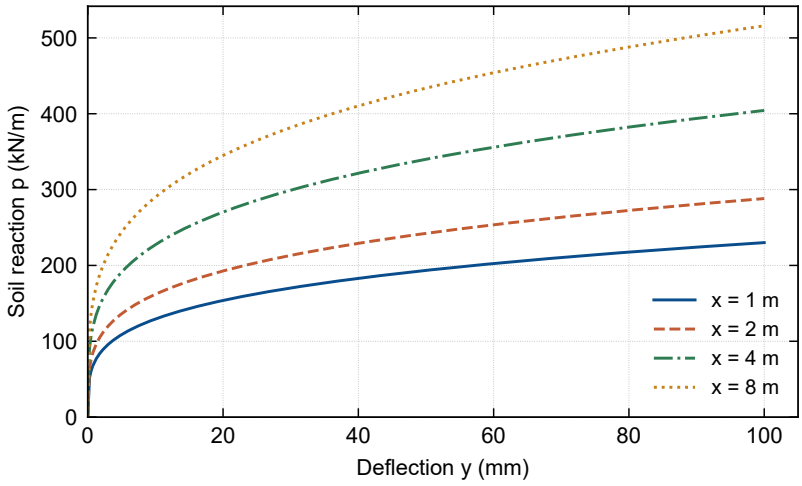

Figure 5.6 — p-y curves of stiff clay without free water (c_u = 100 kPa, static), computed for a pile of 0.6 m width at four depths below the top of the layer

5.5 Sand (Reese)

Basis: Reese, Cox and Koop (1974). With $\alpha = \varphi'/2$, $\beta = 45° + \varphi'/2$, $K_0 = 0.4$ and $K_a = \tan^2(45° - \varphi'/2)$, the resistances of the shallow wedge and of flow around the pile at depth are

$$p_{st} = \gamma' x \left[\frac{K_0\, x \tan\varphi' \sin\beta}{\tan(\beta-\varphi')\cos\alpha} + \frac{\tan\beta}{\tan(\beta-\varphi')}\left(b + x\tan\beta\tan\alpha\right) + K_0\, x \tan\beta\left(\tan\varphi' \sin\beta - \tan\alpha\right) - K_a\, b \right] \tag{5.17}$$

$$p_{sd} = K_a\, b\, \gamma' x \left(\tan^8\beta - 1\right) + K_0\, b\, \gamma' x \tan\varphi' \tan^4\beta \tag{5.18}$$

and $p_s = \min(p_{st}, p_{sd})$. The curve consists of four parts (Figure 5.1):

1. an initial straight line $p = kxy$;
2. a parabola $p = C\, y^{1/n}$ between the intersection with the initial line, at $y_k = (C/kx)^{n/(n-1)}$, and point m;
3. a straight line from point m ($y_m = b/60$, $p_m = B\, p_s$) to point u ($y_u = 3b/80$, $p_u = A\, p_s$);
4. a horizontal line $p = p_u$ beyond y_u.

$$m = \frac{p_u - p_m}{y_u - y_m}, \qquad n = \frac{p_m}{m\, y_m}, \qquad C = \frac{p_m}{y_m^{1/n}} \tag{5.19}$$

When the initial line meets the curve beyond y_m, the parabola is omitted. The coefficients A and B depend on x/b and on the loading (Table 5.2); Solgroup interpolates linearly between the tabulated values and uses the last value beyond $x/b = 5$.

Table 5.2 — Coefficients *A* and *B* for sand (Reese et al., 1974)

x/*b*	0	0.5	1.0	1.5	2.0	2.5	3.0	4.0	≥ 5.0
A_s (static)	2.83	2.48	2.11	1.76	1.48	1.23	1.06	0.90	0.88
B_s (static)	2.14	1.83	1.54	1.27	1.05	0.86	0.71	0.53	0.50
A_c (cyclic)	0.75	0.93	1.07	1.11	1.03	0.98	0.94	0.90	0.88
B_c (cyclic)	0.53	0.72	0.83	0.86	0.82	0.77	0.70	0.55	0.55

The criterion was derived from tests on instrumented steel pipe piles of 610 mm diameter in submerged dense sand, under static and cyclic loading (Reese, Cox and Koop, 1974). The ultimate resistance combines a wedge failure near the surface and a flow-around failure at depth; the curve is built from straight, parabolic and straight segments between deflections that depend on the pile width.

© 2026 Solplan. All rights reserved.

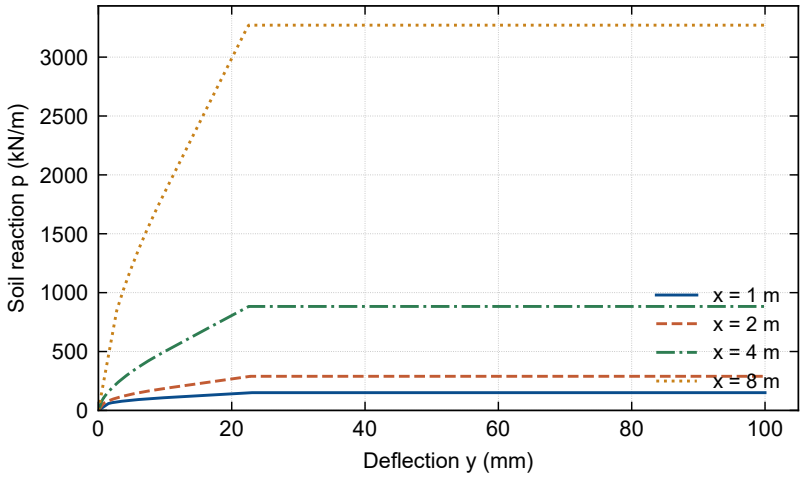

Figure 5.7 — p-y curves of sand, Reese criterion (φ' = 35°, static), computed for a pile of 0.6 m width at four depths below the top of the layer

5.6 API sand

Basis: O'Neill and Murchison (1983); API (2000). The ultimate resistance is

$$p_u = \min\left[\left(C_1\,x + C_2\,b\right)\gamma' x,\;\; C_3\,b\,\gamma' x\right] \tag{5.20}$$

$$C_1 = \frac{\tan^2\beta\,\tan\alpha}{\tan(\beta-\varphi')} + K_0\left[\frac{\tan\varphi'\sin\beta}{\cos\alpha\,\tan(\beta-\varphi')} + \tan\beta\left(\tan\varphi'\sin\beta - \tan\alpha\right)\right] \tag{5.21}$$

$$C_2 = K_p - K_a, \qquad C_3 = K_a\left(\tan^8\beta - 1\right) + K_0\tan\varphi'\tan^4\beta \tag{5.22}$$

with the symbols of Section 5.5 and $K_p = \tan^2(45° + \varphi'/2)$. The curve is

$$p = A\,p_u\tanh\left(\frac{k\,x}{A\,p_u}\,y\right), \qquad A = \max\left(3 - 0.8\,\frac{x}{b},\; 0.9\right)\ \text{(static)}, \quad A = 0.9\ \text{(cyclic)} \tag{5.23}$$

O'Neill and Murchison (1983) evaluated the sand criteria against a database of load tests and proposed the single hyperbolic-tangent expression that was adopted in API RP 2A. It gives curves close to those of the Reese criterion with a simpler shape, and is widely used for offshore piles.

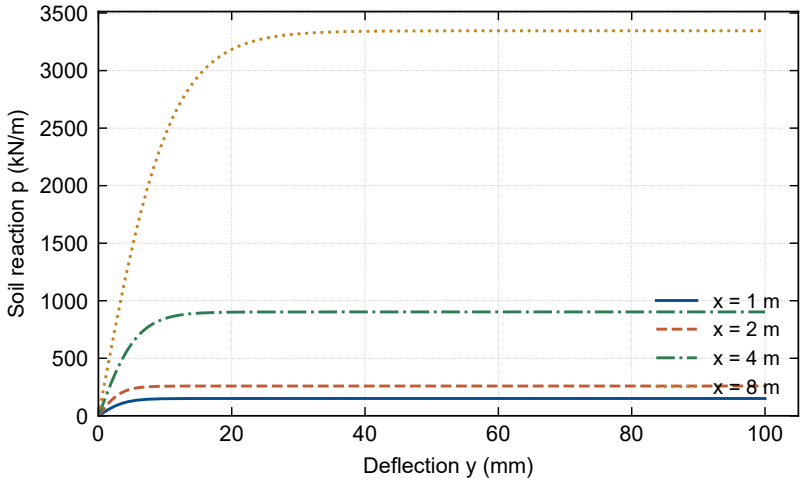

Figure 5.8 — p-y curves of sand, API criterion (φ' = 35°, static), computed for a pile of 0.6 m width at four depths below the top of the layer

© 2026 Solplan. All rights reserved.

5.7 Liquefied sand

5.7.1 Liquefied sand (Rollins)

Basis: Rollins et al. (2005), from full-scale tests in liquefied sand. The curve for a 0.3 m pile is expressed with y in millimetres, z in metres and p in kN/m:

$$p_{0.3} = A\left(B\,y\right)^{C} \le 15\ \text{kN/m} \tag{5.24}$$

$$A = 3\times10^{-7}(z+1)^{6.05},\quad B = 2.80\,(z+1)^{0.11},\quad C = 2.85\,(z+1)^{-0.41}$$

with y limited to 150 mm. For other diameters the reaction is scaled by

$$p = P_d\,p_{0.3},\qquad P_d = 3.81\ln b + 5.6\ \ (0.3 \le b \le 2.6\ m),\qquad P_d = b/0.3\ \ (b < 0.3\ m) \tag{5.25}$$

The logarithmic expression is applied also to diameters above 2.6 m. The model needs no strength parameters; only the effective unit weight of the layer is used. The curves were calibrated for relative densities of about 45 to 55 percent and are recommended to a depth of about 6 m.

The criterion was derived from full-scale tests on piles in sand liquefied by controlled blasting (Rollins et al., 2005). Liquefied sand first offers almost no resistance and then stiffens as it dilates, so the curves are concave upward. The criterion was calibrated for relative densities of about 45 to 55 % and depths of about 6 m.

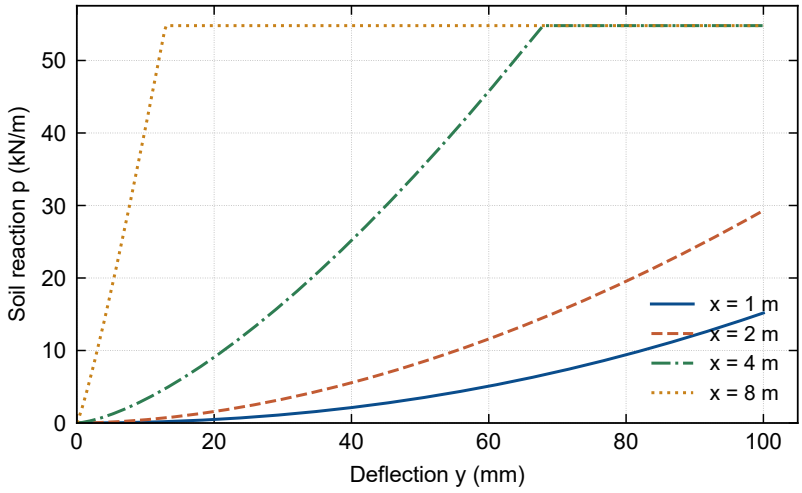

Figure 5.9 — p-y curves of liquefied sand, computed for a pile of 0.6 m width at four depths below the top of the layer

5.7.2 Liquefied sand, hybrid model

Basis: Franke and Rollins (2013). The curve is the lower of the dilative curve above and a residual-strength curve computed with the soft-clay model (Section 5.2, static, J = 0.5) using the residual shear strength S_{ur} and ε_{50}:

$$p = \min\left[p_{dilative}(y),\ p_{residual}(y)\right] \tag{5.26}$$

When S_{ur} is not entered it is estimated from the corrected blow count $(N_1)_{60\text{-cs}}$ with a residual-strength correlation; it is zero for blow counts below 5. Enter S_{ur} and ε_{50} explicitly where site-specific values are available.

Franke and Rollins (2013) combined the dilative curve of liquefied sand with a curve of the soft-clay form that uses the residual strength of the liquefied sand, and take the lower of the two at every deflection. The residual strength can be entered or estimated from the corrected blow count.

© 2026 Solplan. All rights reserved.

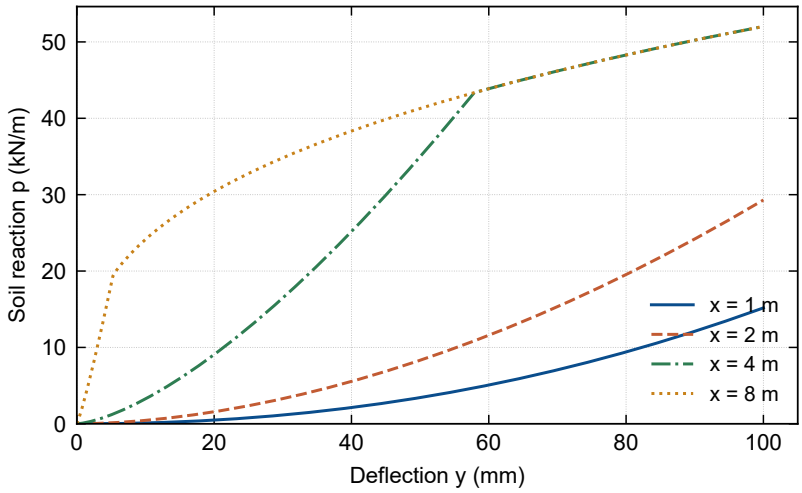

Figure 5.10 — p-y curves of liquefied sand, hybrid model ($(N_1)_{60cs}$ = 10), computed for a pile of 0.6 m width at four depths below the top of the layer

5.8 Cemented soils with cohesion and friction

Basis: the c-φ procedure of Reese and Van Impe (2001). The frictional and cohesive components of the ultimate resistance are computed separately:

$$p_{u\varphi} = \min\left[\sigma'_v\left(C_1\,x + C_2\,b\right),\ \ \sigma'_v\,C_3\,b\right] \tag{5.27}$$

$$p_{uc} = \min\left[\left(3 + \frac{\gamma' x}{c} + 0.5\,\frac{x}{b}\right)c\,b,\ \ 9\,c\,b\right] \tag{5.28}$$

with C_1, C_2, C_3 as in (5.21). The curve is constructed like the sand curve of Section 5.5: an initial line $p = kxy$, a parabola, a straight line from point m ($y_m = b/60$) to point u ($y_u = 3b/80$) and a horizontal line. The resistance at point m combines the two components, $p_m = 1.5p_{u\varphi} + p_{uc}$, with the constant 1.5 in place of the coefficient B of the sand curve; at point u only the frictional component, $p_u = A\,p_{u\varphi}$, remains, so that the straight segment falls when p_m exceeds p_u; the exponent of the parabola is then $n = p_m/(|m|y_m)$. The cohesive component therefore contributes to the peak but is not retained at large deflection. When the initial line meets the straight segment beyond y_m, the parabola is omitted. Both c and φ' must be greater than zero.

Soils such as cemented sands and silts have both cohesion and friction. The criterion described by Reese and Van Impe (2011) adds a cohesive and a frictional part to the ultimate resistance and uses the sand form of the curve.

© 2026 Solplan. All rights reserved.

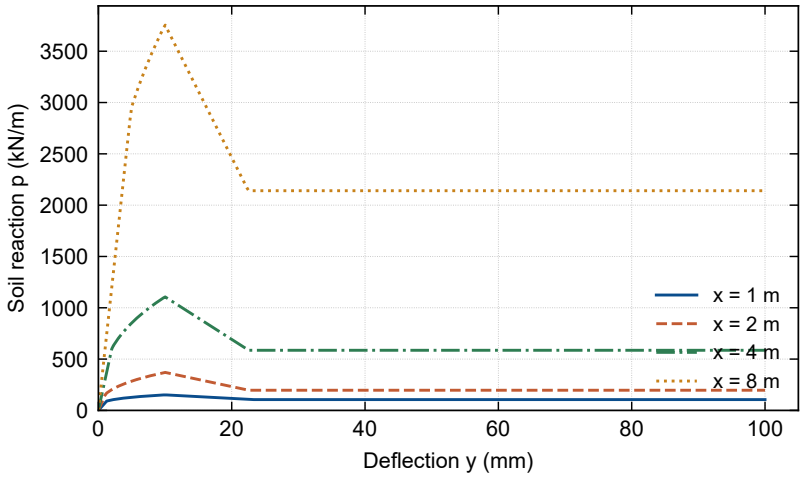

Figure 5.11 — p-y curves of a cemented c-φ soil (*c* = 20 kPa, *φ′* = 30°), computed for a pile of 0.6 m width at four depths below the top of the layer

5.9 Rock

5.9.1 Weak rock

Basis: Reese (1997). With x_r the depth below the top of the rock and the strength reduction factor $\alpha_r = 1 - (2/3)(RQD/100)$, bounded to 1/3–1:

$$p_{ur} = \alpha_r \, q_u \, b \left(1 + 1.4 \frac{x_r}{b}\right) \quad (x_r \le 3b), \qquad p_{ur} = 5.2 \, \alpha_r \, q_u \, b \quad (x_r > 3b) \tag{5.29}$$

$$M_{ir} = k_{ir} \, E_{ir}, \qquad k_{ir} = 100 + 400 \frac{x_r}{3b} \quad (x_r \le 3b), \qquad k_{ir} = 500 \quad (x_r > 3b) \tag{5.30}$$

With $y_{rm} = k_{rm} b$, the curve is

$$p = M_{ir} \, y \quad (y \le y_A), \qquad p = \frac{p_{ur}}{2} \left(\frac{y}{y_{rm}}\right)^{1/4} \quad (y_A < y \le 16 \, y_{rm}), \qquad p = p_{ur} \quad (y > 16 \, y_{rm}) \tag{5.31}$$

$$y_A = \left(\frac{p_{ur}}{2 \, y_{rm}^{1/4} \, M_{ir}}\right)^{4/3} \tag{5.32}$$

The strain factor k_{rm} is usually 0.00005 to 0.0005. With k_{rm} = 0 the curve is the linear $p = M_{ir} y$ without limit. The model is intended for cohesive intermediate geomaterials such as claystone and siltstone, with q_u of about 0.5 to 5 MPa.

The interim criterion of Reese (1997) was derived from load tests on drilled shafts in weak rock. The initial modulus is a multiple of the modulus of the rock mass, and the ultimate resistance depends on the uniaxial compressive strength, reduced by a factor that depends on RQD. It is intended for rock with a uniaxial strength of about 0.5 to 5 MPa.

© 2026 Solplan. All rights reserved.

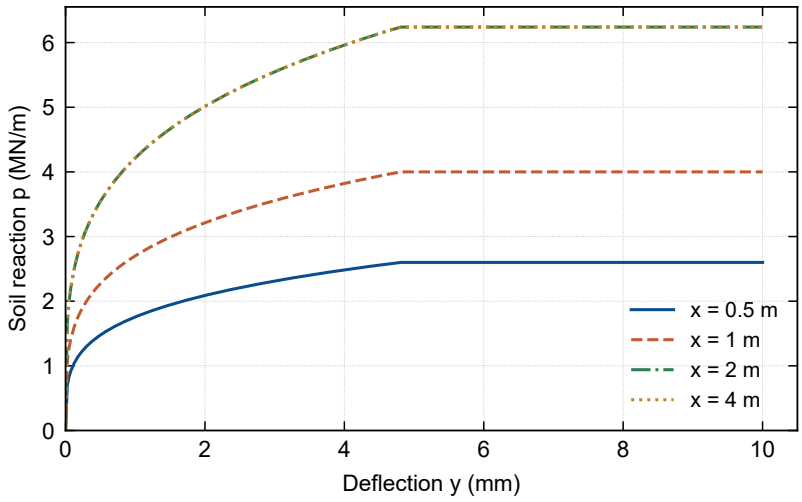

Figure 5.12 — p-y curves of weak rock (q_u = 3 MPa), computed for a pile of 0.6 m width at four depths below the top of the layer

5.9.2 Strong rock

Basis: Reese and Nyman (1978) for vuggy limestone. With $s_u = q_u/2$ and $p_u = b\,s_u$, the curve is bilinear: slope $2000 s_u$ up to $y = 0.0004b$, then slope $100 s_u$ up to p_u. Beyond the deflection at which p_u is reached ($y = 0.0024b$) the rock is assumed to fail in a brittle manner, and the resistance drops to the residual value $0.5\sigma'_v b$.

The criterion was derived from tests on drilled shafts in vuggy limestone (Reese and Nyman, 1978). The response is very stiff and brittle: a steep linear branch, a flatter branch up to the ultimate resistance, and a brittle failure beyond it, as described above. It should be used with caution and confirmed by a load test.

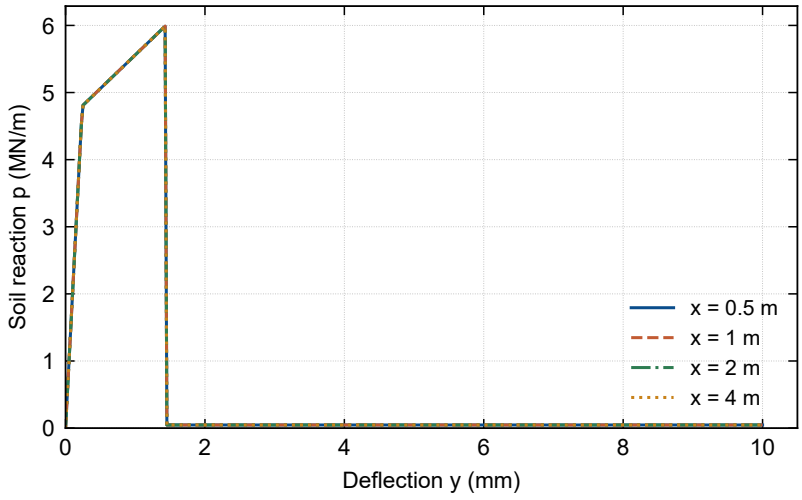

Figure 5.13 — p-y curves of strong rock (q_u = 20 MPa), computed for a pile of 0.6 m width at four depths below the top of the layer

5.9.3 Massive rock

Basis: Liang, Yang and Nusairat (2009), with the rock mass described by the generalised Hoek–Brown criterion (Hoek et al., 2002). The curve is hyperbolic:

$$p = \frac{y}{\dfrac{1}{K_i} + \dfrac{y}{p_u}} \tag{5.33}$$

The initial modulus is

© 2026 Solplan. All rights reserved.

$$K_i = E_m \frac{D}{D_{ref}} e^{-2v} \left(\frac{E_p I_p}{E_m D^4} \right)^{0.284}, \qquad D_{ref} = 0.3048\, m \tag{5.34}$$

where E_m is the rock mass modulus, entered directly or estimated from the intact modulus E_i and the geological strength index as $E_m = E_i\, e^{GSI/21.7}/100$, and $E_p I_p$ the elastic bending stiffness of the pile. The Hoek–Brown parameters are

$$m_b = m_i\, e^{(GSI-100)/28}, \qquad s = e^{(GSI-100)/9} \tag{5.35}$$
$$a = \max\left(0.5,\ 0.65 - GSI/200\right)$$

At the confining stress of interest the criterion is replaced by the instantaneous Mohr–Coulomb parameters φ' and c' (Hoek, 1990). The ultimate resistance is the smaller of the resistance of a three-dimensional wedge near the top of the rock, p_{us}, evaluated with the parameters at a confining stress representative of the wedge (which depends on the depth H below the top of the rock, measured along the pile axis), and the resistance to flow around the pile at depth:

$$p_{ud} = \left(\frac{\pi}{4} p_L + \frac{2}{3} \tau_{max} - p_a \right) D, \qquad p_a = K_a\, \sigma_v' - 2\, c' \sqrt{K_a} \geq 0 \tag{5.36}$$

where p_L is the major principal stress at failure for $\sigma_3 = \sigma'_v$ and $\tau_{max} = 14.23\sqrt{\sigma_{ci}}$ (kPa, with σ_{ci} in kPa) the shear resistance of the pile–rock interface; K_a, φ' and c' are taken at $\sigma_3 = \sigma'_v$. The instantaneous parameters follow from $\sigma_1 = \sigma_3 + \sigma_{ci}(m_b \sigma_3/\sigma_{ci} + s)^a$ with $\Delta = \sigma_1 - \sigma_3$:

$$\sigma_n = \sigma_3 + \frac{\Delta^2}{2\Delta + 0.5\, m_b\, \sigma_{ci}}, \qquad \tau = (\sigma_n - \sigma_3)\sqrt{1 + \frac{m_b\, \sigma_{ci}}{2\Delta}} \tag{5.37}$$
$$\varphi' = 90^\circ - \arcsin\frac{2\tau}{\Delta}, \qquad c' = \tau - \sigma_n \tan\varphi'$$

The wedge resistance uses φ' and c' at $\sigma_3 = \sigma'_{v0} + \gamma' H/3$, where σ'_{v0} is the effective vertical stress at the top of the rock, with $\theta = \varphi'/2$, $\beta = 45^\circ + \varphi'/2$, $K_0 = 1 - \sin\varphi'$ and $K_a = \tan^2(45^\circ - \varphi'/2)$:

$$p_{us} = 2C_1 \cos\theta \sin\beta + C_2 \cos\beta + C_3 \sin\beta - 2C_4 \sin\theta - C_5 \tag{5.38}$$

$$C_1 = H \tan\beta \sec\theta \left(c' + K_0\, \sigma'_{v0} \tan\varphi' + \frac{1}{2} H K_0\, \gamma' \tan\varphi' \right), \qquad C_4 = K_0\, H \tan\beta \sec\theta \left(\sigma'_{v0} + \frac{1}{2}\gamma' H \right) \tag{5.39}$$

$$C_2 = \frac{D \tan\beta\, (\sigma'_{v0} + H\gamma') + H \tan^2\beta \tan\theta\, (2\sigma'_{v0} + H\gamma') + c'(D + 2H \tan\beta \tan\theta) + 2C_1 \cos\beta \cos\theta}{\sin\beta - \tan\varphi' \cos\beta} \tag{5.40}$$

$$C_3 = C_2 \tan\varphi' + c' \sec\beta\, (D + 2H \tan\beta \tan\theta) \tag{5.41}$$

$$C_5 = \gamma' K_0 (H - z_0)\, D \geq 0, \qquad z_0 = \frac{2c'}{\gamma' \sqrt{K_a}} - \frac{\sigma'_{v0}}{\gamma'}$$

In the terms of the wedge, γ' is the average effective unit weight between the ground surface and the depth considered, σ'_v/x.

Liang, Yang and Nusairat (2009) proposed a hyperbolic curve whose initial stiffness comes from an elastic continuum analysis of a shaft in rock and whose ultimate resistance comes from the Hoek–Brown strength of the rock mass, and verified it with load tests on drilled shafts socketed in rock.

© 2026 Solplan. All rights reserved.

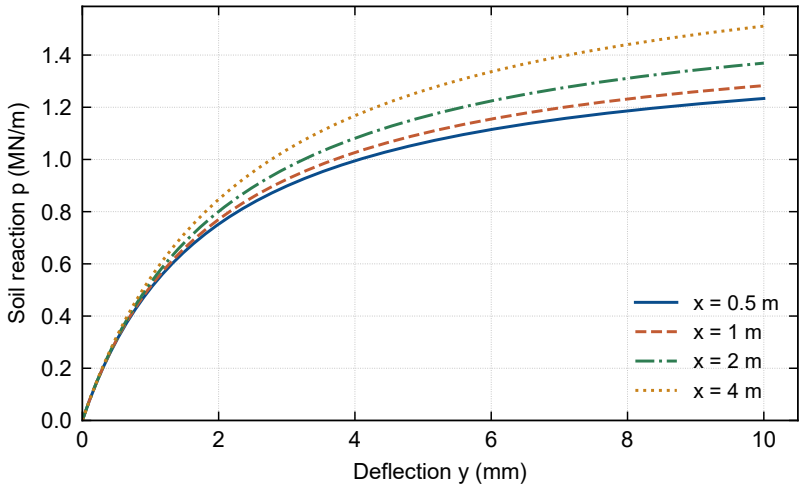

Figure 5.14 — p-y curves of massive rock (q_u = 20 MPa, GSI = 50), computed for a pile of 0.6 m width at four depths below the top of the layer

5.10 Other models

5.10.1 Piedmont residual soil

Basis: Simpson and Brown (2006). The secant modulus degrades logarithmically with the normalised deflection:

$$E_s = E_{si} \quad \left(\frac{y}{b} \le 0.001\right), \qquad E_s = E_{si}\left[1 + \lambda \ln\left(\frac{y/b}{0.001}\right)\right] \quad \left(0.001 < \frac{y}{b} \le 0.0375\right) \tag{5.42}$$

$$p = E_s\, b\, y$$

where $\lambda = -1/(1 + \ln 37.5) = -0.2162$, so that the secant modulus at $y/b = 0.0375$ is $E_{si}/(1 + \ln 37.5)$; beyond that deflection the resistance is constant at $0.00811 E_{si} b^2$. The initial modulus E_{si} (force/length^3) is derived from one field test, selected with the layer, with the correlations of Simpson and Brown (2006): $E_{si} = 22 N_{60}$ lb/in^3 from the SPT blow count, or $0.8136 q_c$, $0.076 E_D$ or $0.235 E_M$ per inch from the cone tip resistance, the dilatometer modulus or the Ménard pressuremeter modulus. Only the value of the selected test is used.

Simpson and Brown (2006) derived the criterion for the residual soils of the Piedmont region, which are weathered in place from rock and keep part of its structure. The initial modulus comes from one in-situ test: the standard penetration test, the cone, the flat dilatometer or the pressuremeter.

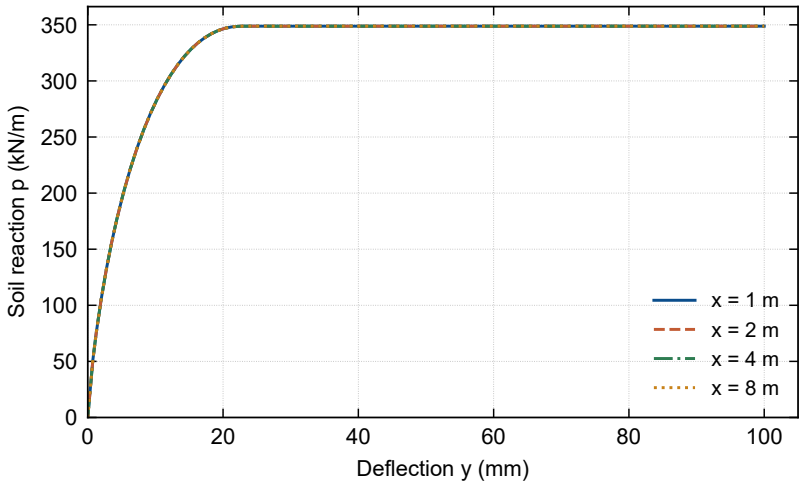

Figure 5.15 — p-y curves of Piedmont residual soil (N_{60} = 20), computed for a pile of 0.6 m width at four depths below the top of the layer

© 2026 Solplan. All rights reserved.

5.10.2 Loess

Basis: Johnson, Parsons, Dapp and Brown (2006), from load tests of drilled shafts in loess with cone penetration data. With the cone resistance q_c, reduced near the surface to $q_c(0.5 + 0.5z/2b)$ for $z < 2b$:

$$p_u = \frac{0.409\, q_c\, b}{1 + 0.24 \log_{10} N}, \qquad E_i = \frac{p_u}{y_{ref}}, \qquad p = \frac{E_i\, y}{1 + y_h}, \qquad y_h = \frac{y}{y_{ref}} \left(1 + 0.10\, e^{-y/y_{ref}} \right) \tag{5.43}$$

with y_{ref} = 2.97 mm and N the number of cycles of the load case (1 for static loading, at most 10).

The criterion of Johnson et al. (2006) was derived for loess, a wind-deposited silt with a weak cementation, from cone penetration tests and lateral load tests on drilled shafts. The ultimate resistance is proportional to the cone resistance and decreases with the number of load cycles.

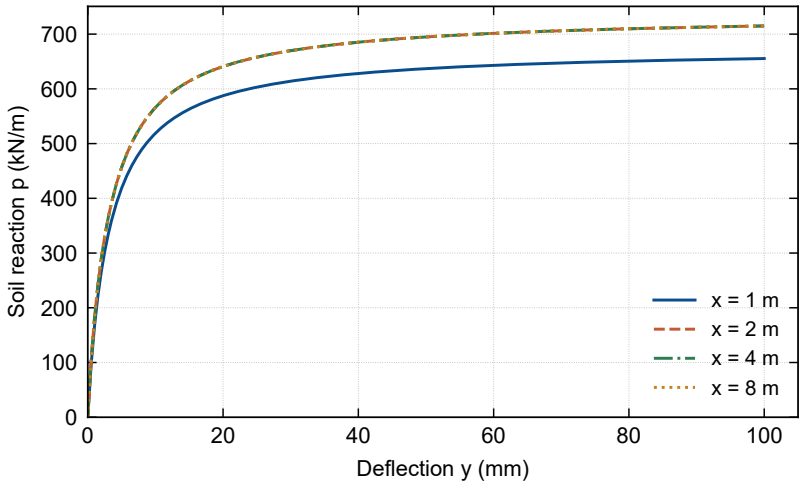

Figure 5.16 — p-y curves of loess (q_c = 3 MPa), computed for a pile of 0.6 m width at four depths below the top of the layer

5.10.3 Elastic subgrade

The reaction is linear, $p = k_h b\, y$, with the modulus of subgrade reaction k_h (force/length^3) constant within the layer. A maximum stress transfer σ_{max} can be entered, which limits the reaction to $p \le b \cdot \sigma_{max}$; zero means no limit.

The elastic subgrade is a linear spring, optionally limited by a maximum stress transfer. It is not a soil criterion: it is used for comparison with closed-form solutions, for materials with a known linear modulus, and for sensitivity studies.

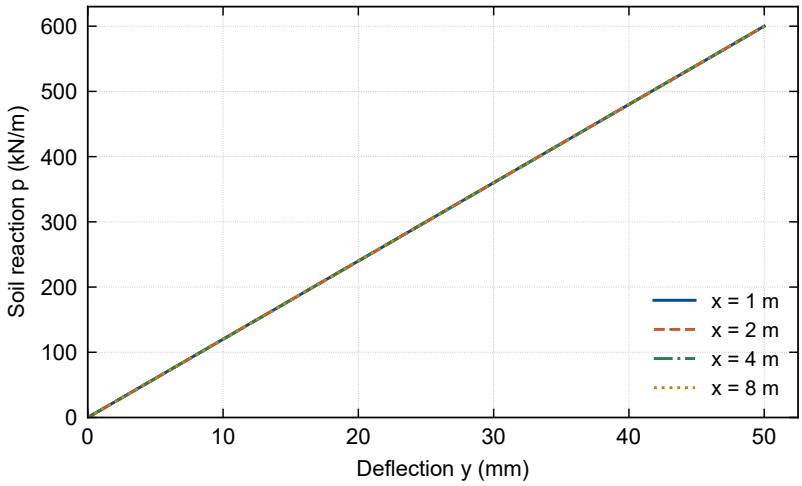

Figure 5.17 — p-y curves of an elastic subgrade (E_s = 20 MN/m³), computed for a pile of 0.6 m width at four depths below the top of the layer

© 2026 Solplan. All rights reserved.

5.10.4 User-defined curves

A set of user-defined p-y curves gives curves at two or more depths, positive downward from the global elevation zero; the set is assigned to piles (Assign ▸ Pile ▸ p-y Set) and is used when the option *User-defined p-y curves* is on. Each curve is the polygon through its points, with a constant reaction beyond the last point. At a node between two depths of the set, the secant modulus is interpolated linearly between the two curves. The depths of the set must reach the tip of the pile; otherwise the load case stops with a message. A layer whose model is *User-defined p-y* takes its lateral resistance from the set assigned to the pile; the depth of a user curve is not corrected for batter or layering.

5.11 Selection of a p-y criterion

The criterion of a layer should be chosen for the soil and the conditions of the site, not for the result it gives. The criteria differ most in the response of the soil near the ground surface, which governs the response of the pile, and in the effect of repeated loading. Table 5.3 summarises the conditions for which each criterion was developed.

Table 5.3 — Choice of the p-y criterion

Soil and conditions	Criterion	Remarks
Soft to firm clay, normally or lightly overconsolidated, below the water table	Soft Clay (Matlock); variants with user *J* or initial *k*	cyclic form for wave, traffic or other repeated loads
Stiff overconsolidated clay with free water at or above the ground surface	Stiff Clay with Free Water	strong loss of resistance under cyclic load by erosion of the clay near the surface
Stiff clay above the water table, or where free water cannot reach the ground surface	Stiff Clay without Free Water; variant with user *k*	the free-water criterion assumes erosion of the clay by water, which cannot occur here
Sand and gravel, above or below the water table	Sand (Reese) or API Sand (O'Neill)	the two give similar curves; the API form is customary offshore
Sand liquefied by an earthquake	Liquefied Sand (Rollins) or hybrid model	calibrated for loose to medium-dense sand at shallow depth
Soils with both cohesion and friction: cemented sand, silt, residual soil	Silt / c-phi Soil (Cemented Sand)	both c and φ' must be given
Residual soils of crystalline rock	Piedmont Residual	modulus from an in-situ test
Loess and similar weakly cemented silts	Loess	from the cone resistance
Weak rock, q_u about 0.5 to 5 MPa	Weak Rock	rock mass modulus and RQD needed
Strong rock, q_u above about 5 MPa	Strong Rock (Vuggy Limestone) or Massive Rock	massive rock for a rock mass described by GSI and m_i; strong rock for brittle limestone
Measured response of a test pile, or a soil not covered by the criteria	User-defined p-y	curves at several depths, interpolated between them
Comparison with closed-form solutions; a material with a known linear response	Elastic Subgrade	linear, with an optional limit on the stress

Where the soil cannot be placed clearly in one class, or its parameters are uncertain, analyses with two criteria or with a range of parameters show how much the design depends on the choice. A lateral load test at the site remains the best way to select and calibrate the criterion.

5.12 Battered piles

The p-y criteria were derived from tests on vertical piles. For a battered pile two effects are considered:

- **Depth of the soil curves.** The ultimate resistance of the near-surface wedge and the effective stress depend on the depth below the ground surface. With the option *Adjust Depth for Batter Piles* the depth of each node is measured vertically, so that a node at a distance x along a pile battered at an angle β from the vertical uses the

© 2026 Solplan. All rights reserved.

curve at the depth $x \cos \beta$; without it the distance along the pile is used. The deflection of the pile is measured normal to its axis in both cases.

- **Direction of the batter relative to the load.** Model tests in sand (Awoshika and Reese, 1971) showed that the lateral resistance of a battered pile differs from that of a vertical pile, and that it is larger for one sense of the lateral load relative to the batter and smaller for the other. The effect is not included in the curves automatically; where it matters, it can be represented by p-multipliers or by a lateral reduction set on the piles concerned.

In a group, battered piles carry much of the horizontal load by axial force (Example 2 of the User Manual). The axial response of the battered piles then governs the horizontal stiffness of the group, and the estimated side friction of driven piles in sand is corrected for the batter (Chapter 6).

5.13 Layered soil

The ultimate resistance of the shallow wedge in a layer depends on the soil above it. Solgroup applies the equivalent-depth method of Georgiadis (1983). For a layer whose top lies at depth H_i, an equivalent depth h_i' is found such that the ultimate resistance of the layer material, integrated from the ground surface to h_i', equals the resistance actually provided by the overlying layers:

$$\int_0^{h_i'} p_{u,i}(x)\,dx = \sum_{j<i} \int_{\text{layer } j} p_{u,j}(x)\,dx \tag{5.44}$$

Within layer i the wedge terms of the p-y curve are then evaluated at the depth $x - H_i + h_i'$, while the effective stress remains that at the actual depth. The correction is switched on with the option *Use Layering Correction (Georgiadis)*, and is omitted where a layer lies below a layer of the same model when the option *Skip correction when the soil above is of the Same Type* is set.

The depths are measured from the ground surface of each pile, which differs from the ground surface of the profile on sloping ground or where a pile has a ground elevation of its own, while the layers keep their elevations. The part of a layer above the ground of a pile gives that pile no resistance and does not enter the sum above, and where the ground of a pile lies inside a layer, that layer starts at the ground of the pile. The effective stress is computed from the ground of the pile; for sand below the ground of the pile it is the actual overburden, and the depth used by the weak-rock and liquefied-sand curves is counted from the first node below the ground of the pile.

5.14 Default parameters

When ε_{50} or the modulus gradient k is entered as zero, Solgroup assigns a default value following the recommendations published with the model:

Table 5.4 — Basis of default parameters

Parameter	Models	Default depends on
ε_{50}	soft clay; stiff clays; cemented soils	undrained shear strength (consistency of the clay), after Matlock (1970) and Reese et al. (1975)
k, clay	stiff clay with free water; modified soft clay with initial k	undrained shear strength and type of loading (static or cyclic), after Reese et al. (1975)
k, sand	sand (Reese); API sand	friction angle and position relative to the water table, after Reese et al. (1974) and API (2000)
k, cemented soils	silt (cemented soils)	cohesion, friction angle, position relative to the water table and type of loading

The default is a generic value for the soil type. For design, determine ε_{50} and k from site-specific tests where possible and enter them. The effect of a default on the curves can be inspected in the generated p-y curves (Display ▸ Show Soil Curves).

The defaults that Solgroup uses are listed below for representative strengths; between the listed values they are interpolated or taken from the band of the strength, as published with the models.

© 2026 Solplan. All rights reserved.

Table 5.5 — Default ε_{50} against the undrained shear strength

c_u (kPa)	Soft clay criteria	Stiff clay criteria
10	0.020	0.011
20	0.020	0.011
40	0.010	0.011
75	0.005	0.007
150	0.005	0.005
300	0.004	0.004

Table 5.6 — Default modulus gradient *k* of stiff clay

c_u (kPa)	*k*, static (MN/m³)	*k*, cyclic (MN/m³)
50	136	54
100	271	109
200	543	217
400	543	217

Table 5.7 — Default modulus gradient *k* of sand

φ' (°)	*k*, above the water table (MN/m³)	*k*, below the water table (MN/m³)
28	4.2	3.8
30	12.9	9.4
33	27.7	17.6
36	44.5	26.2
40	70.1	39.7

© 2026 Solplan. All rights reserved.

6 Soil response for axial loading

6.1 Load-transfer curves

The axial response of a pile (Section 4.2) is built from two kinds of load-transfer curves:

- shaft curves, which give the unit shaft resistance t as a fraction of its ultimate value f at a node as a function of the local movement z of the pile relative to the soil (t-z curves);
- a tip curve, which gives the tip resistance q as a fraction of its ultimate value q_{ult} as a function of the movement w of the tip (Q-w curve).

The unit shaft resistance per unit length of the pile is $t \cdot \pi_s$, with the perimeter π_s of the section, and the tip force is $q \cdot A_{tip}$. For each soil layer the user enters the *ultimate unit side friction* f and the *ultimate unit tip resistance* q_{ult}, or zero to have them estimated from the strength of the soil (Section 6.5). The shape of the curves depends on the installation of the pile (driven pile or drilled shaft, Assign ▸ Pile ▸ Type) and on the type of the soil, which follows the lateral model of the layer:

Table 6.1 — Type of the axial curves by lateral soil model

Lateral soil models	Axial curves
Soft and stiff clays (all variants)	clay
Sand (Reese), API sand, liquefied sand	sand
Silt / c-φ soil	sand curves; the ultimate values combine cohesion and friction
Weak, strong and massive rock	clay
User-defined p-y curves	clay curves of API RP 2A, with the entered ultimate values

The normalised shapes of the curves are compared in Figure 6.1: the shaft resistance of driven piles is mobilised within a few millimetres, independently of the pile size, and in clay it falls to a residual value beyond the peak; the shaft resistance of drilled shafts and all tip resistances are mobilised over displacements proportional to the diameter, so that the tip of a large pile needs a settlement of several percent of its diameter to reach its capacity.

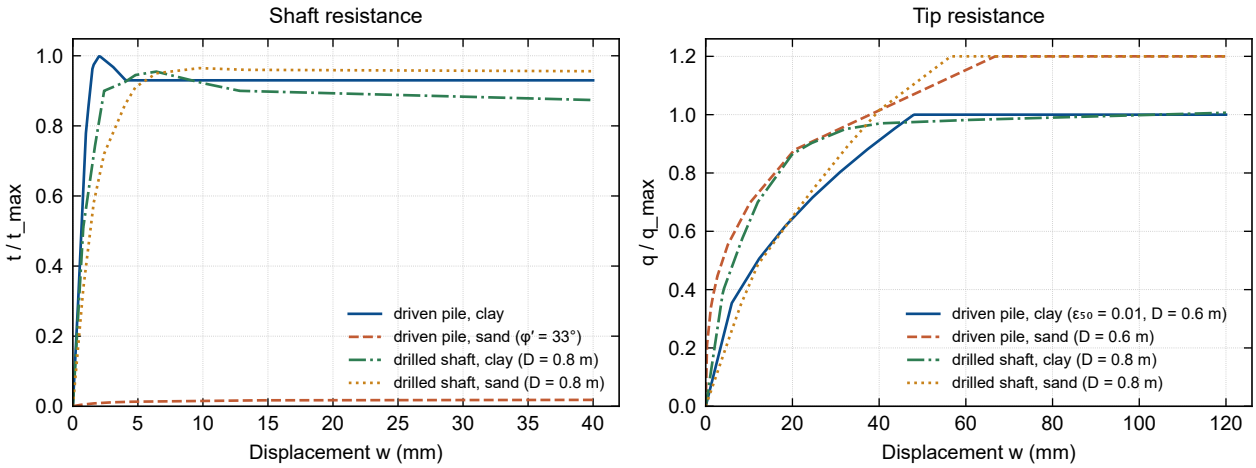

Figure 6.1 — Normalised shaft (t-z) and tip (Q-w) curves of driven piles and drilled shafts

6.2 Driven piles

6.2.1 Shaft resistance in clay

The t-z curve of clay follows the measurements of Coyle and Reese (1966) on instrumented piles in clay. The fraction of the ultimate shaft resistance depends on the absolute movement of the pile:

© 2026 Solplan. All rights reserved.

Table 6.2 — t-z curve for clay, driven piles

Movement *z* (mm)	0	0.25	0.51	1.02	1.52	2.03	3.05	≥ 4.06
t/*f*	0	0.18	0.38	0.79	0.97	1.00	0.97	0.93

The resistance peaks at a movement of about 2 mm and decreases to a residual value of 0.93*f*. Between the tabulated points the curve is linear.

For layers whose lateral resistance is given by user-defined p-y curves, the t-z curve of API RP 2A for clay is used, in terms of the movement relative to the pile diameter *D*:

Table 6.3 — t-z curve of API RP 2A for clay

z/*D*	0	0.0016	0.0031	0.0057	0.0080	0.0100	≥ 0.0200
t/*f*	0	0.30	0.50	0.75	0.90	1.00	0.80

6.2.2 Shaft resistance in sand

The t-z curve of sand is the hyperbola of Mosher (1984):

$$t = \frac{z}{\frac{1}{E_s} + \frac{z}{f}} \tag{6.1}$$

where E_s is the initial slope of the curve, which increases with the friction angle from about 6 000 lb/ft^2 per inch at φ' = 28° to 18 000 lb/ft^2 per inch at φ' = 38° (about 11 to 34 MN/m^3). The curve is evaluated at fixed movements of up to 64 mm and is linear between them.

6.2.3 Tip resistance in clay

The tip curve of clay follows the approach of Skempton (1951), which relates the movement of the tip to the strain of the soil in a laboratory test:

$$\frac{q}{q_{ult}} = 0.5\left(\frac{w}{w_{50}}\right)^{1/2} \le 1, \qquad w_{50} = 2\,\varepsilon_{50}\,D \tag{6.2}$$

so that the full tip resistance is reached at $w = 4w_{50}$. ε_{50} is that of the layer at the tip; when it is zero, a default that decreases with the strength of the clay is used, from 0.02 for soft clay to 0.004 for hard clay. For rock, the strain factor k_{rm} takes the place of ε_{50}. For layers of user-defined p-y curves the Q-z curve of API RP 2A is used:

Table 6.4 — Q-z curve of API RP 2A

w/*D*	0	0.002	0.013	0.042	0.073	≥ 0.100
q/q_{ult}	0	0.25	0.50	0.75	0.90	1.00

6.2.4 Tip resistance in sand

The tip curve of sand is a power law in the movement of the tip, with a critical movement proportional to the diameter (Vijayvergiya, 1977):

$$\frac{q}{q_{ult}} = \left(\frac{w}{z_c}\right)^n, \qquad z_c = 0.05\,D, \qquad n = \begin{cases} 1/2 & \varphi' \le 31^\circ \\ 1/3 & 31^\circ < \varphi' \le 38^\circ \\ 1/4 & \varphi' > 38^\circ \end{cases} \tag{6.3}$$

The curve is evaluated at fixed movements of up to 127 mm and is linear between them.

6.3 Drilled shafts

For drilled shafts the curves are the normalised trend curves of Reese and O'Neill (1987), in terms of the movement relative to the diameter of the shaft:

© 2026 Solplan. All rights reserved.

Table 6.5 — Normalised load-transfer curves for drilled shafts

z/*D* or *w*/*D*	0.001	0.002	0.003	0.005	0.008	0.012	0.016	0.100
Side, clay: *t*/*f*	0.51	0.72	0.90	0.925	0.955	0.925	0.90	0.835
Side, sand: *t*/*f*	0.335	0.58	0.72	0.86	0.95	0.965	0.96	0.95

Table 6.6 — Normalised tip curves for drilled shafts

w/*D*	0.005	0.010	0.015	0.025	0.030	0.040	0.050	0.070	0.100
Tip, clay: q/q_{ult}	0.395	0.56	0.70	0.865	0.90	0.95	0.97	0.98	0.99
Tip, sand: q/q_{ult}	0.175	0.345	0.485	0.65	0.73	0.88	1.015	1.195	1.46

In sand the tip resistance continues to increase beyond the movement at which q_{ult} is defined; the value q_{ult} of a drilled shaft in sand is the tip resistance at a movement of 5 % of the diameter.

6.4 Curves of the pile head

The load–displacement and torque–rotation curves of the head follow from the curves along the pile by the load-transfer procedure of the single pile. Figure 6.2 shows them for a pile of the 3 × 3 group of the examples, once as a driven pile and once as a drilled shaft in the same soil. The driven pile reaches 5,142 kN in compression and −2,146 kN in tension; the drilled shaft 3,342 kN and −2,000 kN. The two kinds of pile use different unit resistances and different load-transfer curves; the tip of a drilled shaft, in particular, mobilises its resistance only at a movement of several per cent of the diameter. In tension only the side resistance acts, and the two curves are closer. The torque reaches 643 kN·m and 596 kN·m.

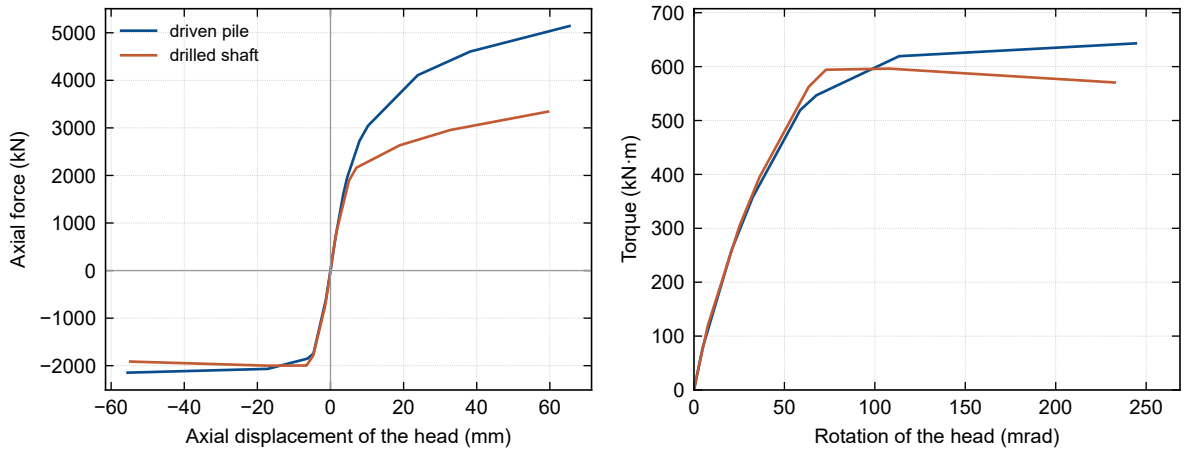

Figure 6.2 — Load–displacement (left) and torque–rotation (right) curves of the head of a driven pile and a drilled shaft in the same soil

6.5 Estimated ultimate values

When the ultimate unit side friction or tip resistance of a layer is entered as zero, it is estimated from the parameters of the layer at the depth of each node, with the vertical effective stress σ'_v:

Table 6.7 — Estimated ultimate unit resistances

Soil	Side friction *f*	Tip resistance q_{ult}
Driven piles		
Clay	$f = \alpha\, c$, with α of API RP 2A (below)	$9c$
Sand	$f = K\,\sigma'_v \tan(\varphi' - 5°)$, $K = 0.8$	$N_q\,\sigma'_v$
Silt / c-φ	sum of the clay and sand terms	$9c + N_q\,\sigma'_v$
Rock	$0.1 q_u$	$9 q_u$

© 2026 Solplan. All rights reserved.

Soil	Side friction f	Tip resistance q_{ult}
Drilled shafts (Reese and O'Neill, 1988; O'Neill and Reese, 1999)		
Clay	$0.55c$	$9c$
Sand	$f = \beta\,\sigma'_v$, $\beta = 1.5 - 0.245\sqrt{z}$ (z in m), $0.25 \le \beta \le 1.2$	by friction angle: practically zero for $\varphi' < 30°$, 1 530 kPa for $30° \le \varphi' < 36°$, 3 830 kPa above

The adhesion factor of API RP 2A is

$$\alpha = 0.5\,\psi^{-0.5} \quad (\psi \le 1), \qquad \alpha = 0.5\,\psi^{-0.25} \quad (\psi > 1), \qquad \psi = \frac{c}{\sigma'_v} \tag{6.4}$$

It is not limited to 1, which gives values above 1 in very soft, normally consolidated clay near the surface; for $\psi > 1$ and $c < 24$ kPa (500 lb/ft^2) the factor is 1. The bearing capacity factor N_q is interpolated linearly in the friction angle:

Table 6.8 — Bearing capacity factor for estimated tip resistance in sand

φ' (°)	20	25	30	35	40
N_q	8	12	20	40	50

For a driven pile with batter angle β in sand, the estimated side friction is multiplied by $\cos\beta + \sin\beta/K$, because the normal stress on the inclined shaft combines the horizontal and the vertical effective stress. The input echo of the run lists the entered values, where zero means estimated; the resulting axial and torsional curves can be inspected with **Display ▸ Show Soil Curves…** and **Display ▸ Show Assigns ▸ Generated L-D Curve**. Estimated values are generic and should be replaced by values from site investigation or load tests where these are available.

As an illustration, Table 6.9 and Table 6.10 give the estimated values for a few strengths, at a vertical effective stress of 50 kPa for the clays and 100 kPa for the sands. They are computed with the functions of the analysis.

Table 6.9 — Estimated ultimate values in clay (σ'_v = 50 kPa)

c (kPa)	Driven, f (kPa)	Driven, q_{ult} (kPa)	Drilled, f (kPa)	Drilled, q_{ult} (kPa)
25	17.7	225	13.8	225
50	25.0	450	27.5	450
100	42.0	900	55.0	900

Table 6.10 — Estimated ultimate values of driven piles in sand (σ'_v = 100 kPa)

φ' (°)	f (kPa)	N_q	q_{ult} (kPa)
30	37.3	20	2,000
33	42.6	32	3,200
36	48.1	42	4,200

The estimates are generic correlations. Values from the site investigation or from load tests, entered in the soil layers, are always preferable; the estimates are best used to check the order of magnitude of the entered values.

NOTE The unit side friction and tip resistance are characteristic of the soil and of the installation method. The curves above describe the shape of the response; the ultimate values govern the capacity of the piles and should be determined with care.

© 2026 Solplan. All rights reserved.

7 Group effects

7.1 Closely spaced piles

When piles are spaced closely, the zones of soil that resist their lateral movement overlap. A pile behind another pile in the direction of the movement (a trailing pile) acts in soil already loaded by the pile in front of it (the leading pile), and two piles side by side share the soil between them. The resistance of each pile is therefore lower than that of a single pile, the more so the closer the spacing. Full-scale and model tests (Brown, Morrison and Reese, 1988; Rollins, Peterson and Weaver, 1998; Rollins et al., 2006) show that the reduction can be represented by multiplying the p-y curve of the single pile by a factor $f_{\mathrm{m}} \le 1$, the p-multiplier:

$$p_{\mathrm{group}}(y) = f_m \, p_{\mathrm{single}}(y) \tag{7.1}$$

A y-multiplier f_{y} may also be given; it divides the soil reaction, so that the combined factor on the reaction is $f_{\mathrm{m}}/f_{\mathrm{y}}$. Group factors act only on the lateral soil resistance; they do not change the axial curves of the piles. The factors are defined in sets (Define ▸ Soil ▸ Lateral Group Effect (p-y)). One set is selected for the model in the analysis options, and a load case may use another set, for example a table method whose leading row follows the load direction of that case.

7.2 Factors by rows

For the methods based on rows, the piles are grouped into rows perpendicular to a load direction stored with the set. Piles whose positions along that direction differ by less than a quarter of the pile diameter belong to the same row. Row 1 is the leading row: the row furthest in the direction of the load, which pushes into undisturbed soil. Rows 2, 3 and so on are trailing rows. Reversing the load direction changes which row leads. Each row has p- and y-multipliers for movement along the load direction and transverse to it. The p-multiplier of each row is given by one of the following methods:

- **Manual:** the factors of each row are entered.
- **AASHTO LRFD Table 10.7.2.4-1:** the factors depend on the ratio of the centre-to-centre spacing of the rows to the diameter, s/D, taken as the mean spacing of the rows in the load direction:

Table 7.1 — p-multipliers of AASHTO LRFD Table 10.7.2.4-1

s/D	Row 1 (leading)	Row 2	Row 3 and higher
3	0.80	0.40	0.30
5	1.00	0.85	0.70

Between the two spacings the factors are interpolated linearly. Outside the range of the table they are held at the value of the nearest row: the program does not extrapolate, and it does not assume that the group effect vanishes at spacings above $5D$. Where the design code allows a factor of 1.0 at wider spacings, that row is added with the user-table method.

- **Reese & Van Impe** and **User table:** a table of factors for the leading row, the second row and the third and further rows at several values of s/D, entered from the reference chosen by the user, and interpolated in the same way.

The factors computed by a method are shown in the table of the set and can be checked or overwritten before they are used.

7.3 Factors for each pile from the positions of all piles

The method *Closely-spaced piles* computes a factor for every pile from the positions of all other piles relative to the direction of the movement of the cap, following Reese and Van Impe (2011). For a pile i and another pile j at the distance $s = r\,b$, where b is the reference diameter, the interaction factor is

$$\beta_a = \min\left(1,\ 0.64\, r^{0.34}\right) \qquad \text{piles side by side} \tag{7.2}$$

© 2026 Solplan. All rights reserved.

$$\beta_b = \min\left(1,\ 0.70\,r^{0.26}\right) \ \text{pile } i \text{ leading}, \qquad \beta_b = \min\left(1,\ 0.48\,r^{0.38}\right) \ \text{pile } i \text{ trailing} \tag{7.3}$$

for piles in line with the movement, and for piles in a skewed position, at an angle ψ between the line joining them and the direction of movement,

$$\beta = \sqrt{\left(\beta_b \cos\psi\right)^2 + \left(\beta_a \sin\psi\right)^2} \tag{7.4}$$

The factor of pile i is the product of its interaction factors with all other piles, $f_i = \Pi_{j \neq i}\, \beta_{ij}$. Factors are computed for the two horizontal global directions and combined according to the direction φ of the movement of the cap:

$$f = \sqrt{\left(f_x \cos\phi\right)^2 + \left(f_y \sin\phi\right)^2} \tag{7.5}$$

The direction of movement is either taken from the analysis of the load case, or a reference direction stored with the set. The reference diameter is that of the first pile, or the average of the two piles of each pair.

7.3.1 Example computation

For a 3 × 3 group of piles of b = 0.6 m at a spacing of 1.8 m ($3b$) and a movement of the cap along +X, the factor of the centre pile P5 is the product of eight interaction factors (Table 7.2). Here *du* is the distance of P5 ahead of the other pile in the direction of movement and *dv* the distance across it. The piles side by side (P2, P8) give $\beta_a = 0.64 \cdot 3^{0.34}$; P4, which P5 leads, gives $\beta_b = 0.70 \cdot 3^{0.26}$; P6, which P5 trails, gives $\beta_b = 0.48 \cdot 3^{0.38}$, the strongest reduction; the diagonal piles combine the two factors with the angle of 45°.

Table 7.2 — Interaction factors of the centre pile P5, movement along +X

Other pile	*du* (m)	*dv* (m)	*r* = *s*/*b*	*β*
P1	+1.8	+1.8	4.24	1.000
P2	+0.0	+1.8	3.00	0.930
P3	−1.8	+1.8	4.24	0.920
P4	+1.8	+0.0	3.00	0.931
P6	−1.8	+0.0	3.00	0.729
P7	+1.8	−1.8	4.24	1.000
P8	+0.0	−1.8	3.00	0.930
P9	−1.8	−1.8	4.24	0.920

The product is f_{P5} = 0.496. The factors of all piles for a movement along +X and along the diagonal (45°) are shown in plan in Table 7.3 and Table 7.4; the leading row (largest X) has the largest factors, and the corner piles of each row have larger factors than the middle pile, which has neighbours on both sides.

Table 7.3 — p-multipliers of the 3 × 3 group in plan, movement along +X (to the right)

P7: 0.58	P8: 0.58	P9: 0.87
P4: 0.50	P5: 0.50	P6: 0.81
P1: 0.58	P2: 0.58	P3: 0.87

Table 7.4 — p-multipliers of the 3 × 3 group in plan, movement at 45°

P7: 0.74	P8: 0.70	P9: 0.87
P4: 0.54	P5: 0.50	P6: 0.70
P1: 0.58	P2: 0.54	P3: 0.74

7.4 Factors for each pile by direction

With the method *Per pile, x/y directions* the p- and y-multipliers of every pile are entered for the two horizontal global directions and combined with the direction of the movement of the cap as in (7.5).

© 2026 Solplan. All rights reserved.

7.5 Reduction along the depth

Test results show that the reduction of resistance in a group is not uniform with depth. Factors that vary along the pile can be entered as lateral reduction sets and assigned to piles (Chapter 4); they multiply the reaction together with the group factors.

7.6 Effect of the spacing

Figure 7.1 shows the 3 × 3 group of the examples, with piles 0.6 m in diameter, under a horizontal load of 900 kN in X, with the p-multipliers of the AASHTO table for spacings from 3 to 8 diameters. At 3 diameters the leading row carries 46.2% of the horizontal load and the trailing row 24.5%; the cap moves 14.98 mm, against 6.30 mm when the factors are omitted. At 5 diameters and more the table gives the factors 1.0, 0.85 and 0.7, the shares become 37.3%, 33.4% and 29.3%, and the movement 7.44 mm.

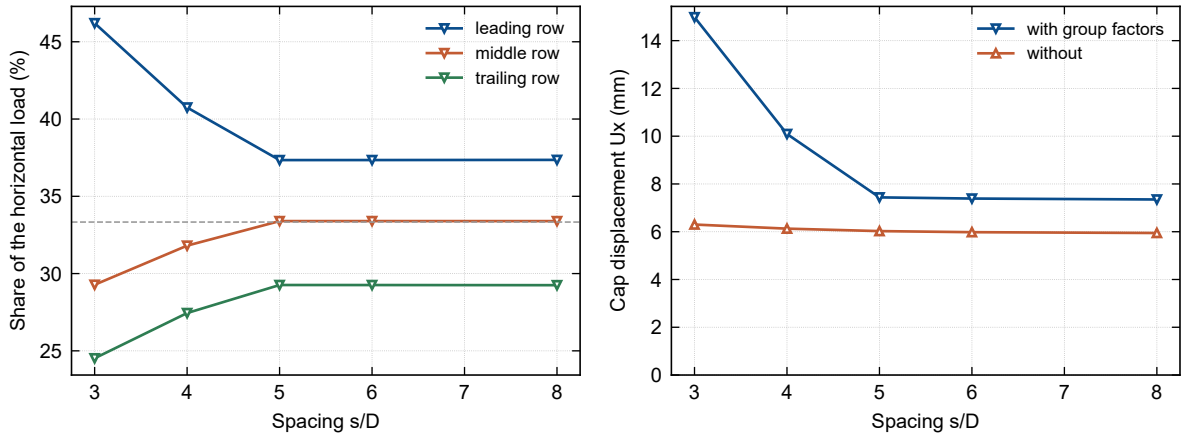

Figure 7.1 — Share of the horizontal load of each row and movement of the cap against the spacing, 3 × 3 group with AASHTO p-multipliers

Because all piles are tied to one cap and move together, a row with a smaller p-multiplier takes a smaller part of the load rather than deflecting more. The reduction of the soil resistance increases the movement of the whole group; the leading row, which keeps most of its resistance, carries the largest shear.

7.7 Axial group effects

The efficiency of a group of piles under axial load can be lower or higher than one, depending on the soil, the installation and the spacing. In cohesionless soil, driving piles at close spacing densifies the soil and can increase the capacity of the group; in cohesive soil, closely spaced piles may fail as a block. Published efficiencies vary widely (O'Neill, 1983; Reese and Van Impe, 2011), and Solgroup does not compute them. When the option *Reduction factors for axial loads* is switched on, a factor entered for each pile multiplies the axial force of its load–displacement curve at every displacement; the displacements of the curve are not changed. With the option off, the factors are ignored.

NOTE Group factors describe the interaction of piles through the soil only approximately. They should be chosen from the design code or from published tests that resemble the foundation, and the sensitivity of the results to them should be checked.

© 2026 Solplan. All rights reserved.

8 Axial resistance of pile groups

8.1 Efficiency of a group

The axial capacity of a group of closely spaced piles can differ from the sum of the capacities of the individual piles. The ratio of the two is the efficiency of the group,

$$\eta = \frac{Q_{group}}{\sum_i Q_i} \tag{8.1}$$

and the settlement of a group under the same load per pile is generally larger than the settlement of a single pile, because the zones of soil stressed by the individual piles overlap below and around the group (Poulos and Davis, 1980). Solgroup analyses the axial response of each pile with its own load-transfer curves and includes the interaction through the cap; the reduction of the capacity or the stiffness by the interaction through the soil is introduced with an axial load reduction factor for each pile (Assign ▸ Pile ▸ Axial Load Reduction Factor), which multiplies the loads of the axial load–displacement curve of the pile and is used when the option *Reduction factors for axial loads* is selected.

8.2 Piles in cohesionless soils

Driving displacement piles into loose to medium-dense sand densifies the sand between the piles. Load tests on groups of driven piles in such sands have shown efficiencies greater than one, increasing as the spacing decreases to about two to three diameters (O'Neill, 1983). In dense sand, or for bored piles that do not densify the soil, efficiencies close to or below one have been measured. A reduction factor of one, that is the capacity of the single pile, is therefore usually adequate for driven piles in sand at spacings of three diameters or more; for bored piles in sand a factor below one may be appropriate where the installation loosens the soil.

8.3 Piles in cohesive soils

In clay the capacity of a closely spaced group may be limited by the failure of the block of soil enclosed by the piles, sliding along the perimeter of the group and bearing at its base, instead of the failure of the individual piles (Whitaker, 1957). The block capacity of a group of width B, length L in plan and depth D is

$$Q_{block} = 2\,(B + L)\,D\,\bar{c} + B\,L\,N_c\,c_{base} \tag{8.2}$$

with the mean undrained strength $\bar{c}$ along the sides of the block, the strength c_{base} below its base and a bearing capacity factor N_{c} of about 9 for deep blocks. The capacity of the group is the smaller of the block capacity and the sum of the capacities of the piles. At spacings of about three diameters or more the individual failure usually governs; at smaller spacings the block can govern, and the efficiency then falls below one. Where the block governs, the axial reduction factor of the piles can be set to the ratio of the block capacity to the sum of the pile capacities. Empirical efficiency formulas based on the geometry of the group alone have been proposed but are not supported by the test evidence and are not recommended.

8.4 Settlement of the group

The settlement of a group under working loads is governed by the compressibility of the soil below the tips of the piles, which is stressed by the whole group. The load-transfer analysis gives the settlement of the piles as single piles, joined through the cap; it does not include the additional settlement caused by the overlap of the stressed zones. For groups in compressible soil, the settlement of the group should be checked separately, for example by treating the group as an equivalent raft at a depth of about two thirds of the pile length and computing the consolidation settlement of the soil below it, and the axial reduction factors chosen so that the settlement of the analysed group matches the estimate.

© 2026 Solplan. All rights reserved.

9 Section mechanics

9.1 Method

The bending response of nonlinear sections is obtained from a moment–curvature analysis by fibre integration. The concrete area is divided into thin strips parallel to the neutral axis; reinforcing bars, strands, casings and cores are represented at their actual positions. For a given curvature φ and neutral-axis depth c the strain varies linearly over the section,

$$\varepsilon(z) = \phi\,(c - z) \tag{9.1}$$

where z is measured from the compressed face. For each curvature the neutral axis is found such that the resultant normal force equals the axial thrust, and the moment and secant stiffness follow:

$$\sum_i \sigma(\varepsilon_i)\,A_i = P, \qquad M = \sum_i \sigma(\varepsilon_i)\,A_i\,(z_g - z_i), \qquad EI = \frac{M}{\phi} \tag{9.2}$$

with z_g the depth of the centroid. The curvature is increased stepwise until the extreme compressive strain reaches the end of the concrete stress–strain curve or the reinforcement reaches its limiting strain.

A nonlinear section is analysed for a list of axial thrusts entered with the section, and one moment–curvature curve is computed for each thrust. Whether the moment is held at its previous maximum where the computed moment decreases, for example immediately after cracking, is an option of the section (Section 9.7).

9.2 Concrete

Unconfined concrete in compression follows a parabola up to the strain ε_0 at peak stress and a linear descending branch to the strain $\varepsilon_u = 0.0038$:

$$f_c = f_c'\left[\frac{2\varepsilon}{\varepsilon_0} - \left(\frac{\varepsilon}{\varepsilon_0}\right)^2\right] \quad (0 \le \varepsilon \le \varepsilon_0), \qquad f_c = f_c'\left[1 - 0.15\,\frac{\varepsilon - \varepsilon_0}{\varepsilon_u - \varepsilon_0}\right] \quad (\varepsilon_0 < \varepsilon \le \varepsilon_u) \tag{9.3}$$

$$\varepsilon_0 = \frac{1.7\,f_c'}{E_c}, \qquad E_c = 4733\sqrt{f_c'}\ \text{(MPa)} \tag{9.4}$$

In tension the same parabola applies up to the rupture stress $f_r = 0.623\sqrt{f'_c}$ MPa ($0.332\sqrt{f'_c}$ MPa for prestressed sections); beyond cracking the tensile stress is zero. Values of E_c and f_r entered by the user replace the derived values. The parabola is that of Hognestad (1951).

9.3 Confined concrete

When confinement is selected, the concrete inside the transverse reinforcement follows the model of Mander, Priestley and Park (1988), while the cover follows the unconfined law. With the effective lateral confining stress f'_l derived from the transverse reinforcement,

$$f_{cc}' = f_c'\left(2.254\sqrt{1 + 7.94\,\frac{f_l'}{f_c'}} - 2\,\frac{f_l'}{f_c'} - 1.254\right), \qquad \varepsilon_{cc} = 0.002\left[1 + 5\left(\frac{f_{cc}'}{f_c'} - 1\right)\right] \tag{9.5}$$

$$f_c = \frac{f_{cc}'\,\xi\,r}{r - 1 + \xi^r}, \qquad \xi = \frac{\varepsilon}{\varepsilon_{cc}}, \qquad r = \frac{E_c}{E_c - f_{cc}'/\varepsilon_{cc}} \tag{9.6}$$

The ultimate strain of the confined concrete, which ends the moment–curvature curve, is taken as (Priestley, Seible and Calvi, 1996)

$$\varepsilon_{cu} = 0.004 + \frac{1.4\,\rho_s\,f_{yh}\,\varepsilon_{su}}{f_{cc}'} \tag{9.7}$$

© 2026 Solplan. All rights reserved.

with the volumetric ratio ρ_s and yield stress f_{yh} of the transverse reinforcement and ε_{su} = 0.09.

9.4 Reinforcing and structural steel

Steel is elastic–perfectly plastic with modulus E_s and yield stress f_y. When strain hardening is selected, the stress beyond the onset of hardening ε_{sh} is

$$f_s = f_y\left[\frac{m\,e+2}{60\,e+2}+\frac{e\,(60-m)}{2\,(30\,q+1)^2}\right]\le f_u, \qquad m=\frac{(f_u/f_y)(30q+1)^2-60q-1}{15\,q^2} \tag{9.8}$$

with $e = |\varepsilon| - \varepsilon_{sh}$ and $q = \varepsilon_{su} - \varepsilon_{sh}$ (Park and Paulay, 1975; Thompson and Park, 1978). Without strain hardening the steel is elastic–perfectly plastic. Steel pipes, H sections, casings and cores are integrated with the same law over their actual geometry. Steel C sections (with or without stiffening lips) about the strong axis, T sections about the weak axis, box sections and the AISC shape families (W, M, S and HP shapes, channels, tees, single and double angles, and hollow structural sections) are described by the width of steel across the bending axis at each distance from the extreme fibre, assembled from plates, rounded corners and rings. Unsymmetrical shapes bend about the geometric axis through their actual centroid. Dimensions of AISC shapes are taken from the AISC Shapes Database, version 14.1 (AISC, 2013).

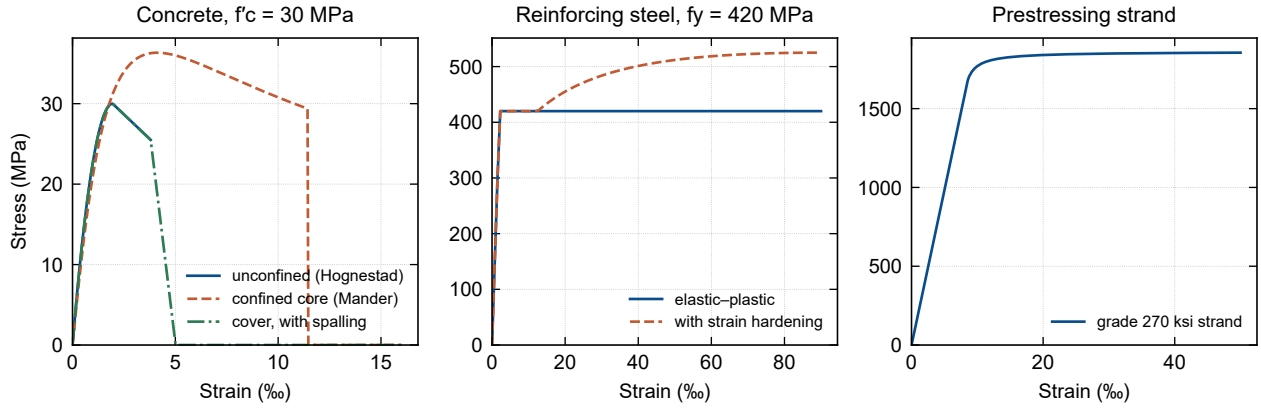

Figure 9.1 — Stress–strain relations used by the moment–curvature analysis: concrete of 30 MPa unconfined and confined by a spiral of US #4 bars at 150 mm in a 0.8 m pile, reinforcing steel of 420 MPa, and prestressing strand

In the confined section of Figure 9.1 the core reaches a strength of 36.3 MPa at a strain of 4.1‰, and keeps a large part of it to much larger strains, while the cover spalls once its crushing strain is exceeded. The gain in strength is modest; the gain in deformation capacity, and with it the ductility of the section, is large.

9.5 Prestressed sections

Seven-wire strands follow the stress–strain relations of the PCI Design Handbook (PCI, 2010): linear with modulus 196.5 GPa (28 500 ksi) up to the limit of proportionality, then

$$f_{ps} = f_{pu} - \frac{A}{\varepsilon_{ps} - B} \tag{9.9}$$

with (ε_{lim}, A, B) = (0.0076, 0.04, 0.0064) for grade 250, (0.0086, 0.04, 0.007) for grade 270, and (0.0088846, 0.0835, 0.0071) for grade 300, stresses in ksi. Prestressing bars are elastic–plastic with modulus 200 GPa (29 000 ksi) and the strength of the selected bar (smooth bars 145 or 160 ksi; deformed bars 150, 157 or 160 ksi depending on the size), and carbon-fibre composite cables are linear-elastic up to rupture. The list of strand and bar sizes, with their areas, depends on the selected strand type. The effective prestress, the prestress force reduced by the fraction of losses, is introduced as an initial strain of the tendons.

© 2026 Solplan. All rights reserved.

9.6 Bending stiffness in the pile analysis

The bending stiffness of a node of a nonlinear section is the secant stiffness of its moment–curvature relation, $EI = M/\varphi$, at the moment of the node in the current iteration (Section 4.1.4), and it varies along the pile with the moment. The relation used for a node is that of the axial thrust of the pile: between two consecutive thrusts of the list the stiffness is interpolated linearly in the axial force. The axial thrusts of the list should therefore bracket the axial forces that the piles carry in the load cases; an axial force outside the list uses the nearest curve.

Below the first computed point the uncracked stiffness is used. When the moment exceeds the largest moment of the relation, the section has reached the end of its computed response; the stiffness of the last point is used and the run reports it. The relation can also be entered by the user, for each axial thrust, as moment–curvature pairs, and for sections whose reinforcement is not symmetric a separate branch for negative moments can be used when the option *Allow non-symmetric nonlinear sections* is on.

Figure 9.2 shows the moment–curvature relation and the secant stiffness of a bored pile of 0.8 m diameter with 16 bars of 420 MPa steel, cover 75 mm, in concrete of 30 MPa (the section of the Getting started tutorial of the User Manual), for axial thrusts of 0, 1,500 and 3,000 kN.

Table 9.1 — Bored pile 0.8 m: stiffness and moment capacity against axial thrust

Thrust (kN)	Initial *EI* (kN·m²)	*M* at which *EI* has halved (kN·m)	Largest moment (kN·m)	*EI* at the largest moment (kN·m²)	Ratio to the initial *EI*
0	682,132	196	1,003	48,083	0.07
1,500	655,972	528	1,312	83,314	0.13
3,000	626,448	951	1,536	121,924	0.19

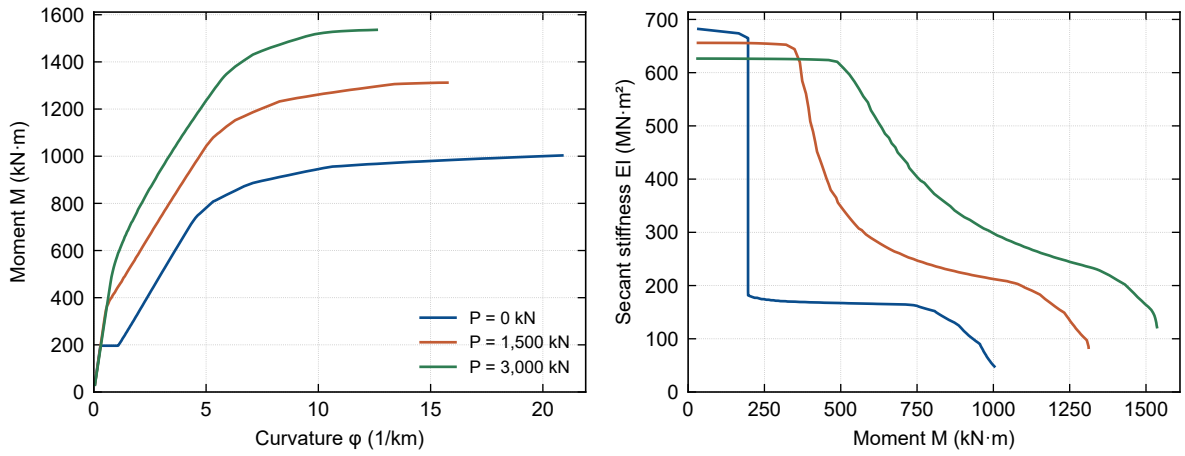

Figure 9.2 — Moment–curvature (left) and secant bending stiffness against moment (right) of a 0.8 m bored pile for three axial thrusts

The stiffness stays at its uncracked value until the concrete in tension cracks, then falls quickly. Without axial force it has halved at 196 kN·m, a fifth of the capacity; at the largest moment it is 7% of the initial value. Axial compression delays the cracking and raises the capacity, so that at 3,000 kN the stiffness halves only at 951 kN·m and keeps 19% of its initial value at the largest moment. Two consequences follow for the analysis of a group. First, the piles of a group under a moment carry different axial forces and therefore have different stiffnesses, and the piles in tension crack first. Second, a fixed-head pile whose section cracks near the head attracts less moment there and deflects more (Example 12 of the User Manual), so that an analysis with the uncracked stiffness overestimates the head moment and underestimates the deflection.

Elastic sections have constant stiffness *EI*. The stiffness about the two axes of a section (EI_{22} and EI_{33}) are computed separately for sections that are not circular.

© 2026 Solplan. All rights reserved.

9.7 Section options

Equivalent diameter for p-y curves. The width b used to generate the p-y curves of a pile can be replaced by an equivalent diameter, for sections that are not circular; the bending stiffness and the moment–curvature relation keep the actual dimensions.

Equivalent elastoplastic moment–curvature (CALTRANS). Following the Caltrans Seismic Design Criteria (Caltrans, 2013), the computed curve (φ_k, M_k) is replaced by a bilinear one. The anchor point a is the first yield of the reinforcement or of the steel tube (the first cracking of the concrete for prestressed sections), and the elastic stiffness is $EI_{el} = M_a/\varphi_a$. The plastic moment M_p makes the areas under the two curves equal beyond the anchor,

$$\sum_{k \geq a+2} \left(\varphi_k - \varphi_{k-1} \right) \frac{\min \left(EI_{el}\, \varphi_k,\ M_p \right) - M_k}{2} = 0 \tag{9.10}$$

and is found numerically. The idealised curve is $M = EI_{el}\, \varphi$ up to the idealised yield curvature $\varphi_y' = M_p/EI_{el}$ and $M = M_p$ up to the last computed curvature φ_u; the plastic curvature capacity is $\varphi_u - \varphi_y'$.

Adjusted softening. With the option on (the default), each moment of the computed curve is replaced by the largest moment reached at a smaller curvature, so that the curve, and with it the bending stiffness used in the pile analysis, does not follow a falling branch after the peak. With the option off the computed moments are used as they are.

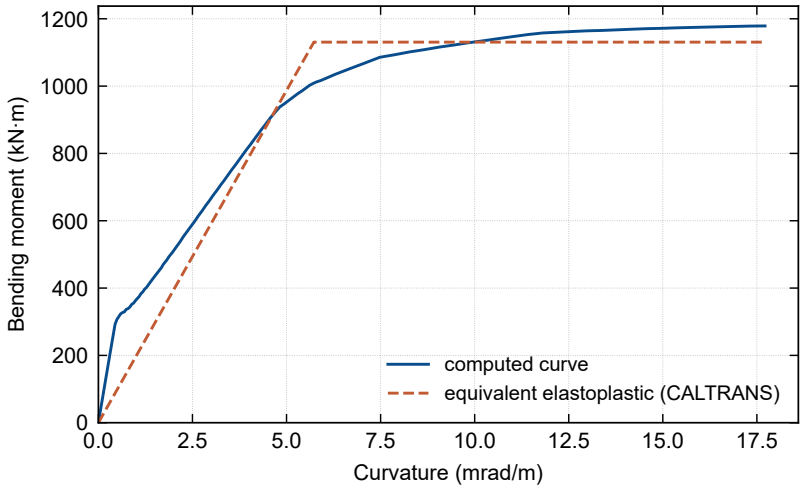

Figure 9.3 — Moment–curvature of a 0.8 m bored pile at a thrust of 1 000 kN and its equivalent elastoplastic idealisation

© 2026 Solplan. All rights reserved.

10 Structural checks of the piles

Besides the forces and the deflections, Solgroup reports quantities that compare the actions in the piles with the strength of their sections: a plastic hinge for elastic sections with a specified moment capacity, the total normal stress of elastic sections, and demand/capacity ratios of the combinations. This chapter defines them.

10.1 Elastic section with a specified moment capacity

A section of the behaviour *Elastic with specified moment capacity* is elastic up to its moment capacity and then yields without further increase of moment. In each bending plane its moment–curvature relation is

$$M = EI\,\phi \quad (\,|\,\phi\,|\, \le \phi_y), \qquad M = M_p\,\mathrm{sign}(\phi) \quad (\,|\,\phi\,|\, > \phi_y), \qquad \phi_y = \frac{M_p}{EI} \tag{10.1}$$

with the moment capacity M_p of the plane: the Moment capacity about axis 3 for bending with EI_{33}, and about axis 2 for bending with EI_{22}. The relation is used like the moment–curvature relation of a nonlinear section (Section 9.6): where the moment of a node reaches M_p, its secant stiffness drops to M_p/φ and a hinge forms. The moment along the pile can then not grow further at that point, and additional load is carried by a redistribution of the moments to other parts of the pile and to the other piles, at the price of larger deflections.

Figure 10.1 compares the reference group of Chapter 13 with elastic sections and with the same sections given a capacity of 200 kN·m, under horizontal loads from 300 to 1 500 kN.

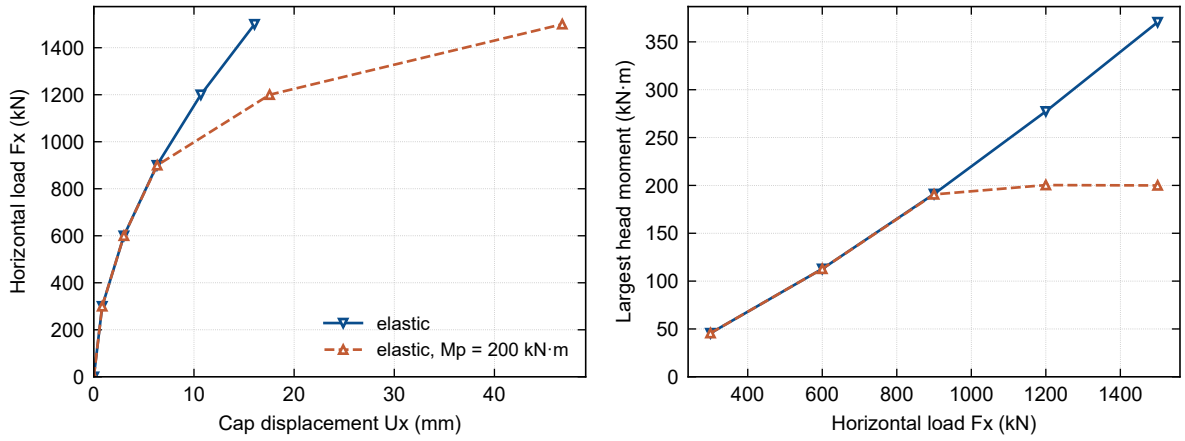

Figure 10.1 — Load–displacement curve (left) and head moment (right) of a group with elastic sections and with a moment capacity of 200 kN·m

Up to 900 kN the head moments stay below the capacity and the two models coincide. At 1 200 kN the elastic piles would carry 277 kN·m at the heads; with the capacity the head moment stays at 200 kN·m, hinges form at the heads, and the cap moves 17.6 instead of 10.7 mm. At 1 500 kN the displacement is 46.8 mm against 16.0 mm. The largest moment anywhere along the piles, 202.5 kN·m, exceeds the capacity by about one per cent, which is the tolerance of the iteration on the secant stiffness. A group whose heads have all hinged still carries load through the bending of the piles below the heads and through the soil, but its stiffness has fallen sharply; the load at which the first hinge forms is the useful limit of an elastic design.

10.2 Total stress of elastic sections

For elastic sections the normal stress at the extreme fibre is computed at every node from the axial force N and the moments of the two bending planes. For circular and annular sections, and for general sections without a rectangular or H outline, the resultant moment acts on the same section modulus S in every direction:

© 2026 Solplan. All rights reserved.

$$\sigma = \frac{|N|}{A} + \frac{\sqrt{M_2^2 + M_3^2}}{S} \tag{10.2}$$

For other shapes the two bending stresses are added at the corner, each with the section modulus of its plane:

$$\sigma = \frac{|N|}{A} + \frac{|M_3|}{S_{33}} + \frac{|M_2|}{S_{22}} \tag{10.3}$$

The axial term is taken as a magnitude, so the stress is the largest normal stress in compression or tension. No total stress is given for nonlinear sections, whose strength is described by their moment–curvature relation.

10.3 Demand/capacity ratios

For load combinations of the type Linear Add the program computes, at every node of every pile, the ratio of the bending moment and of the shear force to the factored capacity of the section at that node:

$$\mathrm{D/C}_M = \sqrt{\left(\frac{M_{(2)}}{\phi_b M_{n,33}}\right)^2 + \left(\frac{M_{(3)}}{\phi_b M_{n,22}}\right)^2} \tag{10.4}$$

$$\mathrm{D/C}_V = \sqrt{\left(\frac{V_2}{\phi_v V_{n,2}}\right)^2 + \left(\frac{V_3}{\phi_v V_{n,3}}\right)^2} \tag{10.5}$$

where $M_{(2)}$ is the moment of bending in the plane of local axis 2, resisted by the capacity about axis 3, and $M_{(3)}$ that in the plane of axis 3; V_2 and V_3 are the shear forces along the two axes. The capacities are those of the Design (LRFD) tab of the section used at the node, so that a pile with a section along its length is checked against the section of each segment, unless the combination gives capacities of its own, which then apply to all piles. The resistance factors φ_b and φ_v are properties of the combination, by default 0.90 and 0.75. When only one of the two capacities of a pair is entered, it is used for both axes; when both are zero, or the resistance factor is zero, no ratio is computed and the result is left empty. Load cases, and combinations of other types, have no ratios.

A nonlinear section obtains its moment capacities from **Compute moment capacity from M-φ**: the capacity about axis 3 is the largest moment of the moment–curvature curve at the first axial thrust of the list of the section, and the capacity about axis 2 the largest moment of the curve of the section turned through 90°, which equals the first for a section symmetric in both planes. Because the capacity depends on the axial force, the first thrust of the list should be the one that governs the design.

As an example, the worked example of the User Manual is given capacities M_n = 250 kN·m and V_n = 300 kN in both planes and analysed under the combination 1.4D (Figure 10.2). The moment ratio is largest at the fixed head, 0.300; the head moment of 67.5 kN·m divided by 0.90 × 250 kN·m gives 0.300, the same value. The shear ratio reaches 0.203.

© 2026 Solplan. All rights reserved.

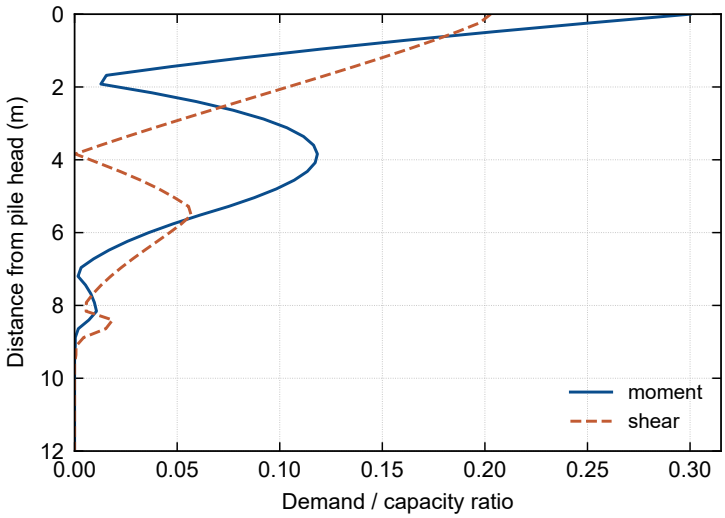

Figure 10.2 — Demand/capacity ratios of moment and shear along a pile of the worked example under 1.4D

© 2026 Solplan. All rights reserved.

11 Embedded pile cap

11.1 Soil resistance on the cap

A pile cap cast below the ground surface is pushed against the soil when it moves laterally, and the passive resistance of that soil adds to the lateral resistance of the piles. Tests on full-scale pile groups (Mokwa and Duncan, 2001) show that this resistance can be a large part of the lateral capacity of a foundation at small deflections. When the soil resistance on the cap is included, Solgroup describes it with the p-y criteria of the soil layers in contact with the cap, treating the front face of the cap like a wide pile (Reese and Van Impe, 2011):

- The zone of contact extends over the thickness of the cap, from the bottom of the cap at the elevation of the pile heads to the top of the cap, or between elevations entered by the user.
- The width of the face is the equivalent diameter entered with the cap; zero selects the diagonal of the cap in plan, which suits a load in any horizontal direction.
- The resistance at a depth is given by the p-y curve of the layer at that depth, with the equivalent diameter as the width, at the lateral movement of the cap.

The resistance acts on the cap only; it does not change the soil reaction of the piles below the cap.

11.2 Method of analysis

Equivalent lateral load. The soil reaction is taken to vary linearly over the contact zone, from zero at the ground surface to the value of the p-y curve at the bottom of the cap, for the current movement of the cap. Its resultant is applied to the cap as a horizontal force opposing the movement. In a three-dimensional model the resultant is resolved into the two horizontal directions in proportion to the components of the movement of the cap.

Equivalent lateral springs. The contact zone is divided into a number of equal increments (between 1 and 20). At each of their end points the reaction is taken from the p-y curve of the layer at the depth of the point below the top of the soil, at the movement of the cap at that point, which includes the effect of the rotation of the cap. In a three-dimensional model the reaction at a point acts along the resultant horizontal movement of that point. The reactions are integrated over the thickness and applied to the cap as forces and moments. Because every point uses its own depth and its own movement, this method generally gives a larger resistance than the equivalent load.

In both methods the resistance is recomputed in every iteration of the cap, so that its nonlinearity is included in the equilibrium of (2.6).

11.3 Effect on the lateral response

Figure 11.1 shows the horizontal load against the movement of the cap for the 3 × 3 group of the examples with the pile heads 1.5 m below the ground surface, so that the cap, 1 m thick, lies wholly in the soft clay. At F_x = 900 kN the cap moves 4.44 mm without resistance on the cap, 4.00 mm with the equivalent lateral load and 3.83 mm with the equivalent lateral springs; the soil on the cap carries 48 kN and 68 kN respectively. At 1800 kN the corresponding movements are 15.93, 14.75 and 14.28 mm, with 74 and 105 kN on the cap.

© 2026 Solplan. All rights reserved.

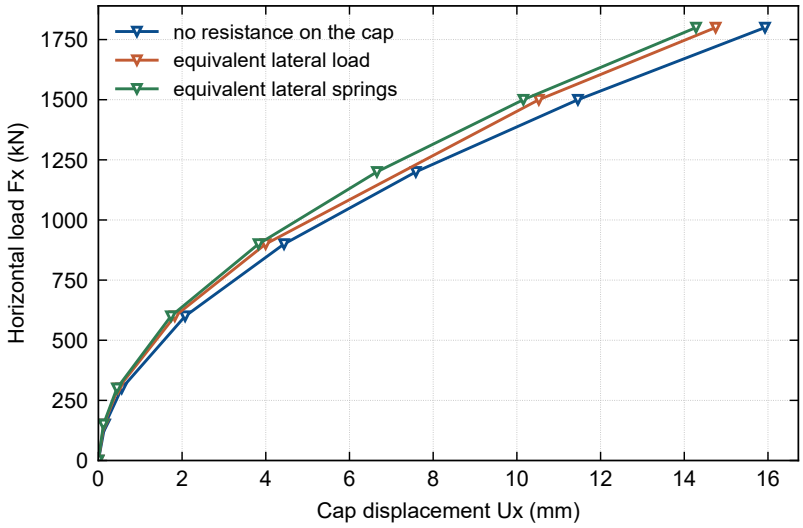

Figure 11.1 — Horizontal load against the movement of an embedded cap in soft clay, without and with the soil resistance on the cap

The resistance of the cap grows with the movement but less than in proportion to it, as the p-y curves of the soil in contact soften. In soft clay near the surface the contribution is a small part of the load; in stiff clay or dense sand, and for a deeper or thicker cap, it is larger, because the ultimate resistance of the p-y curves grows with the strength of the soil and with the depth. The springs give the larger resistance of the two methods, as explained above.

NOTE The soil in front of a cap may be disturbed by excavation and backfilling, may shrink away from the cap, or may be removed later. Include its resistance only where it can be relied on for the life of the structure.

© 2026 Solplan. All rights reserved.

12 Foundation stiffness and pushover

12.1 Stiffness of the foundation

A structural model of a bridge pier, a building or a jetty often represents the pile foundation by springs at the base of the structure. The stiffness of the foundation relates the forces on the cap to the movement of its reference point,

$$\mathbf{F} = \mathbf{K}\,\mathbf{U} \tag{12.1}$$

where $\mathbf{K}$ is a 6×6 matrix (3×3 in the vertical plane of a two-dimensional idealisation). Because the response of the piles is nonlinear, $\mathbf{K}$ depends on the level of loading. Solgroup computes it in two ways, selected on the **Foundation Stiffness** page of a load case.

12.1.1 Based on the nonlinear soil response

The cap is loaded with one component of the load of the case at a time; the other components are zero. For each component j the analysis is repeated at a series of load levels, the load factors of the case times the component. At each level the secant flexibility

$$S_{ij} = \frac{U_i}{P_j} \tag{12.2}$$

is the movement U_i of the cap per unit of the load P_j applied at that level, and the stiffness matrix of the level is the inverse of the flexibility matrix, $\mathbf{K} = \mathbf{S}^{-1}$. The coupling terms of $\mathbf{K}$ therefore follow from the inverse of the full matrix, not from the reciprocals of the individual flexibilities. When only the diagonal terms are requested, $K_{ii} = 1/S_{ii}$. A component whose load is zero in the case is not swept; its diagonal term is reported as 1.0 with a warning. The stiffness decreases as the load level increases, which shows how far the response of the foundation departs from a linear spring.

12.1.2 Based on equivalent elastic springs

The nonlinear analysis is carried out at the load of the case, or with the load scaled so that the movement of the cap reaches a target deflection within a tolerance. The scaling is found by a secant iteration on the load factor; the target can be given at several factors of the target deflection, and either all components of the load or only the component associated with the target are scaled. In the state reached, every pile is replaced by linear springs:

- lateral springs at the nodes, equal to the soil reaction divided by the deflection at that node, times the length of the increment;
- an axial spring at the head, equal to the axial force divided by the axial movement of the head, and a torsional spring equal to the torque divided by the rotation (zero for a head pinned in both planes);
- for nonlinear sections, an equivalent elastic bending stiffness of the section.

Each pile is then condensed statically to its head, as a beam on these springs, with the head connection of the pile, and the stiffness matrices of the heads are assembled through the kinematics of the cap ((2.7)). The axial force of the piles can be included through the geometric stiffness of the beam, which softens the piles in compression and stiffens them in tension. The result is a symmetric matrix that reproduces, with linear springs, the movement of the nonlinear group at the target deflection.

NOTE A foundation stiffness is valid for the level of loading at which it was computed. For a structural analysis with loads of different magnitude, compute the stiffness at the corresponding levels.

12.1.3 Comparison of the two methods

Figure 12.1 compares the diagonal terms of the stiffness of the 3 × 3 group of the examples under F_x = 900 kN, F_z = −2,700 kN and M_y = 600 kN·m, at fractions of this load from 0.2 to 1. The lateral stiffness K_{11} falls from 552,763 kN/m at 0.2 of the load to 146,699 kN/m at the full load with the nonlinear sweep, and from 580,121 to 150,619

© 2026 Solplan. All rights reserved.

kN/m with the equivalent springs. The vertical stiffness K_{33}, about 4,601,049 kN/m, does not change, because the axial forces stay on the initial part of the load–displacement curves of the piles; the rotational stiffness K_{55} changes little for the same reason, as it comes mostly from the axial forces of the piles.

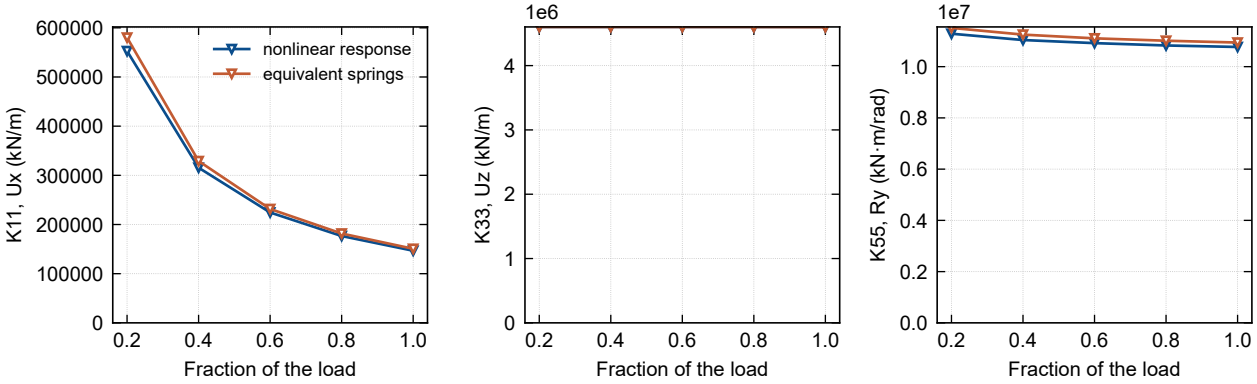

Figure 12.1 — Diagonal stiffness of a 3 × 3 group against the fraction of the load, from the nonlinear sweep and from equivalent springs

The diagonal terms of the two methods agree within a few per cent. The coupling term between the horizontal movement and the rotation, K_{15}, differs more (−113,345 against −300,429 kN at the full load), because the sweep loads one component at a time while the springs describe the state of the piles under all components together. Where the coupling matters to the structural model, the method should be chosen to match the way the structure loads the foundation.

12.2 Pushover analysis

A pushover analysis follows the response of the group to an increasing load. The load of the case is multiplied by a series of up to 25 load factors, generated from a first to a last factor with an arithmetic or a logarithmic ramp. Each factor is a complete analysis of the group under the factored load. Components of the load can be held constant, so that for example the vertical load stays at its service value while the horizontal load and the moment increase. The loads along the piles and the soil movements are factored with the cap load unless they are held constant as well.

The result is the path of the cap movement against the load factor, shown with the special plots. The analysis continues until the last factor or until the group no longer reaches equilibrium; the last converged factor then marks the load at which the foundation, as modelled, fails.

© 2026 Solplan. All rights reserved.

13 Parametric studies

This chapter shows how the main parameters of a pile group govern its response. Each study changes one parameter of a reference model and keeps the others; all results were computed by Solgroup 1.0.16. Unless stated otherwise the reference is the group of the worked examples: nine piles of 0.6 m diameter and 24 m length in a 3 × 3 arrangement at 1.8 m (three diameters), under a rigid cap with fixed heads, in soft clay over stiff clay and dense sand, loaded with F_x = 900 kN and F_z = −2 700 kN at the cap. The studies are illustrations of trends, not design rules; the numbers belong to these models.

13.1 Length of the piles

The length of the piles of the reference group is varied from 6 to 30 m (Figure 13.1).

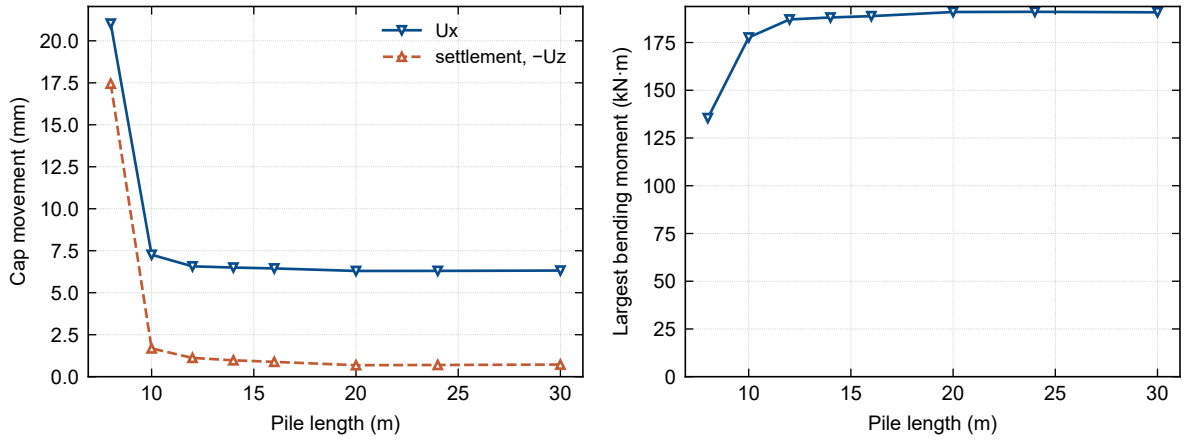

Figure 13.1 — Cap movement (left) and largest bending moment (right) against the length of the piles

Piles of 6 m do not carry the vertical load: their tips are in the soft clay, the axial load–displacement curves are exhausted and the run does not converge. At 8 m the group carries the load, but the short piles rotate in the soil as rigid bodies: the cap moves 21.0 mm horizontally and settles 17.4 mm, and the largest moment lies 3.6 m below the heads. From about 10 to 12 m the piles behave as long, flexible piles: the horizontal movement settles at about 6.3 mm and the head moment at about 191 kN·m, and a longer pile no longer changes the lateral response, because the lower part of the pile does not deflect. The settlement keeps falling as more shaft resistance is mobilised, until about 20 m; beyond that the elastic shortening of the longer pile slightly outweighs the additional resistance. The length that matters for the lateral response is therefore much smaller than the length needed for the axial capacity.

13.2 Batter of the piles

The two outer rows of the reference group, normal to the load, are battered outward by 0 to 20°; the middle row stays vertical (Figure 13.2).

© 2026 Solplan. All rights reserved.

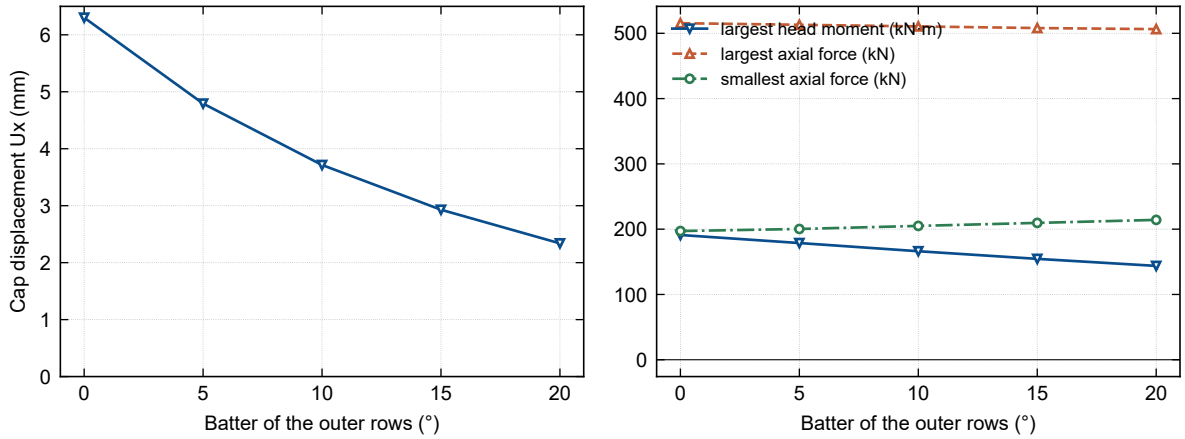

Figure 13.2 — Cap displacement (left) and pile forces (right) against the batter of the outer rows

A batter of 5° already reduces the horizontal movement from 6.30 to 4.79 mm, and 20° to 2.34 mm, because the axial stiffness of a pile is much larger than its lateral stiffness and the inclined piles carry part of the load axially. The head moments fall with the displacement, from 191 to 144 kN·m. The range of the axial forces narrows slightly, because the smaller head moments transfer less moment to the cap. In a real group the gain in lateral stiffness must be weighed against the larger axial forces of the battered piles under the governing combinations, the bending of battered piles in settling ground and the cost of driving them.

13.3 Free length and axial load

Four steel pipe piles of 610 × 12 mm at 2.4 m stand in water, with 6 m of soft clay over medium sand and 30 m of embedment; the free length above the seabed is varied from 0 to 16 m. A horizontal load of 200 kN acts with no vertical load, and again with 8 000 kN, 2 000 kN per pile (Figure 13.3).

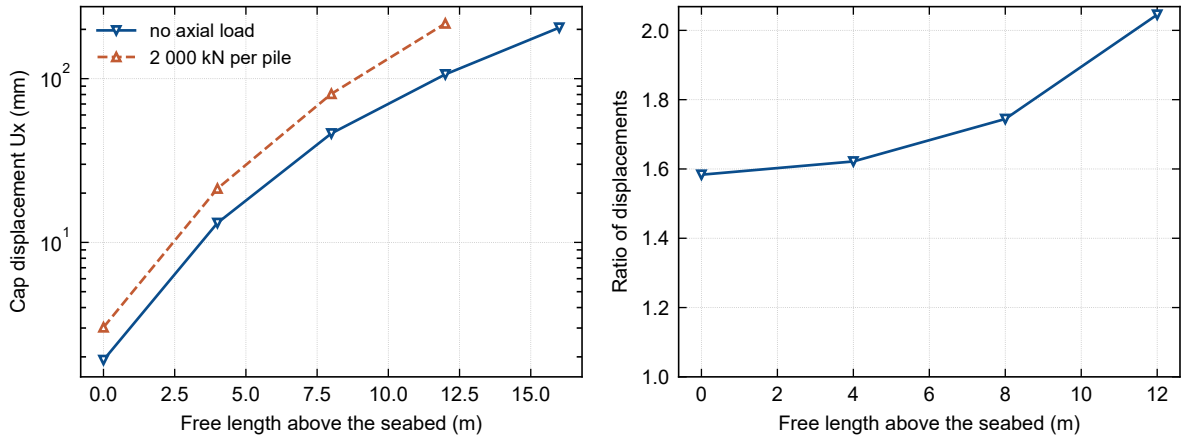

Figure 13.3 — Cap displacement against the free length (left, logarithmic scale) and ratio of the displacements with and without the axial load (right)

Without axial load the displacement grows steeply with the free length, from 1.9 mm at the seabed to 205 mm at 16 m. The axial load amplifies it through the second-order moment $P{\cdot}y$ of each pile ((4.1)): the ratio of the displacements grows from 1.58 at the seabed to 2.05 at 12 m. At 16 m with the axial load the analysis does not converge: the axial force has consumed the lateral stiffness left by the long free length and the soft clay, the behaviour of a pile close to buckling. For free-standing piles the amplification should be read from the analysis with the axial load of each combination, and a case that fails to converge only when the axial load is present should be treated as a sign of instability, not as a numerical difficulty.

© 2026 Solplan. All rights reserved.

13.4 Number of piles

Square groups of 1 to 25 piles at three diameters carry 100 kN horizontally and 300 kN vertically per pile, without reduction for group effects and with the factors of the method *Closely-spaced piles* (Figure 13.4).

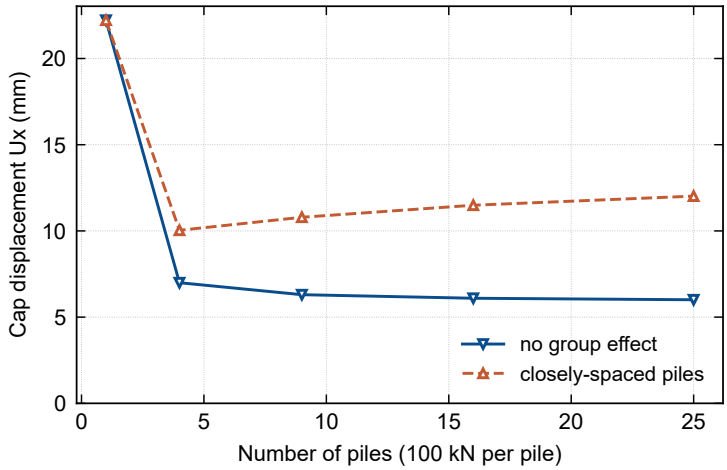

Figure 13.4 — Cap displacement against the number of piles at the same load per pile

The single pile under a cap moves 22.2 mm, much more than any group, because a single pile cannot stop the rotation of its cap and behaves as a free-head pile; in a group the push and pull of the piles holds the cap, and the heads act as fixed. Without group effects the displacement then changes little with the number of piles. With the factors of closely spaced piles it grows with the size of the group: the ratio of the displacements with and without the factors is 1.43 for 2 × 2 piles, 1.71 for 3 × 3 and 2.00 for 5 × 5, because the piles inside a large group are shadowed by more piles in front of them and beside them (Chapter 7). Ignoring the group effect in a large group of closely spaced piles can therefore halve the computed displacement.

13.5 Rotational restraint of the pile heads

The heads of the reference group are connected to the cap by rotational springs of stiffness 10^2 to 10^7 kN·m/rad, and compared with pinned and fixed heads (Figure 13.5).

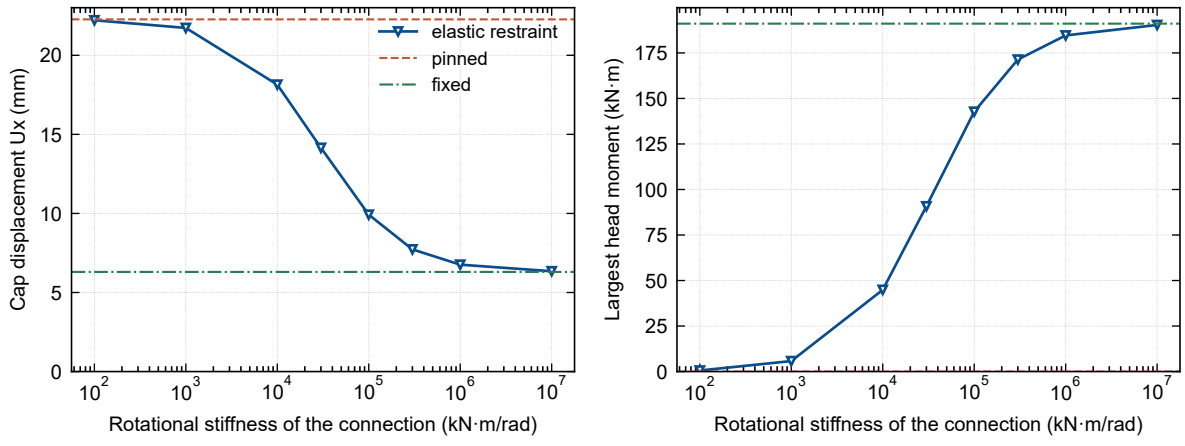

Figure 13.5 — Cap displacement (left) and head moment (right) against the rotational stiffness of the connection

Below about 10^3 kN·m/rad the connection behaves as a pin, and above about 10^6 kN·m/rad it approaches a fixed head; the transition lies where the stiffness of the connection is comparable with the rotational stiffness of the pile head in the soil. The largest moment along the pile does not follow the head moment: pinned heads have no moment at the head but 194 kN·m in the soil, fixed heads 191 kN·m at the head, and at 30,000 kN·m/rad the largest moment

© 2026 Solplan. All rights reserved.

is only 126 kN·m, the head moment and the moment in the soil being of similar size. The stiffness of the connection, which is rarely known precisely, therefore affects both the displacement and the distribution of the moments; where it is uncertain, the two limits should be analysed.

13.6 Thickness of a flexible cap

A 3 × 3 group at 2.4 m carries a vertical load of 5 400 kN at the centre of a flexible cap whose thickness is varied from 0.3 to 3.0 m, and of a rigid cap (Figure 13.6).

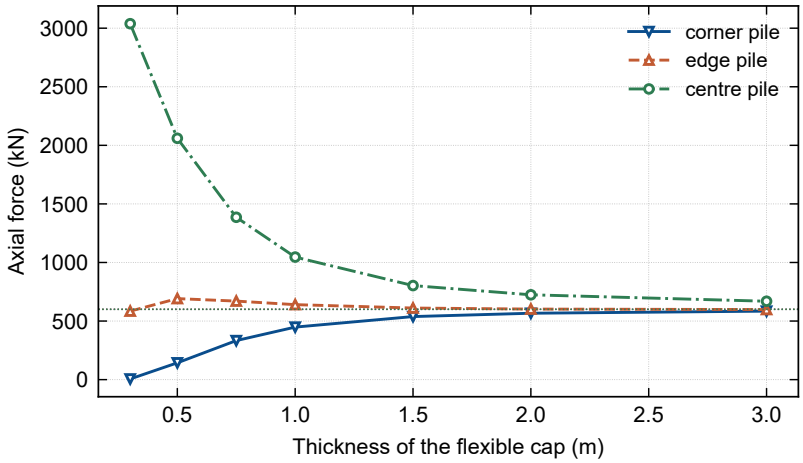

Figure 13.6 — Axial forces of the corner, edge and centre piles against the thickness of the flexible cap; the dotted lines are the values under a rigid cap

Under the rigid cap the nine identical piles carry 600 kN each. A thin cap bends under the central load and the centre pile takes most of it: 3,038 kN at 0.3 m, while the corner piles are left with 6 kN. As the cap thickens the forces approach those of the rigid cap, but slowly: at 3.0 m, more than the pile spacing, the centre pile still carries 669 kN, 12 % more than under a rigid cap, the whole load acting at one point, directly above it. Whether a cap may be taken as rigid depends on the stiffness of the piles as well as on the cap; with stiff, end-bearing piles or concentrated column loads the flexible cap should be used.

13.7 Mesh of a flexible cap

The cap of 0.5 m thickness of the previous study is meshed with elements from 1.2 m down to 0.15 m (Figure 13.7); the number of plates grows from 36 to 1,600.

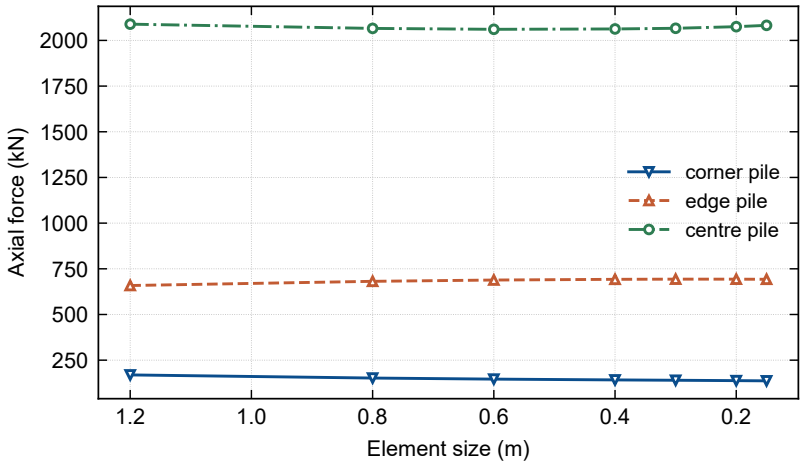

Figure 13.7 — Axial forces of the corner, edge and centre piles against the element size of the mesh of a flexible cap 0.5 m thick

© 2026 Solplan. All rights reserved.

Table 13.1 — Pile forces against the element size

Element size (m)	Plates	Corner (kN)	Edge (kN)	Centre (kN)	Largest change to the finest mesh
1.20	36	169	659	2,089	23.7 %
0.80	64	152	681	2,066	11.2 %
0.60	100	146	689	2,061	6.9 %
0.40	256	142	692	2,063	3.7 %
0.30	400	140	693	2,066	2.3 %
0.20	900	138	693	2,075	0.8 %
0.15	1,600	137	693	2,082	0.0 %

The coarse mesh of 1.2 m, one element per half spacing, already gives the distribution between the piles, but its corner force is 24 % off. At 0.4 m, about one sixth of the pile spacing, the forces are within 4 % of the finest mesh. Beyond that the edge forces no longer change, while the force of the centre pile keeps rising slowly: the load is applied at a single node above it, and in a plate with shear deformation the deflection under a point load grows without limit as the mesh is refined. A concentrated column load is therefore better represented as a pressure over the area of the column, and a mesh of about a sixth of the pile spacing is a reasonable start, to be confirmed by one refinement.

13.8 Depth of a soil movement

The reference group carries only its vertical load, and a free-field soil movement of 100 mm at the ground surface, decreasing linearly to zero at a depth of 2 to 12 m, is assigned to all piles (Figure 13.8).

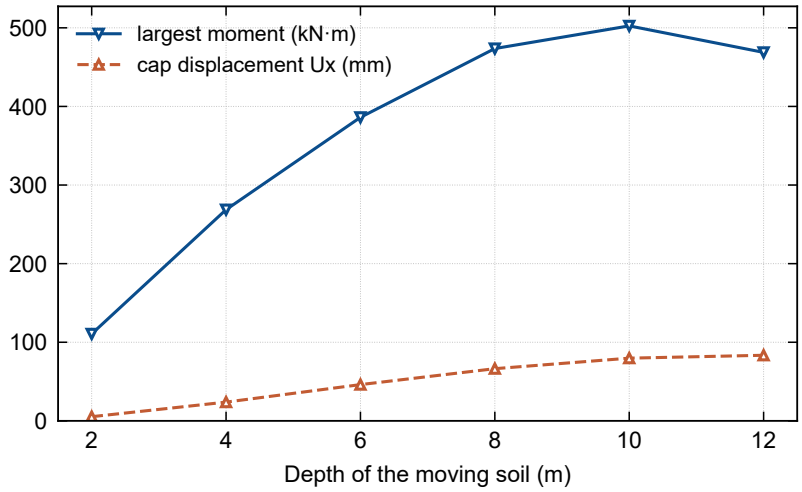

Figure 13.8 — Largest moment and cap displacement against the depth of the moving soil, with 100 mm of movement at the surface

A shallow movement of 2 m moves the cap only 5.3 mm: the piles reach far into stable soil, which holds them, and the moving layer flows around them. As the moving zone deepens, the stable soil has less leverage and the group is carried along: at 12 m the cap moves 83 mm, close to the 100 mm of the surface. The largest moment grows from 111 kN·m to a maximum of 502 kN·m at a depth of 10 m, and moves from the heads to the boundary between the moving and the stable soil (10.1 m below the heads at 10 m). The most severe case for the bending of the piles is therefore not the deepest movement but an intermediate one, at which the piles are loaded over a large length and still restrained below; the depth of the moving zone, which is often uncertain, should be varied over its plausible range.

© 2026 Solplan. All rights reserved.

13.9 Choice of the p-y criterion

One pile of 0.6 m diameter under its own cap, which acts as a free head, carries 150 kN horizontally. The upper 8 m of soil is described in turn by four criteria for a clay of c_u = 50 kPa and ε_{50} = 0.01, and by two criteria for a sand of φ' = 35°, with the same unit weights; the soil below is unchanged (Figure 13.9, Table 13.2).

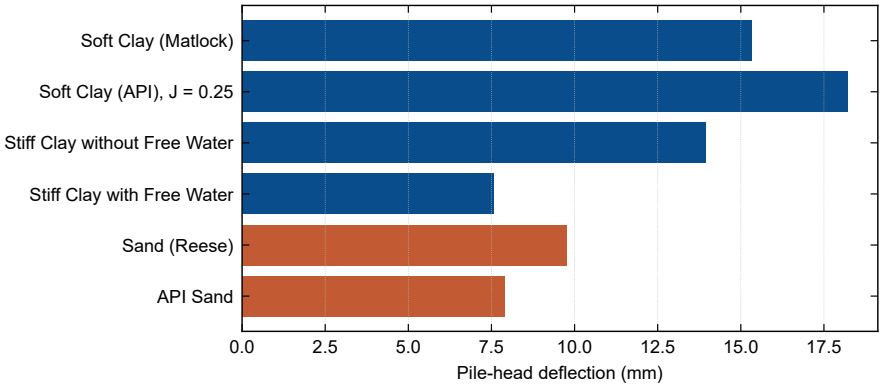

Figure 13.9 — Pile-head deflection under 150 kN for the same soil described by different p-y criteria

Table 13.2 — Response of one pile for different p-y criteria

Criterion of the upper 8 m	Head deflection (mm)	Largest moment (kN·m)	Depth of the largest moment (m)
Soft Clay (Matlock)	15.3	219	2.9
Soft Clay (API), J = 0.25	18.2	226	2.9
Stiff Clay without Free Water	13.9	218	2.6
Stiff Clay with Free Water	7.6	185	1.9
Sand (Reese)	9.8	196	2.2
API Sand	7.9	184	1.9

For the same strength the four clay criteria give head deflections between 7.6 and 18.2 mm, a factor of more than two, while the largest moments differ much less, by about a fifth. The criterion of stiff clay with free water is the stiffest here because its curves start with the initial modulus $k\,x$ and its peak lies at a smaller deflection; the API form of soft clay with J = 0.25 is the softest, because the smaller J lowers the ultimate resistance near the surface. The two sand criteria differ by about a quarter in deflection. The deflection of a laterally loaded pile is thus more sensitive to the choice of the criterion than to most other inputs, while its moment is less so; the criterion should match the soil and the loading for which it was derived (Section 5.11), and where the choice is uncertain, the analysis should be repeated with the alternatives.

© 2026 Solplan. All rights reserved.

14 Verification

This chapter compares results of Solgroup 1.0.16 with closed-form solutions and with conditions that the solution must satisfy exactly. The soil-response curves themselves are empirical; their validity rests on the field tests reported in the publications cited in Chapter 4. All results in this chapter were computed with Solgroup 1.0.16.

14.1 Long pile on a linear subgrade

For a long pile of constant bending stiffness EI on a linear subgrade $p = k\,y$, without axial force, (4.1) has the closed-form solution of Hetényi (1946). With $\lambda = (k/4EI)^{1/4}$, the head shear and moment needed to impose a head deflection y_0 are

$$V_{\text{fixed}} = 4\,EI\,\lambda^3 y_0, \qquad M_{\text{fixed}} = 2\,EI\,\lambda^2 y_0, \qquad V_{\text{pinned}} = 2\,EI\,\lambda^3 y_0 \tag{14.1}$$

for a fixed head (no rotation) and a pinned head (no moment). The pile has EI = 100,000 kN·m², k = 20,000 kN/m² and length $L = 10/\lambda$ = 21.15 m; the head deflection is 10 mm. The closed form gives V_{fixed} = 422.95 kN, M_{fixed} = 447.21 kN·m and V_{pinned} = 211.47 kN. Table 14.1 gives the ratio of the computed to the exact values for increasing numbers of increments.

Table 14.1 — Long pile on a linear subgrade: computed / exact

Increments n	h (m)	V_{fixed}	M_{fixed}	V_{pinned}
50	0.423	0.99025	0.98020	1.01005
100	0.211	0.99752	0.99501	1.00250
200	0.106	0.99938	0.99875	1.00063
400	0.053	0.99984	0.99969	1.00016

The error decreases by a factor of four each time the increment length is halved, as expected of the central finite-difference scheme. With the default number of increments of a typical pile the error of the head forces is a fraction of a per cent.

14.2 Symmetric group under a rigid cap

Four identical piles at the corners of a square of side 3.0 m are joined by a rigid cap. Each pile has a linear axial spring of stiffness k_a = 200,000 kN/m. By symmetry, a vertical load P = 4,000 kN at the centre must be shared equally, and the cap must settle $P/(4k_a)$ = 5.000 mm; a horizontal load H = 200 kN must likewise be shared equally between the pile heads.

Table 14.2 — Symmetric group under a rigid cap

Quantity	Result
Largest deviation of a pile axial force from $P/4$, relative to P	0.0e+00
Settlement of the cap (mm), exact 5.000	5.000
Largest deviation of a pile shear force from $H/4$, relative to H	5.3e−05
Residual of the equilibrium of the cap under H, relative to H	6.6e−13

The vertical load is shared exactly and the settlement equals the exact value. The equilibrium of the cap under the horizontal load is satisfied to the precision of the arithmetic.

14.3 Equilibrium of the worked example

In the worked example of the User Manual (SPL-SG-002, chapter “Worked example”), a rectangular group of nine piles in layered clay and sand carries a vertical load of 5,400 kN, a horizontal load of 300 kN and a moment. The sums of the pile head forces are 5,907.84 kN (axial) and 300.00 kN (shear), equal to the applied loads.

© 2026 Solplan. All rights reserved.

14.4 Independence of the position of the group

The response of a group cannot depend on where it lies in the global coordinate system. The worked example was moved as a whole, piles and cap together, to site coordinates and analysed again. Table 14.3 gives the largest difference of all cap displacements and pile head forces, relative to the largest value.

Table 14.3 — Worked example moved to site coordinates

X (m)	Y (m)	Largest relative difference
300,000	700,000	1.8e−12
500,000	9,200,000	2.6e−11

14.5 Axial forces in a ring of piles

Eight identical piles on a ring of radius R = 3 m under a rigid cap carry a vertical load of 8 000 kN, a horizontal load of 600 kN and a moment of 2 400 kN·m about the horizontal axis perpendicular to the horizontal load (Example 18 of the User Manual). With a rigid cap and identical piles, the change of the axial force of a pile is proportional to its distance from the axis of bending. The moment of inertia of the ring about any horizontal axis through its centre is $I = nR^2/2$, and the moment carried by the axial forces is the applied moment plus the bending moments of the fixed pile heads, which act on the cap:

$$\Delta N_{max} = \frac{\left(M + \sum M_{head}\right) R \cos\alpha}{I} \tag{14.2}$$

where α is the angle between the direction of the load and the nearest pile. The head moments are those of the analysis; the check concerns the distribution of the axial forces by the cap.

Table 14.4 — Largest change of the axial force in the ring

Direction of load	ΣM_{head} (kN·m)	ΔN, (14.2) (kN)	ΔN, Solgroup (kN)
0°, towards a pile	1,030.0	285.8351	401.3814
22.5°, between two piles	1,030.0	264.0768	379.6232

The two agree to the fourth decimal for both directions.

14.6 Equilibrium of battered piles

In a group with battered piles the horizontal load is carried partly by the shears of the piles and partly by the horizontal components of their axial forces. The shear of a pile acts perpendicular to its axis, so for a pile battered by the angle β in the plane of the load, horizontal equilibrium of the cap requires

$$\sum_i V_i \cos\beta_i + \sum_i \pm N_i \sin\beta_i = F_x \tag{14.3}$$

with the sign of each axial term given by the direction in which the tip of the pile points. The dolphin of Example 19 of the User Manual (six steel pipes, F_x = 600 kN) was analysed with vertical piles, with the front row battered 10° and with both rows battered 10°.

Table 14.5 — Horizontal equilibrium of the dolphin

Piles	Axial components (kN)	Left side of (14.3) (kN)
All vertical	0.000	600.000000
Front row battered	289.275	600.000000
Both rows battered	218.745	600.000000

In each arrangement the shears and axial forces of the pile heads balance the applied load, which checks the transformation between the local axes of a battered pile and the global axes of the cap.

© 2026 Solplan. All rights reserved.

14.7 A rectangular section in its two planes

For a nonlinear section that is not symmetric about both axes, the curve of the second bending plane is computed from the section turned through 90°. For a rectangular concrete section of 400 × 500 mm with ten bars (Example 21 of the User Manual) the ratio of the gross moments of inertia is 4.1667/2.6667 = 1.5625. Without axial load the initial stiffnesses of the two moment–curvature curves are 142,542 and 90,596 kN·m^2, a ratio close to that of the gross section; the small excess comes from the reinforcement, which lies farther from the neutral axis in the stronger plane. A ratio near one, or below one, would show that the second curve was not turned.

14.8 Moment–curvature of a steel pipe

For a steel pipe of an elastic–perfectly plastic material the moment at a given curvature and axial force follows from the equilibrium of the stresses over the section alone. The moment–curvature curves of a pipe of 0.508 m diameter and 0.012 m wall, with f_y = 345 MPa and E = 199.948 GPa, were compared with an independent integration of the stresses over 40,000 thin strips, in which the axial strain at the centroid was found by bisection for each curvature so that the resultant equals the axial force. The squash load is P_y = 6,451 kN and the plastic moment without axial force $M_p = f_y Z$ = 1,018.7 kN·m.

Table 14.6 — Moment–curvature of a steel pipe: computed against independent integration

P/P_y	Axial force (kN)	Largest moment, Solgroup (kN·m)	Same curvature, integration (kN·m)	Largest difference along the curve
0	0	1,009.4	1,011.3	0.30%
0.25	1,613	924.3	926.2	0.30%
0.50	3,226	685.5	687.5	0.30%

The initial bending stiffness is 114,693 kN·m^2, against EI = 115,042 kN·m^2. The difference is the same at every curvature and every axial force, which shows that it comes from the representation of the wall by a finite number of fibres and not from the material law or the equilibrium of the axial force. The curve ends at a strain of five times the yield strain, where the moment is still slightly below M_p.

14.9 Torsion of a rigid cap

Nine identical piles in a square of 3 m spacing are joined by a rigid cap and have linear lateral, axial and torsional responses, as in Section 14.2. A torque M_z = 900 kN·m about the vertical axis through the centre of the cap rotates the cap by 0.2158 mrad. Every pile head then moves normal to its radius by the rotation times the radius, so that with identical linear piles the lateral force of each pile must be proportional to its distance from the centre, the centre pile must carry no lateral force, and the forces and torques of the piles must balance the applied torque.

Table 14.7 — Torsion of a rigid cap on linear piles

Quantity	Result
Lateral force of an edge pile (radius 3 m), kN	24.730
Lateral force of a corner pile (radius 3√2 m), kN	34.974
Spread of force / radius among the eight outer piles, relative to its mean	0.0e+00
Lateral force of the centre pile, kN	5.5e−16
Sum of the torques of the pile heads, kN·m	9.71
Residual of the equilibrium of the cap, relative to M_z	2.2e−14

The forces of the corner and edge piles are in the ratio $\sqrt{2}$ of their radii, the centre pile carries no lateral force, and the equilibrium is satisfied to the precision of the arithmetic. The torsional resistance of the individual piles is a small part of the total, as stated in Section 4.3.

© 2026 Solplan. All rights reserved.

14.10 p-y curves against the published equations

The p-y curves of the analysis were compared with the published equations of Chapter 5, evaluated by hand for a layer that starts at the ground surface without a water table (γ = 18 kN/m^3), at a depth x = 3 m and a width b = 0.6 m.

Table 14.8 — p-y curves: hand calculation and Solgroup

Model and quantity	Hand calculation	Hand (kN/m)	Solgroup (kN/m)
Soft clay, c_u = 25 kPa, ε_{50} = 0.01, J = 0.5: p_u	$(3 + \gamma x/c_u + J\,x/b)\,c_u\,b \le 9\,c_u\,b$	114.90	114.90
Soft clay: p at $y_{50} = 2.5\,\varepsilon_{50}\,b$	$0.5\,p_u$	57.45	57.45
API sand, φ' = 35°: $A\,p_u$ (large y)	C_1 = 2.970, C_2 = 3.419, C_3 = 53.79; A = 0.9	532.79	532.79
Elastic subgrade, E_s = 20 MN/m³: p at y = 10 mm	$E_s\,b\,y$	120.00	120.00

The values agree to the precision shown: the curves of the analysis are the published curves, evaluated with the parameters of the layer. The same comparison can be made for any layer with **Define ▸ Soil ▸ Printing Depths for p-y Curves**, which prints the curves generated at chosen depths.

© 2026 Solplan. All rights reserved.

Appendix A References

- AASHTO (2020). *LRFD Bridge Design Specifications*, 9th ed., Article 10.7.2.4. American Association of State Highway and Transportation Officials.
- AISC (2013). *Shapes Database*, version 14.1. American Institute of Steel Construction.
- American Petroleum Institute (2000). *Recommended Practice for Planning, Designing and Constructing Fixed Offshore Platforms — Working Stress Design*, API RP 2A-WSD, 21st ed.
- Awoshika, K., & Reese, L. C. (1971). *Effect of Batter on Piles Subjected to Lateral Load*. Research Report 3-5-71-117, Center for Highway Research, The University of Texas at Austin.
- Brown, D. A., Morrison, C., & Reese, L. C. (1988). Lateral load behavior of pile group in sand. *Journal of Geotechnical Engineering*, 114(11), 1261–1276.
- Bryant, L. M., & Matlock, H. (1977). Three-dimensional analysis of framed structures with nonlinear pile foundations. *Proceedings, Offshore Technology Conference*, OTC 2955.
- Caltrans (2013). *Seismic Design Criteria*, version 1.7. California Department of Transportation.
- Coyle, H. M., & Reese, L. C. (1966). Load transfer for axially loaded piles in clay. *Journal of the Soil Mechanics and Foundations Division*, ASCE, 92(SM2), 1–26.
- Franke, K. W., & Rollins, K. M. (2013). Simplified hybrid p-y spring model for liquefied soils. *Journal of Geotechnical and Geoenvironmental Engineering*, 139(4), 564–576.
- Georgiadis, M. (1983). Development of p-y curves for layered soils. *Proceedings, Geotechnical Practice in Offshore Engineering*, ASCE, 536–545.
- Hetényi, M. (1946). *Beams on Elastic Foundation*. University of Michigan Press.
- Hoek, E. (1990). Estimating Mohr–Coulomb friction and cohesion values from the Hoek–Brown failure criterion. *International Journal of Rock Mechanics and Mining Sciences*, 27(3), 227–229.
- Hoek, E., Carranza-Torres, C., & Corkum, B. (2002). Hoek–Brown failure criterion — 2002 edition. *Proceedings, North American Rock Mechanics Symposium*, Toronto, 267–273.
- Hognestad, E. (1951). *A Study of Combined Bending and Axial Load in Reinforced Concrete Members*. Bulletin 399, University of Illinois Engineering Experiment Station.
- Ibrahimbegovic, A. (1993). Quadrilateral finite elements for analysis of thick and thin plates. *Computer Methods in Applied Mechanics and Engineering*, 110, 195–209.
- Ibrahimbegovic, A., Taylor, R. L., & Wilson, E. L. (1990). A robust quadrilateral membrane finite element with drilling degrees of freedom. *International Journal for Numerical Methods in Engineering*, 30, 445–457.
- Johnson, R., Parsons, R. L., Dapp, S., & Brown, D. A. (2006). *Soil Characterization and p-y Curve Development for Loess*. Kansas Department of Transportation.
- Liang, R., Yang, K., & Nusairat, J. (2009). p-y criterion for rock mass. *Journal of Geotechnical and Geoenvironmental Engineering*, 135(1), 26–36.
- Mander, J. B., Priestley, M. J. N., & Park, R. (1988). Theoretical stress–strain model for confined concrete. *Journal of Structural Engineering*, 114(8), 1804–1826.
- Matlock, H. (1970). Correlations for design of laterally loaded piles in soft clay. *Proceedings, Offshore Technology Conference*, OTC 1204.
- Mokwa, R. L., & Duncan, J. M. (2001). Experimental evaluation of lateral-load resistance of pile caps. *Journal of Geotechnical and Geoenvironmental Engineering*, 127(2), 185–192.
- Mosher, R. L. (1984). *Load-Transfer Criteria for Numerical Analysis of Axially Loaded Piles in Sand*. Technical Report K-84-1, U.S. Army Engineer Waterways Experiment Station.
- O'Neill, M. W. (1983). Group action in offshore piles. *Proceedings, Geotechnical Practice in Offshore Engineering*, ASCE, 25–64.
- O'Neill, M. W., Ghazzaly, O. I., & Ha, H. B. (1977). Analysis of three-dimensional pile groups with nonlinear soil response and pile–soil–pile interaction. *Proceedings, Offshore Technology Conference*, OTC 2838.

© 2026 Solplan. All rights reserved.

- O'Neill, M. W., & Murchison, J. M. (1983). *An Evaluation of p-y Relationships in Sands*. Report to the American Petroleum Institute, PRAC 82-41-1, University of Houston.
- O'Neill, M. W., & Reese, L. C. (1999). *Drilled Shafts: Construction Procedures and Design Methods*. FHWA-IF-99-025, Federal Highway Administration.
- Park, R., & Paulay, T. (1975). *Reinforced Concrete Structures*. Wiley.
- PCI (2010). *PCI Design Handbook: Precast and Prestressed Concrete*, 7th ed. Precast/Prestressed Concrete Institute.
- Poulos, H. G., & Davis, E. H. (1980). *Pile Foundation Analysis and Design*. John Wiley & Sons, New York.
- Priestley, M. J. N., Seible, F., & Calvi, G. M. (1996). *Seismic Design and Retrofit of Bridges*. Wiley.
- Reese, L. C. (1997). Analysis of laterally loaded piles in weak rock. *Journal of Geotechnical and Geoenvironmental Engineering*, 123(11), 1010–1017.
- Reese, L. C., Cox, W. R., & Koop, F. D. (1974). Analysis of laterally loaded piles in sand. *Proceedings, Offshore Technology Conference*, OTC 2080.
- Reese, L. C., Cox, W. R., & Koop, F. D. (1975). Field testing and analysis of laterally loaded piles in stiff clay. *Proceedings, Offshore Technology Conference*, OTC 2312.
- Reese, L. C., Isenhower, W. M., & Wang, S.-T. (2006). *Analysis and Design of Shallow and Deep Foundations*. Wiley.
- Reese, L. C., & Nyman, K. J. (1978). *Field Load Tests of Instrumented Drilled Shafts at Islamorada, Florida*. Research report, Bureau of Engineering Research, University of Texas at Austin.
- Reese, L. C., & O'Neill, M. W. (1987). *Drilled Shafts: Construction Procedures and Design Methods*. FHWA-HI-88-042, Federal Highway Administration.
- Reese, L. C., & O'Neill, M. W. (1988). Field load tests of drilled shafts. *Proceedings, International Seminar on Deep Foundations on Bored and Auger Piles*, Ghent, 145–191.
- Reese, L. C., O'Neill, M. W., & Smith, R. E. (1970). Generalized analysis of pile foundations. *Journal of the Soil Mechanics and Foundations Division*, ASCE, 96(SM1), 235–250.
- Reese, L. C., & Van Impe, W. F. (2011). *Single Piles and Pile Groups under Lateral Loading*, 2nd ed. CRC Press.
- Rollins, K. M., Gerber, T. M., Lane, J. D., & Ashford, S. A. (2005). Lateral resistance of a full-scale pile group in liquefied sand. *Journal of Geotechnical and Geoenvironmental Engineering*, 131(1), 115–125.
- Rollins, K. M., Olsen, K. G., Jensen, D. H., Garrett, B. H., Olsen, R. J., & Egbert, J. J. (2006). Pile spacing effects on lateral pile group behavior: analysis. *Journal of Geotechnical and Geoenvironmental Engineering*, 132(10), 1272–1283.
- Rollins, K. M., Peterson, K. T., & Weaver, T. J. (1998). Lateral load behavior of full-scale pile group in clay. *Journal of Geotechnical and Geoenvironmental Engineering*, 124(6), 468–478.
- Simpson, M., & Brown, D. A. (2006). *Development of p-y Curves for Piedmont Residual Soils*. North Carolina Department of Transportation.
- Skempton, A. W. (1951). The bearing capacity of clays. *Proceedings, Building Research Congress*, London, Division I, 180–189.
- Stoll, U. W. (1972). Torque shear test of cylindrical friction piles. *Civil Engineering*, ASCE, 42(4), 63–64.
- Thompson, K. J., & Park, R. (1978). Stress–strain model for grade 275 reinforcing steel with cyclic loading. *Bulletin of the New Zealand National Society for Earthquake Engineering*, 11(2), 101–109.
- Vijayvergiya, V. N. (1977). Load-movement characteristics of piles. *Proceedings, Ports '77 Conference*, ASCE, Long Beach, 269–284.
- Welch, R. C., & Reese, L. C. (1972). *Laterally Loaded Behavior of Drilled Shafts*. Center for Highway Research, University of Texas at Austin.
- Whitaker, T. (1957). Experiments with model piles in groups. *Géotechnique*, 7(4), 147–167.

END OF DOCUMENT

© 2026 Solplan. All rights reserved.